

QUARTERLY PROGRESS REPORT

January 1 to March 31, 2016

Florida International University's Continued Research Support for the Department of Energy's Office of Environmental Management

Principal Investigator:

Leonel E. Lagos, Ph.D., PMP®

Prepared for:

U.S. Department of Energy
Office of Environmental Management
Under Cooperative Agreement No. DE-EM0000598



Applied Research Center
FLORIDA INTERNATIONAL UNIVERSITY

Introduction

The Applied Research Center (ARC) at Florida International University (FIU) executed work on four major projects that represent FIU-ARC's continued support to the Department of Energy's Office of Environmental Management (DOE-EM). The projects are important to EM's mission of accelerated risk reduction and cleanup of the environmental legacy of the nation's nuclear weapons program. The information in this document provides a summary of the FIU-ARC's activities under the DOE Cooperative Agreement (Contract # DE-EM0000598) for the period of January 1 to March 31, 2016.

The period of performance for FIU Year 6 under the Cooperative Agreement will be August 29, 2015 to August 28, 2016. The projects have been reorganized for FIU Year 6. Projects 2 and 3 from FIU Year 5 have been combined into a single project (Project 2) focused on soil and groundwater remediation research. The D&D and Workforce Development projects were subsequently renumbered as Projects 3 (D&D) and 4 (Workforce Development). Project 1 (high level waste/waste processing) remains unchanged.

Highlights during this reporting period include:

Program-wide:

- FIU made preparations for the program research review via video-teleconference planned for April 5-6, 2016, between DOE EM and FIU ARC as part of the DOE Cooperative Agreement. All presentations are available for downloading on FIU's DOE Research webpage at <http://doeresearch.fiu.edu>.
- FIU staff and students (DOE Fellows) participated and presented their DOE EM research at this year's Waste Management Symposia (WM16). A total of 15 professional presentations (oral/posters) and 20 student posters were presented.

Project 1- Chemical Process Alternatives for Radioactive Waste:

- Milestone 2015-P1-M18.1.1 and its corresponding deliverable, development of a test plan for using SLIM to detect precursors to DSGRE's, was completed on January 22, 2016 and submitted to DOE EM.
- Milestone 2015-P1-M18.2.1, finalizing the design of the refractory pad inspection tool, was completed on February 26, 2016 and submitted to DOE EM.
- Milestone 2015-P1-M18.2.3 and its corresponding deliverable, finalizing the design of the air supply line inspection tool, was completed on February 26, 2016 and submitted to DOE EM.
- Milestone 2015-P1-M19.1.1, down selection of alternative UT systems, was completed and the corresponding deliverable was submitted to EM-HQ on March 11, 2016.
- Milestone 2015-P1-M19.2.2, completing the baseline testing on the nonmetallic materials, was completed on March 25, 2016. The corresponding deliverable was submitted to EM-HQ on April 8, 2016.

Project 2- Environmental Remediation Science & Technology:

- A deliverable for Task 1, a progress report on the experimental results on autunite mineral biodissolution (Subtask 1.2), was submitted to DOE and site contacts on 2/15/2016.
- FIU has reforecasted the milestones and deliverables associated with the SRS surface water modeling of Tims Branch task forward one month through the end of this performance year, due to technical difficulties related to a server failure at ARC during the last week of January 2016, which caused the loss of many of the data files being developed in support of this research task. Data recovery efforts were pursued but failed to salvage the lost files. The reforecast dates will allow the research team the time needed to regenerate the missing data files and complete the proposed tasks. The circumstances and end path forward, including the new reforecasted dates for this project task, have been closely coordinated with the stakeholders at SRS and DOE HQ. FIU discussed the issue via teleconference with the SRNL collaborators and confirmed the agreement on new milestone and deliverable dates with an email sent to SRS and DOE HQ contacts on February 26, 2016.
- Milestone 2015-P2-M3, complete input of MIKE SHE model configuration parameters for simulation of evapotranspiration (subtask 3.1), was completed by the reforecast date of March 31, 2016. Milestone 2015-P2-M4, complete input of MIKE SHE model configuration parameters for simulation of unsaturated flow (subtask 3.1), which was originally due March 31, 2016, has been reforecast to April 29, 2016.
- A deliverable for Task 1, literature review of geophysical resistivity measurements and microbial communities (subtask 1.3.3), was submitted to DOE and site contacts on March 18, 2016.

Project 3 – Waste and D&D Engineering & Technology Development:

- Milestone 2015-P3-M2.2, associated with the D&D task, was completed with FIU's participation in the ASTM International Conference and embedded ASTM E10 committee meeting on January 24-27, 2016.
- Milestone 2015-P3-M3.2, for the D&D KM-IT task, was met with the deployment of the pilot web-based D&D Fixative Decision Model application to DOE for review on January 15, 2016.
- A deliverable on the preliminary metrics progress report on outreach and training activities for the D&D KM-IT task was complete and sent to DOE by the due date of February 29, 2016.
- FIU completed development and integration of the Global Knowledge Sharing Platform (for collaboration with the United Kingdom), FIU milestone 2015-P3-M3.3, and sent the link to DOE for their review on March 4, 2016.
- A D&D KM-IT workshop with the D&D community was completed during the Waste Management conference by demonstrating the system to conference attendees.

- A draft infographic on the DOE EM Cooperative Agreement was developed and revealed during the FIU Research Review presentations in early April.
- Milestone 2015-P3-M3.4, the addition/editing of four Wikipedia articles, originally due by March 31, has been reforecast to April 15, 2015 due to the coordination needed for the planned FIU Research Review presentations to DOE in early April. The circumstances and path forward, including the new reforecasted date for this project task, have been closely coordinated with the stakeholders at DOE HQ, and was discussed and agreed upon with the DOE Project Lead during regular project teleconferences on March 17 and March 31, 2016.

Project 4- DOE-FIU Science & Technology Workforce Development Initiative:

- Milestone 2015-P4-M4 was completed with the submission of twenty (20) student poster abstracts to the Waste Management Symposia 2016 (WM16).

The program-wide milestones and deliverables that apply to all projects (Projects 1 through 4) for FIU Year 6 are shown on the following table:

Task	Milestone/ Deliverable	Description	Due Date	Status	OSTI
Program-wide (All Projects)	Deliverable	Draft Project Technical Plan	10/16/15	Complete	
	Deliverable	Monthly Progress Reports	Monthly	On Target	
	Deliverable	Quarterly Progress Reports	Quarterly	On Target	
	Deliverable	Draft Year End Report	10/14/16	On Target	OSTI
	Deliverable	Presentation overview to DOE HQ/ Site POCs of the project progress and accomplishments (Mid-Year Review)	02/29/16*	Complete on 04/07/16	
	Deliverable	Presentation overview to DOE HQ/ Site POCs of the project progress and accomplishments (Year End Review)	08/31/16*	On Target	

**Completion of this deliverable depends on availability of DOE-HQ official(s).*

Project 1

Chemical Process Alternatives for Radioactive Waste

Project Manager: Dr. Dwayne McDaniel

Project Description

Florida International University has been conducting research on several promising alternative processes and technologies that can be applied to address several technology gaps in the current high-level waste processing retrieval and conditioning strategy. The implementation of advanced technologies to address challenges faced with baseline methods is of great interest to the Hanford Site and can be applied to other sites with similar challenges, such as the Savannah River Site. Specifically, FIU has been involved in: analysis and development of alternative pipeline unplugging technologies to address potential plugging events; modeling and analysis of multiphase flows pertaining to waste feed mixing processes, evaluation of alternative HLW instrumentation for in-tank applications and the development of technologies to assist in the inspection of tank bottoms at Hanford. The use of field or *in situ* technologies, as well as advanced computational methods, can improve several facets of the retrieval and transport processes of HLW. FIU has worked with site personnel to identify technology and process improvement needs that can benefit from FIU's core expertise in HLW. The following tasks are included in FIU Year 6:

Task No	Task
Task 17: Advanced Topics for Mixing Processes	
Subtask 17.1	Computational Fluid Dynamics Modeling of HLW Processes in Waste Tanks
Task 18: Technology Development and Instrumentation Evaluation	
Subtask 18.1	Evaluation of FIU's Solid-Liquid Interface Monitor for Estimating the Onset of Deep Sludge Gas Release Events
Subtask 18.2	Development of Inspection Tools for DST Primary Tanks
Subtask 18.3	Investigation Using an Infrared Temperature Sensor to Determine the Inside Wall Temperature of DSTs
Task 19: Pipeline Integrity and Analysis	
Subtask 19.1	Pipeline Corrosion and Erosion Evaluation
Subtask 19.2	Evaluation of Nonmetallic Components in the Waste Transfer System

Task 17: Advanced Topics for HLW Mixing and Processing

Task 17 Overview

The objective of this task is to investigate advanced topics in HLW processing that could significantly improve nuclear waste handling activities in the coming years. These topics have been identified by the Hanford Site technology development group, or by national labs and academia, as future methods to simulate and/or process waste streams. The task will focus on

long-term, high-yield/high-risk technologies and computer codes that show promise in improving the HLW processing mission at the Hanford Site.

More specifically, this task will use the knowledge acquired at FIU on multiphase flow modeling to build a CFD computer program in order to obtain simulations at the engineering-scale with appropriate physics captured for the analysis and optimization of PJM mixing performance. Focus will be given to turbulent fluid flow in nuclear waste tanks that exhibit non-Newtonian fluid characteristics. The results will provide the sites with mathematical modeling, validation, and testing of computer programs to support critical issues related to HLW retrieval and processing.

Task 17 Quarterly Progress

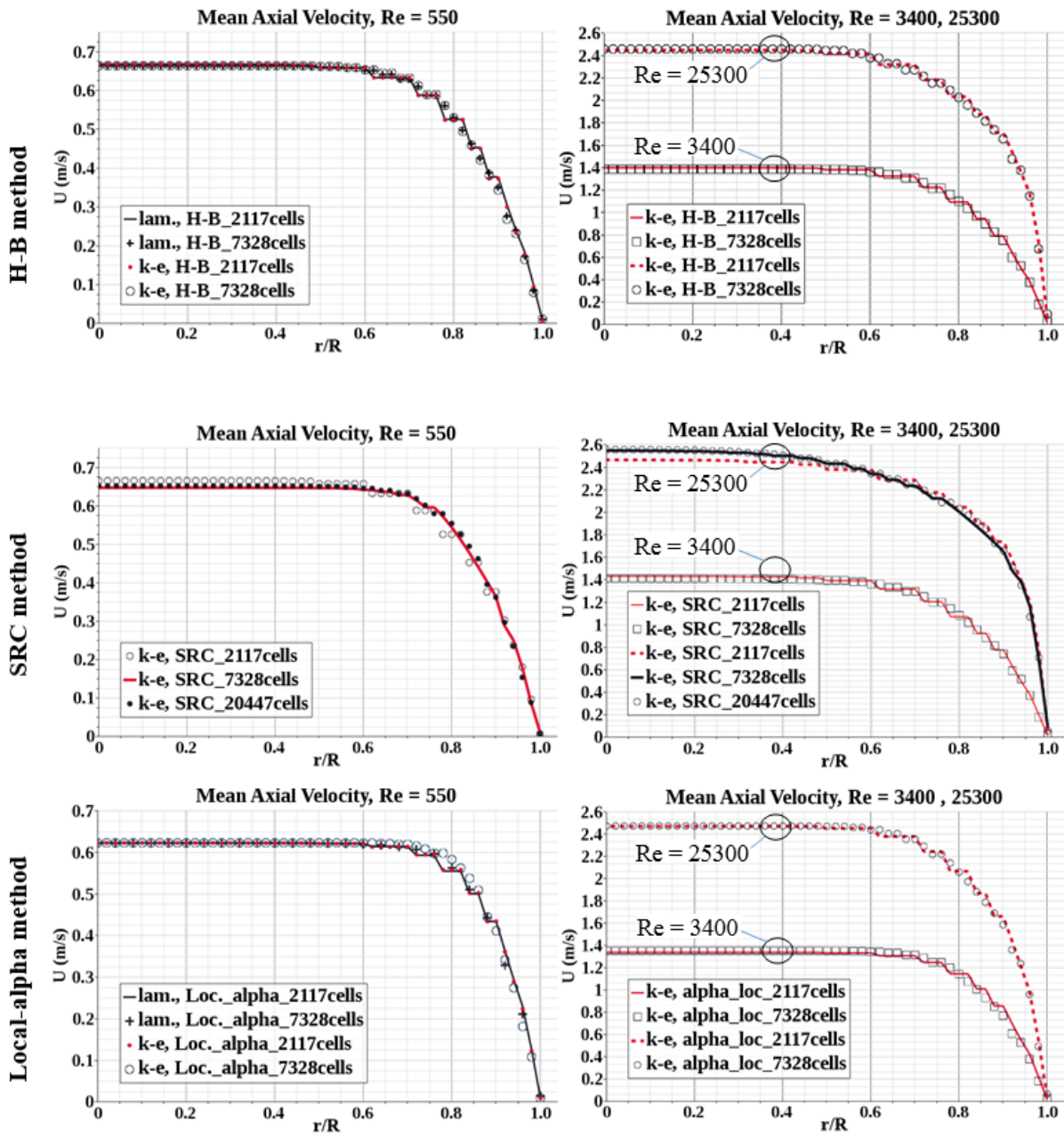
Subtask 17.1: Computational Fluid Dynamics Modeling of HLW Processes in Waste Tanks

During this performance period, a professional poster based on this research task and titled, “Improving the Accuracy of Computational Fluid Dynamics Simulations of Nuclear Waste Mixing using Direct Numerical Simulations,” was prepared and presented during the Waste Management 2016 (WM16) conference in Phoenix, AZ. In addition, a poster titled, “Radial Jet Impingement Correlation Investigation,” was prepared and presented by DOE Fellow Max Edrei at the student poster session at the WM16. In addition, a draft journal article of this research work has been prepared and will be submitted.

FIU investigated variations in the 2-D pipe flow results obtained from a variety of viscosity models and for three regimes of the flow (i.e., laminar, transitional, and turbulent). The viscosity models used are Herschel-Bulkley (H-B), Shear Rate Correction of Gavrilov and Rudyak [1] with the acronym of SRC, Local- α , Global- α , Inverse-Local- α , and Inverse-Global- α . In addition, FIU used finer computational grids containing 7328 (~198×37), 20447 (~393×52), and 28615 (~432×66) cells for grid-independence tests. The purpose of grid refinement was to guarantee that spatially-converged solutions were obtained.

The results for different models and grid sizes are displayed in Figure 1-1. For each model in this figure, the maximum difference between the profiles associated with the same Reynolds number is less than 4%. Further, an error analysis was performed for all models and flow regimes by comparing the numerical data point values with the available experimental data. Tables 1-1 and 1-2 show the calculated error values and improvements of the error for all models that were used in flow simulations. FIU used the converged solutions for calculation of the relative percentage error.

FIU also investigated the computational error associated with the profiles of axial velocity reported by Peltier et al. (2015) for the same flow cases (i.e., laminar, transitional, and turbulent) reported previously. This result is included in the Table 1-3 with the label of “Inkson N. (2015)” which was used originally by Peltier and his colleagues. This table also shows the best results obtained by using the FIU’s proposed α -method. Our comparison shows the competitiveness of the alpha method for the laminar flow and the superiority of this method in the turbulent flow. In the case of the transitional flow, a hybrid alpha method potentially could be developed and be more competitive with the method of Peltier et al. (2015).



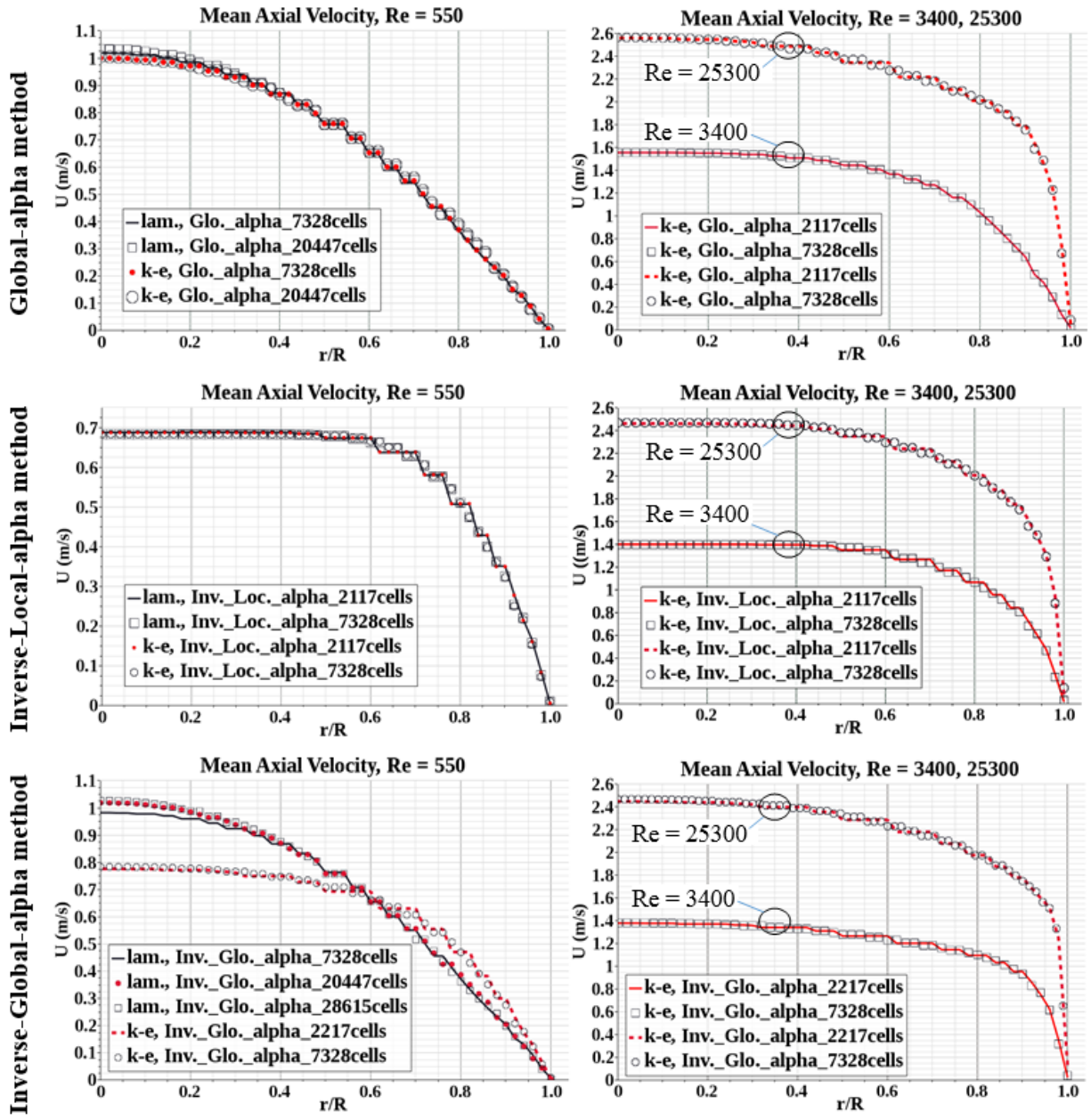


Figure 1-1. Results of various viscosity models under multiple flow conditions.

Table 1-1. Error Analysis Study for Different Methods and Flow Regimes

Flow regime	Laminar ^a (Re = 550)	Laminar ^b (Re = 550)	Transitions (Re = 3400)	Turbulent (Re = 25300)
method	Err _{avē} (%)	Err _{avē} (%)	Err _{avē} (%)	Err _{avē} (%)
H-B	18.2	17.4	28.2	4.5
SRC	-	19.8	26.8	6.2
Local_alpha	25.6	25.8	30.5	6.3
Global_alpha	20.3	19.1	14.7	4.7
Inv._ Local_alpha	14.9	14.5	35.7	3.3
Inv._ Global_alpha	20.4	10.5	52.5	1.7

a: Solved by the laminar solver in STARCCM+

b: Solved by the k-ε solver in STARCCM+

Table 1-2. Improvement of Percent Error for Different Methods and Flow Regimes

Flow regime	Laminar ^b (Re = 550)	Laminar ^c (Re = 550)	Transitions (Re = 3400)	Turbulent (Re = 25300)
method	Err _{imp.} (%)	Err _{imp.} (%)	Err _{imp.} (%)	Err _{imp.} (%)
H-B	N/A	N/A	N/A	N/A
SRC	-	-8.6	4.7	-37.1
Local_alpha	-40.7	-41.7	-8.1	-40.8
Global_alpha	-11.8	-5.1	48.1	26.2
Inv._ Local_alpha	18.4	20.2	-26.7	-5.4
Inv._ Global_alpha	-11.9	42.2	-86.2	61.4

a: Negative values indicate increase of error

b: Solved by the laminar solver in STARCCM+

c: Solved by the k-ε solver in STARCCM+

Table 1-3. Comparison of Error Values for Proposed Method and Peltier et al. (2015)

Flow regime	Laminar (Re = 550)	Transitions (Re = 3400)	Turbulent (Re = 25300)
Method	Err. (%)	Err. (%)	Err. (%)
H-B	17.4	28.2	4.5
SRC	19.8	26.8	6.2
alpha (this work)	10.5	14.7	1.7
Inkson N. (2015) [*]	8.1	5.1	9.2

FIU has evaluated two MATLAB computational packages (MX and ANAFLAME), which have been developed to determine the dissipation rate of the kinetic energy (TDR) for DNS simulations. These methods were based on empirical correlations (modeling the TDR) and direct solutions (based on the 4th and 6th order gradients of the fluctuating components of the velocity field). A combination of user-filed-functions and user-defined functions (UDF) were developed

in the STAR-CCM+ to obtain the fluctuating components of the velocity field and to calculate the turbulent KE and TDR using the direct method. The developed codes were tested to ensure that the UDFs could regenerate the same values of variables that could be obtained directly from the application without utilization of the UDF (e.g., local values of the alpha).

The developed codes in C and C++ and functions were based on the expression for the mean rate of dissipation of energy introduced by Taylor (1953) and Baldi et al. (2003), as:

$$\epsilon = \mu \left(2 \frac{\overline{\delta u^2}}{\delta x} + 2 \frac{\overline{\delta v^2}}{\delta y} + 2 \frac{\overline{\delta w^2}}{\delta k} + \overline{\left(\frac{\delta u}{\delta y} + \frac{\delta v}{\delta x} \right)^2} + \overline{\left(\frac{\delta u}{\delta z} + \frac{\delta w}{\delta x} \right)^2} + \overline{\left(\frac{\delta v}{\delta z} + \frac{\delta w}{\delta y} \right)^2} \right)$$

where, u, v, and w are the fluctuating components of velocity in three coordinate directions (i.e., x, y, and z) and μ is the dynamic viscosity of the non-Newtonian fluid which can be found from different methods (e.g., the alpha method). The most efficient way to obtain the TDR was to use the root-mean-square of the fluctuations, which is in accord with measurements of Baldi et al. (2003). The quickest approach for calculation of the gradient is to use the built-in 1st order gradients method in the application. This approach is acceptable for the data obtained from higher order solvers (i.e., the QDNS solver) which is 2nd order accurate. Figure 1-2 shows the Field-Functions developed in the STAR-CCM+ and a display of the gradient of the fluctuating component of the axial velocity. However, development of a UDF for calculation of higher order gradients is in progress. Figure 1-3 shows equal values obtained of the local alpha that were obtained from different methods (i.e., a field function and a UDF). Through this test, some issues regarding the difference between default conventions used in the STAR-CCM+ for storage and naming of variables and those used for field-functions and user-defined functions were successfully overcome and communication between field functions and UDF was successfully established.

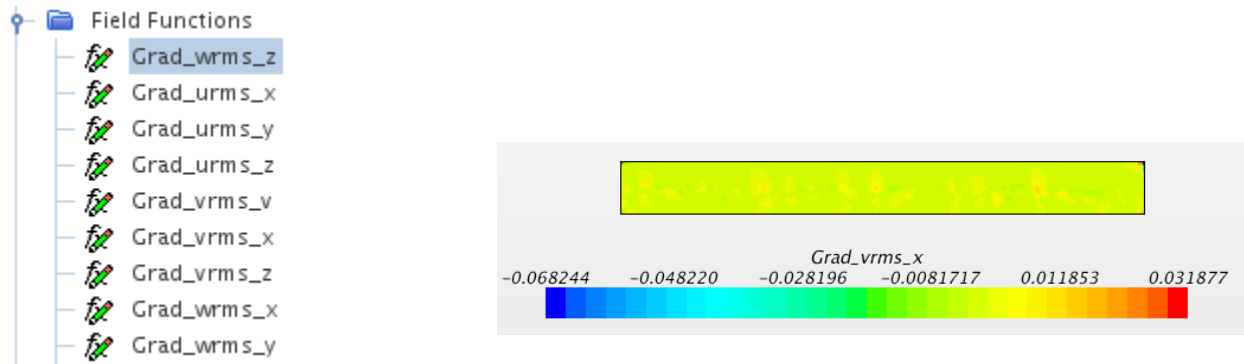


Figure 1-2. Field functions developed to obtain correlations needed to obtain the TDR (left) and visualization (right).

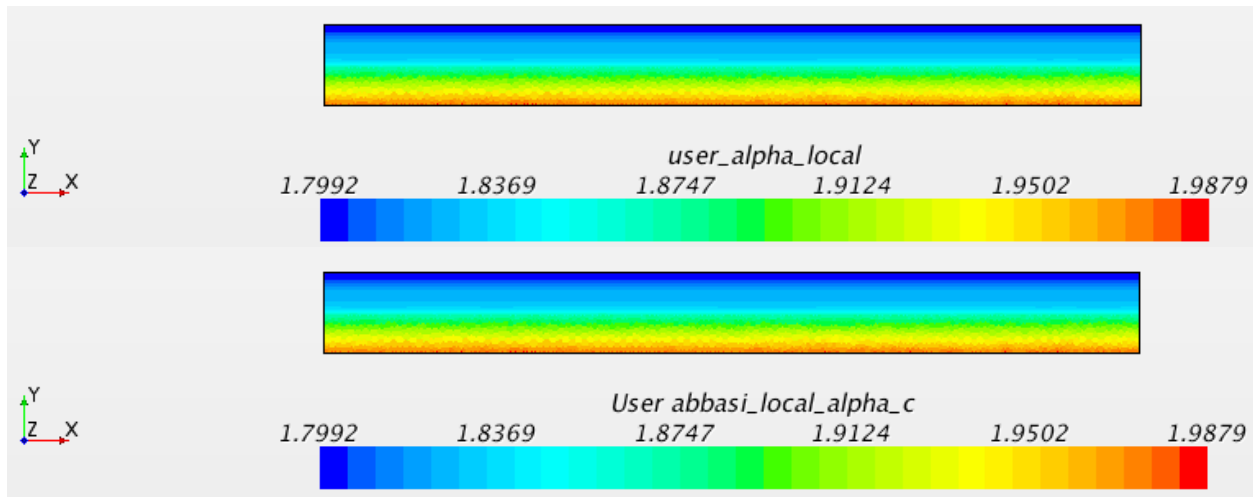


Figure 1-3. Local alpha obtained from the user-field function “user-alpha-local” (top) and the UDF “User abbasi_local_alpha_c” (bottom).

References:

Baldi S., Hann D., Yianneskis M., 2003, On the measurement of turbulence energy dissipation in stirred vessels with PIV techniques, I&EC journal, Volume 42, Issue 26, pp 7006–7016.

Kaneda Y., Ishihara T., Yokokawa M., Itakura K., A. Uno, Energy dissipation rate and energy spectrum in high resolution direct numerical simulations of turbulence in a periodic box, Physics of Fluids 15, L21 (2003); doi: 10.1063/1.153985.

Gavrilov A., Rudyak V.Y., A Model of Averaged Molecular Viscosity for Turbulent Flow of Non-Newtonian Fluids, Journal of Siberian Federal University. Mathematics & Physics 2014, 7(1), 46–57.

Meyer A., Phillips H. E., Sloyan B. M., Polzin K. L., Mixing (MX) Oceanographic Toolbox for EM-APEX* float data applying shear-strain finescale parameterization, IMAS Technical Report 2014/01.

Peltier J, Andri R, Rosendall, Inkson N., Lo S., 2015, Evaluation of RANS Modeling of Non-Newtonian Bingham Fluids in the Turbulence Regime Using STAR-CCM+®, Advanced Simulation & Analysis, BecthelNuclear, Security & Environmental, Cd-adapco™ , Conference: STAR Global Conference 201

Taylor F.R.S., "Statistical Theory of Turbulence", Proc. Roy. Soc. London, A, 1935, vol 151, 421-478.

A second task in 17.1 is the investigation of radial wall jet correlations using STAR-CCM+. During this reporting period, Poreh’s correlation applied to a curved surface jet impingement using a scaled down PJM geometry was investigated. The simulation was run using a standard k-epsilon turbulence model with similar mesh. A 3D model is used due to the lack of an axisymmetric section in a 2D plane of the PJM geometry. Below is the geometric domain used.

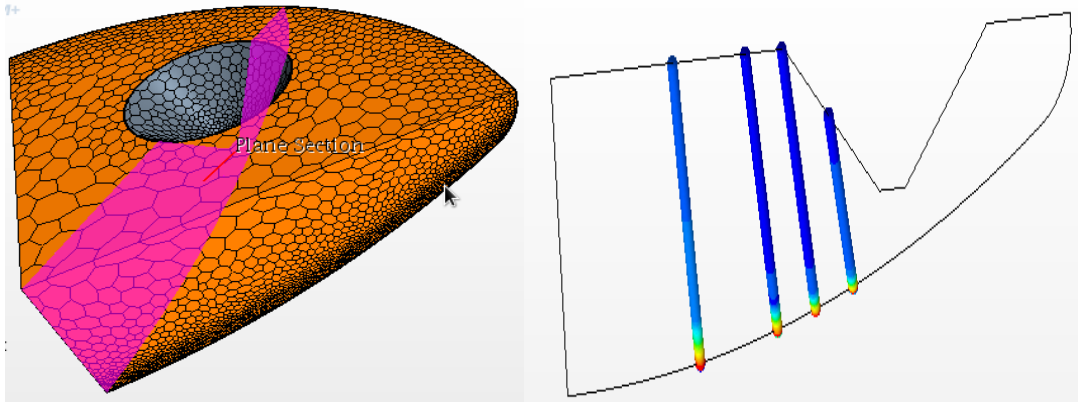


Figure 1-4. CAD of scaled down vessel (left) and plane of symmetry with data collection locations (right).

As can be seen in Figure 1-4, the plane of symmetry is highlighted. This plane is the region from which data is collected. The line probes are at an r/b location of 1, 2, 3 and 5. The following velocity profile was obtained after the simulation was run

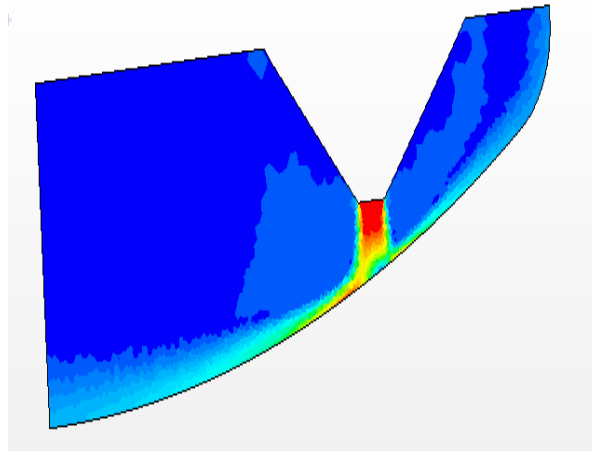


Figure 1-5. Velocity profile domain of PJM symmetry plane.

Similar jet impingement structures are observed in Figure 1-5. The stagnation zone is slightly displaced upward. This is expected based on the literature review of oblique impingement. To establish mesh independence, a mesh sensitivity analysis is conducted.

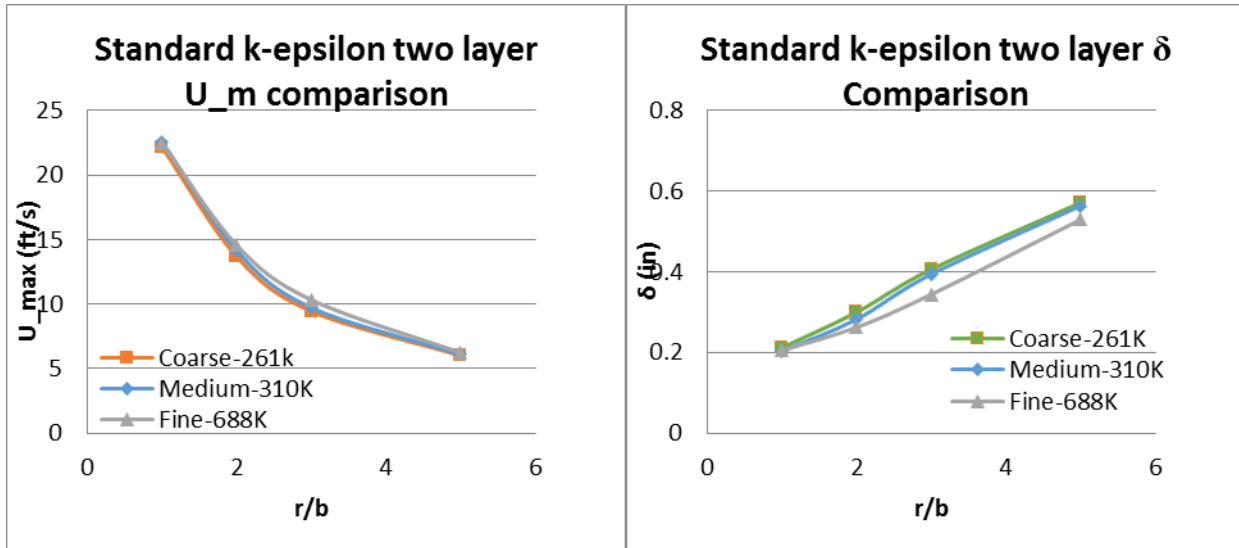


Figure 1-6. Mesh effect on extracted U_{max} and δ .

Figure 1-6 suggests that finer meshing has little effect on the radial jet characteristics. The medium mesh is chosen to move forward in this study.

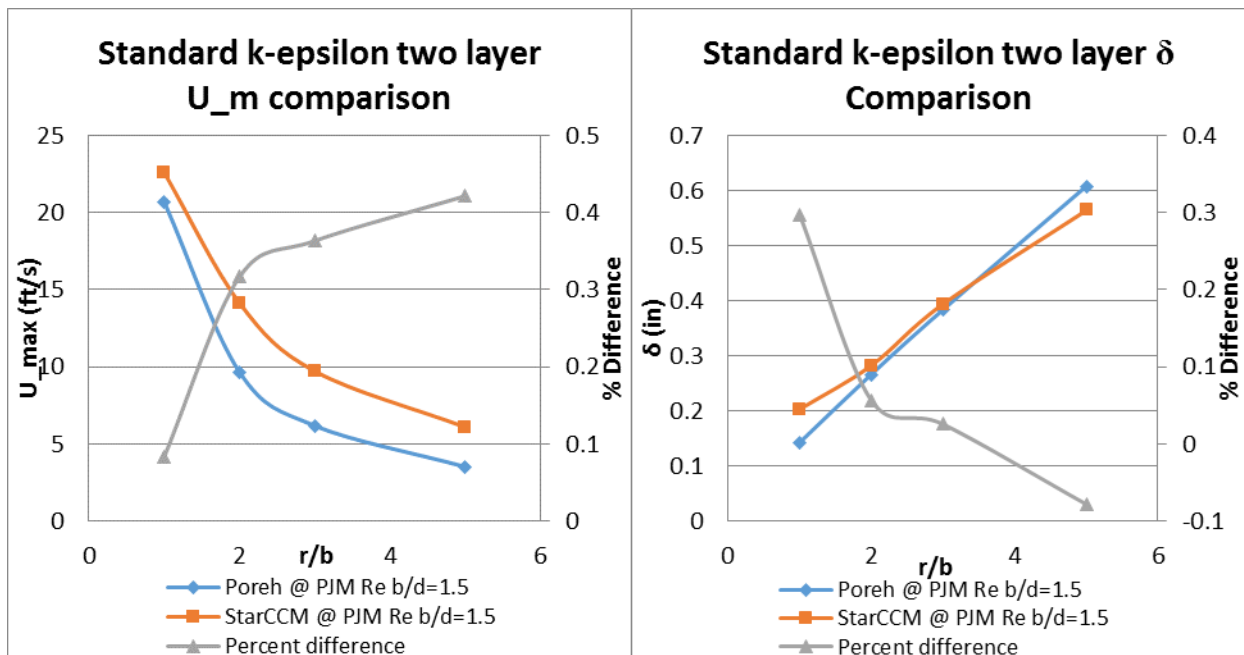


Figure 1-7. Comparison between Poreh's correlation and simulation radial jet characteristics.

It can be seen from Figure 1-7 that the simulation predicts that Poreh's correlation has similar predictive capabilities on a curved PJM vessel as it does on a flat surface. The r/b locations chosen are the only ones applicable to the PJM vessel. Further r/b locations pertain to the impingement of radial jets region, to which the correlations do not apply. As a path forward, further error analysis will be conducted in order to see the exact effect of the curved surface on Poreh's correlations.

Task 18: Technology Development and Instrumentation Evaluation

Task 18 Overview

The objective of this task is to assist site engineers in developing tools and evaluating existing technologies that can solve challenges associated with the high level waste tanks and transfer systems. Specifically, FIU is assisting in the evaluation of using a sonar (SLIM) developed at FIU for detecting residual waste in HLW tanks during pulse jet mixing (PJM). This effort would provide engineers with valuable information regarding the effectiveness of the mixing processes in the HLW tanks. Additionally, the Hanford Site has identified a need for developing inspection tools that provide feedback on the integrity of the primary tank bottom in DSTs. Recently, waste was found to be leaking from the bottom of the primary tank in AY-102. FIU will assist in the development of a technology to provide visual feedback of the tank bottom after traversing through the refractory pad underneath the primary tank.

Task 18 Quarterly Progress

Subtask 18.1: Evaluation of FIU's SLIM for Estimating the Onset of Deep Sludge Gas Release Events

The objective of this task is to assist DOE site scientists and engineers in developing tools and evaluating existing technologies that can solve challenges associated with the high-level waste (HLW) tanks and transfer systems. Specifically, FIU is assisting in the evaluation of using a 3D profiling sonar as part of its Solid-Liquid Interface Monitor (SLIM). SLIM was developed at FIU for imaging the settled solids layer in million gallon HLW tanks and for quantifying the residual waste volume on the floor of HLW conditioning tanks during pulse jet mixing (PJM) operations. This effort would provide engineers with valuable information regarding the effectiveness of the mixing processes in the HLW tanks. In summer 2015, the focus of research was changed to address a new Hanford need to investigate the ability of the 3D sonar to image small increases in HLW volume as an early indication of possible deep sludge gas release events (DSGREs).

Additionally, the Hanford Site has identified a need for developing inspection tools that provide feedback on the integrity of the primary tank bottom in DSTs. Recently, waste was found to be leaking from the bottom of the primary tank in AY-102. FIU will assist in the development of a technology to provide visual feedback of the tank bottom after traversing through the refractory pad underneath the primary tank.

Task 18 Quarterly Progress

Subtask 18.1: Evaluation of FIU's SLIM for Estimating the Onset of Deep Sludge Gas Release Events

A professional poster titled, "Sonar Testing, Imaging and Visualization for Rapid Scan Applications in High-Level Waste Tanks," was prepared and presented at WM16. In addition, a poster titled, "Rapid Imaging of Solids in High Level Waste Tanks at Hanford," was prepared and presented by DOE Fellow Gene Yllanes at the WM16 student poster session.

FIU succeeded in completing a primary objective of this task by imaging a solids layer that is raised 5 mm through insertion of air into a bladder under a solids (sand) layer. This directly mimics the rise in HLW solids from gas generation and retention in a deep sludge layer. This was achieved by putting sand over an empty bladder and adding increments of air to the bladder to raise the top sand layer center point by 10 mm and 20 mm and imaging the solids layer initially and after each increment of air.

The air bladder was taped to a plastic lid and weighted with flat metal pieces to keep it securely on the tank floor and not floating to the surface (Figure 1-8). Paver sand was placed on the bladder and then smoothed over in order to ensure the sand would remain over the entire bladder even after addition of air while underwater. In Figure 1-9, the sand covers the bladder with a slight mounding.



Figure 1-8. Air bladder with metal weights underneath taped to a plastic lid.



Figure 1-9. Same air bladder covered with paver sand to create object to be imaged by the 3D sonar.

In Figure 1-10, the 3D sonar images are shown with: no air in bladder (left); increment of air to raise center point of sand 10 mm (center); and 2nd increment of air to raise the center point of sand to 20 mm (right).

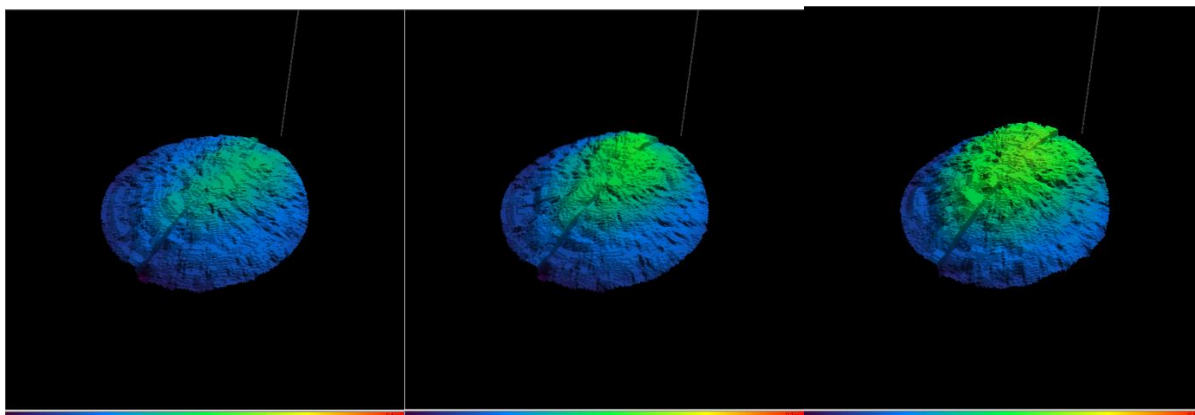


Figure 1-10. Three 3D sonar images are shown with: no air in bladder (left); with 1st increment of air to the bladder; and after 2nd increment of air to the bladder.

Once the sand with an empty bladder was imaged, air was added to the bladder in increments to simulate the rise in HLW solids with gas generation and retention in a deep sludge layer. Figure 1-10 clearly shows that changes as small as 10 mm can be imaged and measured by the 3D sonar. Measurements of the center sand point were taken with a yardstick with mm rulings to measure the 10 mm and 20 mm increases. Earlier tests demonstrated that 5 mm changes in height can be measured with the 3D sonar and, therefore, future testing will identify the resolution of the sonar for changes in the height of the solids layer.

Figure 1-10 (right image) shows the maximum amount of gas that was put into the bladder and the resultant height change was measured to be 20 mm.

This proof-of-principle test results were shared with WRPS scientists and engineers immediately after testing. In addition, a detailed test plan was completed and sent to DOE EM and WRPS for comment in January.

FIU hosted a visit from four WRPS engineers in February to discuss the status of our current tasks. Gary Peterson from DOE EM also participated via teleconference. A number of tasks were discussed, but it was unclear how the SLIM task would contribute to the immediate needs of the site. Suggestions included reducing the number of tasks and placing more effort and resources on fewer tasks. Results from this year would need to be evaluated to see how SLIM could be utilized. Some of the engineers suggested that the next step should simply be to deploy the system in a cold test facility to demonstrate its capability.

FIU processed images within MATLAB software to improve visualization of the settled solids layer on tank floors. FIU's goal on this visualization subtask is to improve the accuracy of the spatial dimensions of the wall locations, settled solids on the floor and any objects in the field of view. FIU discovered that by covering hard smooth objects with sand, the sonar signal has stronger reflections and that the sonar images were more precise, and that there was a reduced need for filtering and processing the data from the sonar images.

In a simple experiment, a tank floor was covered with a thin layer of sand and then a dish was filled with sand and set on the floor. Subsequently, sand was mounded over a plastic bladder with most of the air removed. Two short cardboard cylinders were placed beside each other in the sand in the dish and the cylinders were also filled with sand. In Figure 1-11, the color scale connected with distances from the sonar head is not conducive to visualizing the experimental setup. In Figure 1-11, it is difficult to visualize the change in the height of the sand over the air bladder. After modeling with MATLAB, the location of the objects beneath the sand became clear. The air bladder and the cardboard cylinders are much more visible in Figure 1-12, which displays the processed image in MATLAB. Often the accuracy of the actual sonar data and the images from MATLAB are higher resolution than the display of the commercial sonar. In this particular case, the image spatial resolution (shape of the solids layer) is nearly the same. The MATLAB processing allowed for optimal display of the varying height to maximize the ability of the viewer to see these changes.

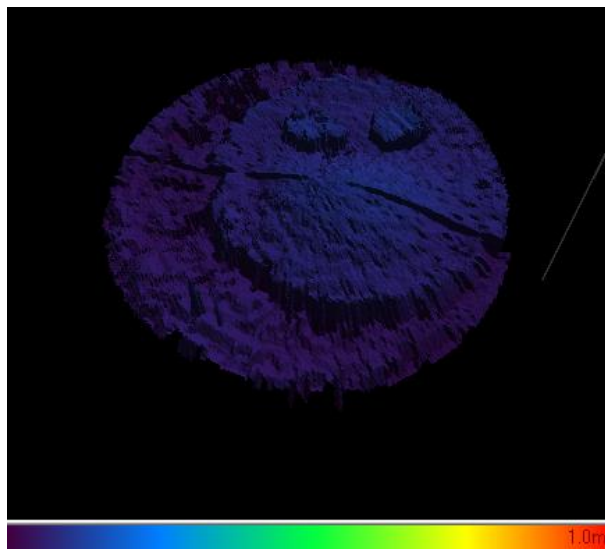


Figure 1-11. Image of experiment from sonar's commercial visualization package.

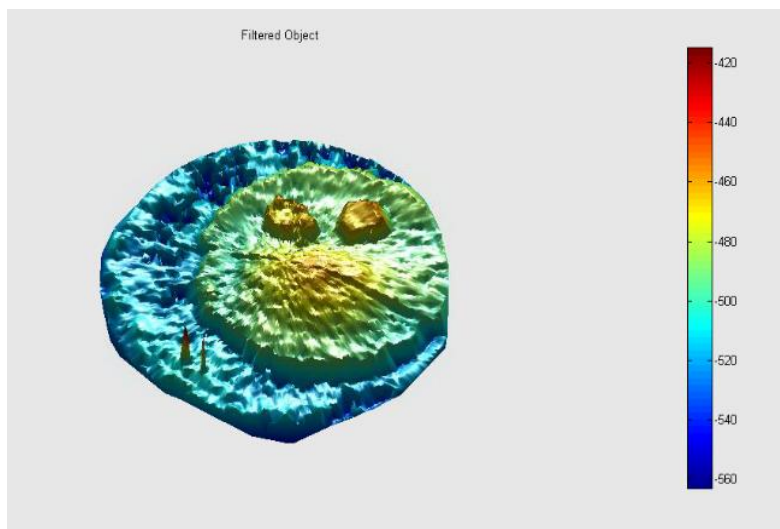


Figure 1-12. Image of experimental results in MATLAB.

FIU also continued performing diagnostics on the sonar system since there is a major fraction of the sonar signal that appears to be scattered in the water around the sonar head where there should be no scattering. By using a delay before accepting a reflected sonar signal, we were able to filter out this anomalous scattering around the sonar. This anomalous scattering contributes to the sonar signal being lost and, hence, to lowering the intensity of the scanning sonar. FIU will again work with the manufacturer to diagnose the problem with the sonar while the approved test plan is executed in April.

Subtask 18.2: Development of Inspection Tools for DST Primary Tanks

DOE Fellow Ryan Sheffield gave a professional presentation based on this research task titled, “Development of Inspection Tools for the AY-102 Double-shell Tank at the Hanford DOE Site,” during WM16. In addition, Ryan also presented a poster titled, “Development of a Miniature Motorized Inspection Tool for the Hanford Site Tank Bottoms,” during the WM16 student poster session. DOE Fellow Erim Gokce also presented during the student poster session with a poster titled, “Modifications/Enhancements to the Robotic Pipe Inspection Tool Utilized for the DOE High Level Waste Project at the Hanford Site.”

Miniature Motorized Inspection Tool

The design and testing of the inspection tool rover have been completed, so remaining issues include finalizing the design and assembly of the unit’s tether. A modification was introduced to the control circuit that reduced the number of power wires from eight to four. The purpose of this modification was to reduce the weight, diameter and drag force so maximum power would be available for navigation and obstacle avoidance. However, there was a concern of reducing the available voltage to the motors and, consequently, reducing the overall available pull force of the device. The inspection tool was tested with the new control circuit and results demonstrated that the maximum pull force had not been reduced and could still pull 4.5 lb.

USB communication was chosen for the camera line since the USB protocol utilizes a maximum of 5 wires which will minimize the drag force of the tether while providing sufficient image quality. The illuminating LEDs can be powered through the USB and is compatible with a majority of the commercially available CMOS camera sensors that are used in micro cameras. A tether casing, which needs to house the camera line and powerlines, was selected and is comprised of a 6-mm expandable braided sleeving as shown in Figure 1-13.



Figure 1-13. Tether with expandable braided sleeving to encase the camera and powerlines.

During the assembly, the sleeving will easily expand to accommodate the number of wires to be inserted. The surface of the sleeve is very smooth, which will assist in minimizing the friction forces, and is fairly elastic so it should easily be able to navigate through sharp turns in the refractory slots.

In addition to the camera and power lines, a thin metal wire will be incorporated into the tether. This line will keep any loads from being applied to the power and camera lines and can be used to remove the unit in case of failure. Lastly, FIU has begun to investigate approaches for minimizing contact of the tether with the corners when making turns. Although this is not a need for traversing the first 17 feet of channel, it will be required when the efforts change to modifying the design to reach the central plenum.

In completing the design of the rover, a milestone was completed (milestone 2015-P1-M18.2.1) in February. The final design was presented to four WRPS engineers visiting FIU and they provided suggestions for the path forward in terms of engineering-scale testbed development, testing and in-tank deployment. Figure 1-14 shows the final design of the inspection tool after introduction of a cap and incorporating the camera and powerlines inside the tether sleeving.



Figure 1-14. Prototype of completed design for the miniature rover inspection tool.

Performance parameters of the inspection tool including maximum pull force and force to weight ratio have already been measured and quantified. This is based on the four magnets incorporated into the design. The magnets not only function to hold the crawler upside down inside the refractory channel, but they also provide the normal force required to convert the output torques of motors to the traction force which pulls the tether. Two key parameters that can influence the magnet force are the distance to the tank bottom and the operating temperature. Limitations on these parameters was also investigated during this performance period.

The magnetic field strength of a magnetic block along the central axis of the field can be calculated via:

$$B(x) = \frac{B_r}{\pi} \left\{ \arctan \left(\frac{lw}{2x\sqrt{4x^2+l^2+w^2}} \right) - \arctan \left(\frac{lw}{2(t+x)\sqrt{4(t+x)^2+l^2+w^2}} \right) \right\}$$

where, B is the flux density, B_r is the residual flux density, l is length of a magnet, w is width of the magnet and t is the thickness. The pull force from steel can be calculated from the following relation:

$$F = B^2 A / 2 \mu_0$$

where A is the area of each surface and μ_0 is the permeability. The physical properties of the neodymium iron boron magnet used in our inspection tool is summarized in Table 1-4.

Table 1-4. Magnet Properties

Dimensions	0.75 in x 0.25 in x 0.10 in
Material	Sintered Neodymium Iron Boron
Tolerance	All dimensions +/- 0.005 in
Temperature Range	40F to 302F
Magnetic Grade	N38SH
Remanence (Br)	12,200 to 12,600 Gauss
Coercivity (Hc)	10,800 to 11,500 Oersted
BHMax	35 to 38 MGOe

Figure 1-15(a) and 1-15(b) show the magnetic field strength and maximum pull force versus air gap for the magnets used in our design.

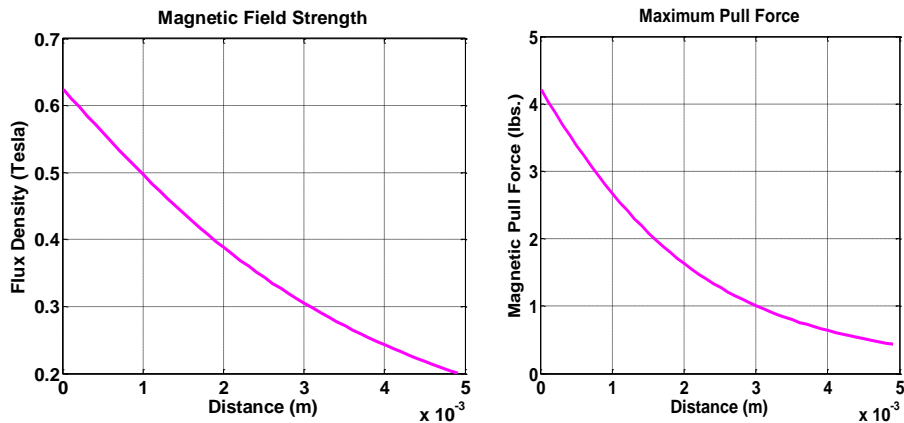


Figure 1-15. (a) Magnetic field strength and (b) maximum pull force with air gap.

Figure 1-15(b) demonstrates that for an air gap less than 1 mm, the pull force of magnet is greater than 2.5 lbs for each magnet block. This means the available normal force from four magnets will be greater than 10 lbs.

Two key temperatures associated with magnets are the maximum operating temperature and the Curie temperature. If the temperature exceeds the maximum operating temperature of the magnet, a percentage of the magnetization is irreversibly lost. The Curie temperature is the temperature at which all magnetization of the magnet is lost.

Figure 1-16 shows the demagnetization curves for neodymium magnets (N38SH) used in the design of our inspection tool. The load line is a line from the origin, with a slope equal to the permeance coefficient of the magnet (0.51 for N38SH grade). The knee is the part of the normal curve where it bends down, becoming a vertical line. At 140°C (284°F), the operating point would be right at the knee of the normal curve. Thus, 284°F is the maximum operating temperature. According to the information provided by site engineers, the maximum operating temperatures of the N38SH magnets will be approximately 170°F which is well below 284°F.

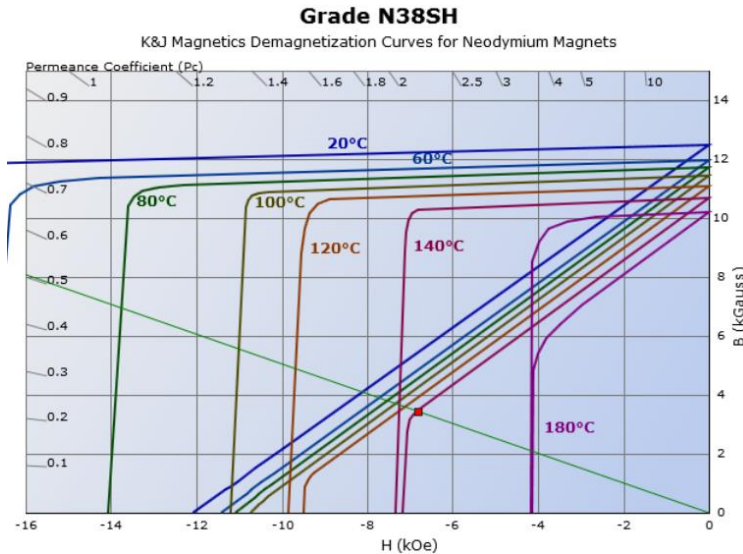


Figure 1-16. Demagnetization (BH) Curves for Neodymium Magnets N38SH.

Peristaltic Crawler

During this period, activities were focused on consolidating the crawler design. This involved minor modifications to the crawler including the grippers being strengthened, as shown in Figure 1-17. The final design uses the original bolted-through-pins at the mechanism hinges. The previous design, using hinges with embedded pin inserts, presented structural issues when the bipartite parts were 3D printed in thermoplastic.

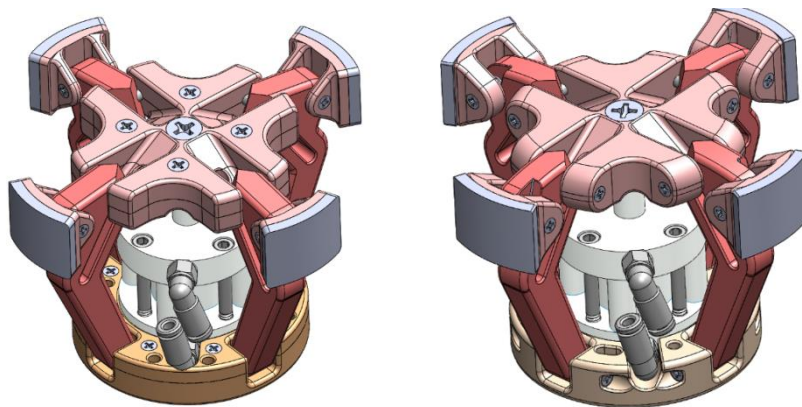


Figure 1-17. Previously improved design (left) and final (right) gripper.

As shown in Figure 1-18, the hinged flat pads used for increasing the contact of the gripping mechanisms were strengthened. The original design with two extension springs was also simplified by using one torsion spring. The springs are necessary to recoil the pads when the mechanism closes, keeping a tight diameter during crawling.

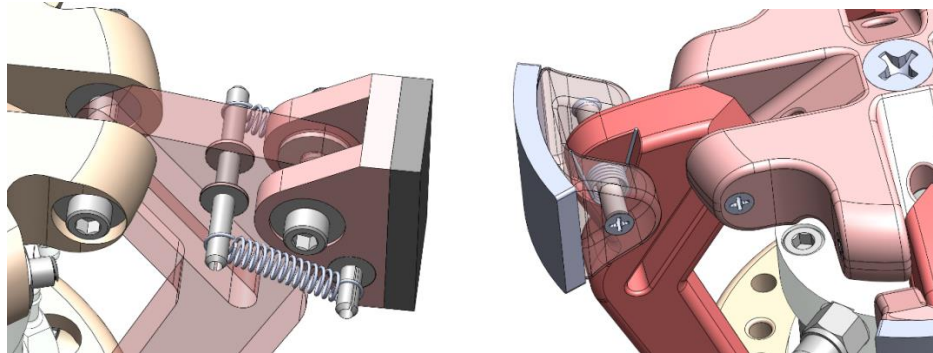


Figure 1-18. Original hinged pad (left) and final design (right).

Another modification was the rearrangement of the control panel layout, where push-to-connect tube fittings were used to lessen the likelihood of leaks (Figure 1-19). Additionally, the embedded microcomputer of the unit was upgraded from a CPU with one core to four cores. A multicore system would be useful for controlling additional instrumentation.

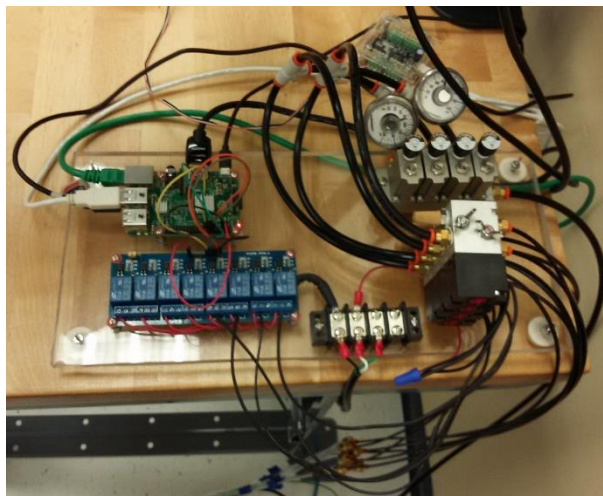


Figure 1-19. Control panel improved layout.

With the objective of integrating additional instrumentation to the crawler, ways to implement a network of sensors were also studied during this period. Among several technologies, the Inter-integrated Circuit (I²C) Protocol was selected. I²C is a protocol intended to allow a “master-slave” network of multiple digital integrated circuits. It requires two wires only, and the basic version of it can communicate with up to 1008 devices at 100 kHz or 400 kHz. To test the protocol, FIU successfully used a MCP9808 temperature sensor. The sensor, shown in Figure 1-20, is a I²C digital temperature sensor with an accuracy of $\pm 0.25^{\circ}\text{C}$, range of -40°C to $+125^{\circ}\text{C}$ and precision of $+0.0625^{\circ}\text{C}$. The testing application was implemented in C++ using the built-in i²c capability of the upgraded microcomputer embedded in the control panel.

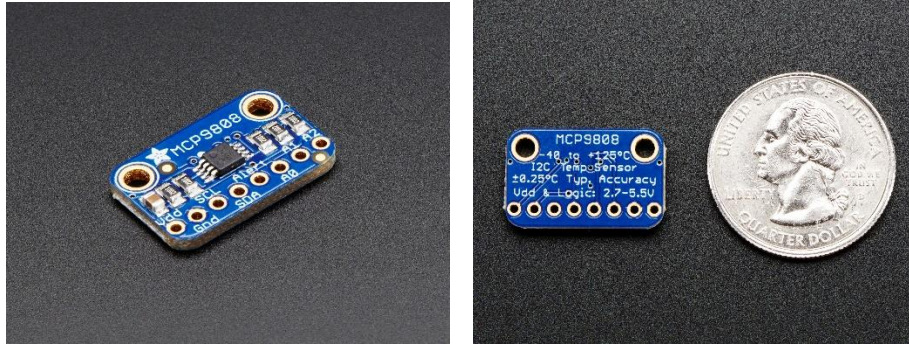


Figure 1-20. MCP9808 precision I2C temperature sensor.

To enhance the remote controlling capability of the crawler, experiments were conducted using inter-process communication across a computer network. A testing client-server application was successfully implemented in C++, in which data from the crawler control panel were transferred between computers using the internet.

A final prototype design of the crawler has been completed, as shown in Figure 1-21 and FIU began manufacturing a new prototype to be used in the future full-scale mockup tests. Shown in Figure 1-22 is the manufactured prototype which incorporates the improvements of our most current design. This system has guides added to keep the unit centered in the pipe and it has the updated design of the four-armed gripper.

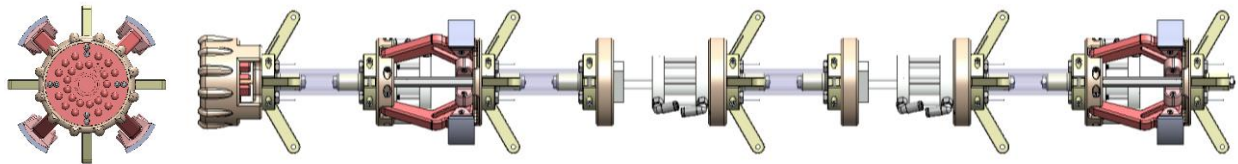


Figure 1-21. Crawler final design.

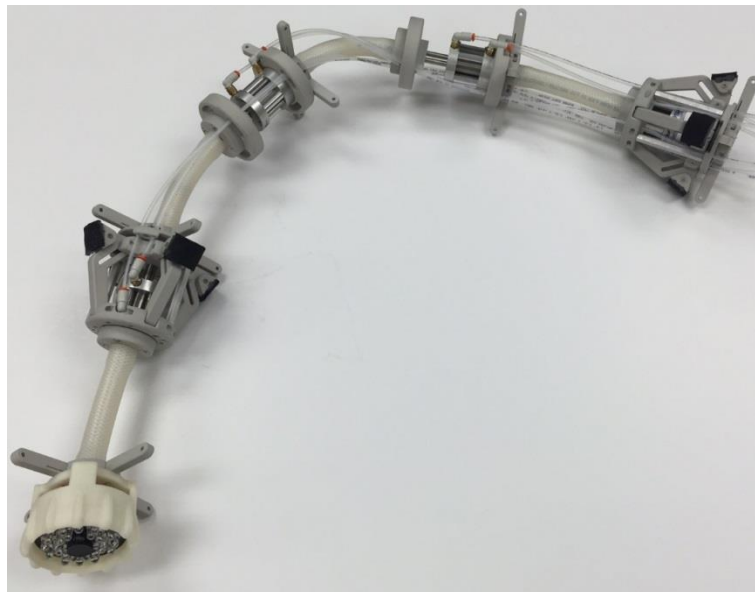


Figure 1-22. New crawler prototype.

During the manufacturing process, minor modifications were made to the design. Bolt through and nut connections were replaced by heat-set inserts. As illustrated in Figure 1-23, the embedment of metal threads in the 3D printed thermoplastic parts streamlined the assembly and improved the layout of the crawler modules.

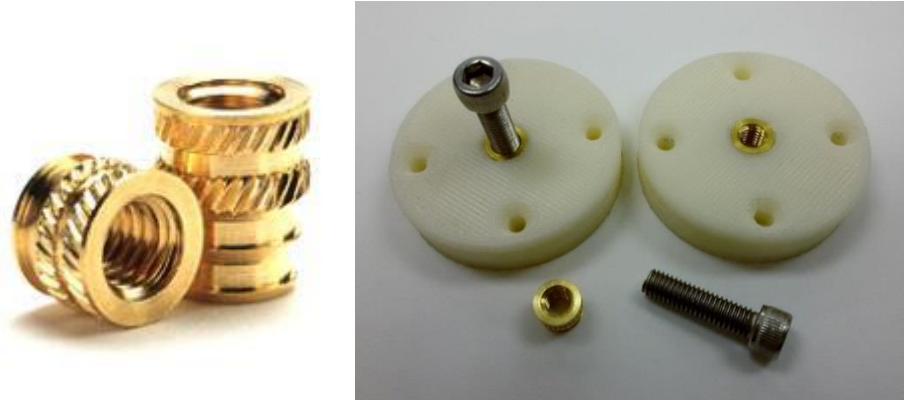


Figure 1-23. Heat-set inserts for plastics.

The testing of the system in a full scale mockup testbed was also discussed with engineers from WRPS. A new testbed will be developed that is representative of the proposed inspection in the AY-102 tank. The pipeline in the testbed will be composed of welded schedule 40 steel pipe and fittings, routed with dimensions shown in Figure 1-24. The vertical lines will be replaced by horizontal runs, which would make the inspection more challenging and the structure more affordable.

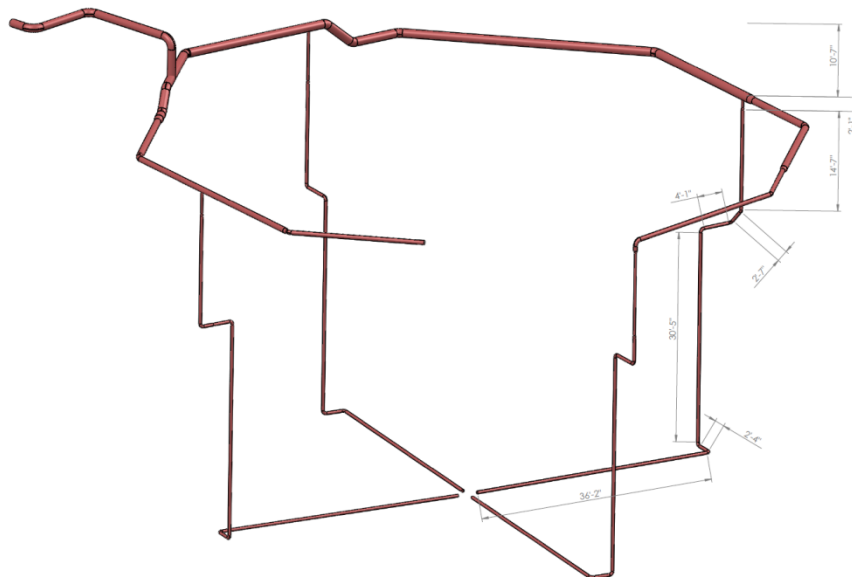


Figure 1-24. Ventilation header of the AY-102 tank at Hanford.

During the month of March, a draft modular full scale design for a mock-up of a primary tank bottom has been developed based on DST documentation provided by WRPS. The draft design includes a portion of the tank bottom with the proper dimensions to incorporate two adjacent refractory channels (Figure 1-25) and it is comprised of a primary tank bottom, the refractory air cooling channels and the 4-inch air supply pipe. The structure will have the actual dimensions of

a portion of tank AZ-241 and AY-102. Figure 1-26 shows a preliminary prototype of the full scale mock-up testbed. The new testbed is being designed to reproduce the inspection conditions of the bottom of the DST primary tanks. The testbed is also being designed to be customizable, which will allow FIU to create exemplars of a variety of DSTs at Hanford. The structure might also be used to evaluate future inspection technologies and other robotic devices.

The mockup is modular and portions of the structure can be replaced to simulate several inspection conditions, such as different configurations of the refractory pad, cooling channels and supply airlines. Defects such as damaged weld beds and bottom cracks could be tested, as well with the influence of thicker steel plates. Currently, the draft design is being evaluated and, due to the considerable size of testbed, several issues need to be considered, including:

- Weight of the testbed and equipment needed for handling
- Sizing of each module to find a balance point between ease of assembly and size of weight of each module
- Optimal location and ergonomics for the test bed
- Safety and handling considerations when handling modules
- Utility requirements

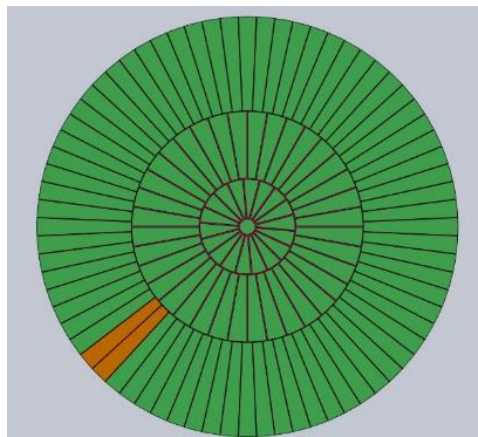


Figure 1-25. CAD of refractory channels.

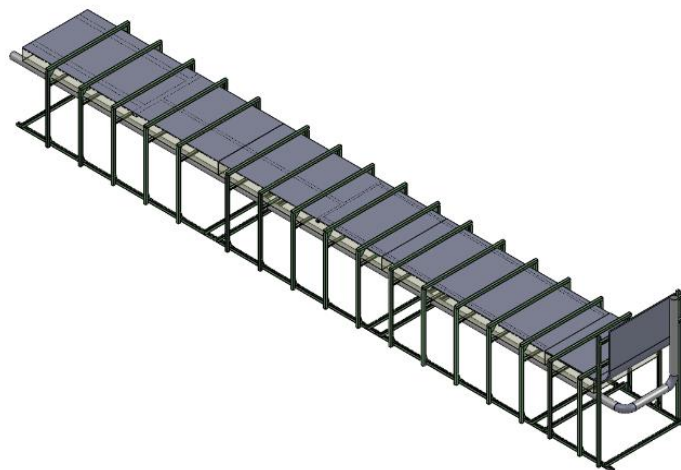


Figure 1-26. Full scale mock-up testbed prototype.

For the peristaltic crawler, a new instrumentation module is being designed to carry a load cell and an embedded computer. The module will be used in the full scale mockup tests, providing feedback from the unit during the inspections. In the current design, a USB cable is used to provide video feedback from the device. This cable is being replaced with an Ethernet cable. The new network cable not only will allow the communication, but will also supply power to the device. This way, multiple additional sensors could be used without the addition of extra cabling and avoiding future modification in the tether.

FIU is also coding the software infrastructure necessary for enabling the simultaneous communication, sensor feedback, and video streaming from the inspection tool to the main control box. The multi-client/server application is being developed in C++ and uses native capabilities of the embedded computer, such as the standard sockets library, and multithreading.

Subtask 18.3: Investigation Using an Infrared Temperature Sensor to Determine the Inside Wall Temperature of DSTs

During this quarter, equipment required for bench scale testing was acquired, calibrated and the initial bench scale test set up procedure was determined.

During the first month, the Raytek IR sensor was ordered; options of heating water in the tank and measuring its temperature were investigated. Two different options to increase the temperature of water in the tank were considered, namely, the water heaters and the Peltier plates. Immersion water heaters can be readily dropped into the tank to increase the water temperature. In this application, the temperature range is from 120°F to 170°F. Typical immersion heaters are shown in Figure 1-27. They represent the portable coil heater, the tank immersion heater and over-the-side tank immersion heater, respectively.



Figure 1-27. Immersion heaters a) portable b) tank c) side mounted tank.

Peltier plates work on the Peltier effect which states that an applied voltage can result in a temperature difference between the intersections of two different materials (semiconductors). There are two sides on a Peltier plate and as one side gets cooler the other side gets hotter with the flow of electricity. In our application, this function of Peltier plates can be used to heat a region. Typical Peltier plates commercially available are shown in Figure 1-28. A major concern with Peltier plates is that the cooler side is to be maintained cool and the hotter side hot, which was investigated for the present application and found not to be a viable option.



Figure 1-28. Peltier plates a) circular, b) square.

In addition, efforts were focused on investigating the thermocouples to be placed at various set points both inside and outside the tank. Thermocouples are temperature sensors made by joining two different metals. With changes in temperature, both metals expand differently, which is related to the voltage difference. There are five types of base metal thermocouples: J, K, T, E, and N. There are also Type R, S, C, and GB thermocouples, which are the noble metal thermocouples. Thermocouples are mainly classified as wireless thermocouples, beaded wire thermocouples, thermocouple probes, and surface probes. Figure 1-29 shows a few typical commercially available thermocouple options.



Figure 1-29. Thermocouples a) high temperature surface probe b) hollow tube thermocouple probe.

In February, all the components required for bench-scale testing were acquired. This included the Raytek IR sensor, an immersion electric coil heater and a carbon steel tank (drum).

The Raytek IR sensor is a miniature pyrometer (non-contact temperature sensor), with a distance spot ratio of 22:1. The system includes a communication box/head and a 100-m connecting cable as shown in Figure 1-30.

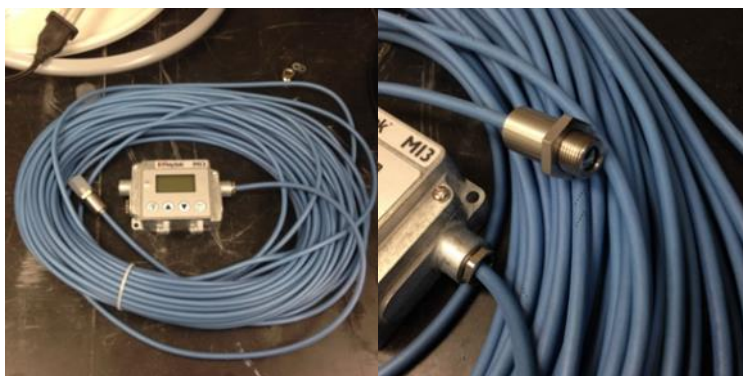


Figure 1-30. a) Raytek IR sensor system; b) sensor (detailed view).

The electric immersion coil is suitable for heating the fluid (water) up to 212°F. A picture of the heater is as shown in Figure 1-31a. The specifications of the immersion coil are 120 volts/1350 watts and its dimensions are 13.5” x 2” x 2 1/4”. A carbon steel tank (drum) has been acquired for initial testing. The drum has an outer diameter of 14 5/8” and a gauge of 20 (thickness - 0.0375”). Height of the drum is 18 7/8” and its capacity is 10 gallons.



Figure 1-31. a) immersion coil and b) carbon steel drum.

The test set up plan includes filling the tank with water and heating it using the coil heater. As the temperature increases, the IR sensor would collect data at intervals according to the test matrix in Table 1-5. To measure the inside water temperature, an immersion thermometer will be used and a few thermocouples will be placed on the walls to cross verify the readings.

Table 1-5. Test Matrix for IR Sensor

Distance (ft)	Y = 1 ft	Y= 2 ft	Y = 3 ft	Y = 4 ft
X = 0.5	T=[120 170°F]	T=[120 170°F]	T=[120 170°F]	T=[120 170°F]
X = 1	T=[120 170°F]	T=[120 170°F]	T=[120 170°F]	T=[120 170°F]
X=1.5	T=[120 170°F]	T=[120 170°F]	T=[120 170°F]	T=[120 170°F]
X = 2	T=[120 170°F]	T=[120 170°F]	T=[120 170°F]	T=[120 170°F]
X = 2.5	T=[120 170°F]	T=[120 170°F]	T=[120 170°F]	T=[120 170°F]

X - Horizontal distance away from the tank; Y- vertical height; T -temperature of water.

During the last month of this quarter, assembly, calibration and testing of the Raytek MI3 infrared sensor were conducted. The Raytek MI3 sensor required additional electrical connections for power source and emissivity calibrations. Initial temperature measurement tests were conducted using the power supply assembled at FIU-ARC. Measurements included the ambient air temperature, a glass beaker with heated coolant and a hot coffee pot (metallic tank). In order to verify the Raytek MI3 sensor readings, a laser gun (handheld IR sensor) was also used to measure the temperatures. For emissivity calibration settings, an external electrical circuit was fabricated by combining three single-pull double-throw (SPDT) switches. The switch circuit symbol and the assembled electrical circuit is shown in Figure 1-32.



Figure 1-32. Switch circuit symbol (left), circuit assembly – open (center), circuit assembly – closed (right).

Depending on the combinations of 0 (low) and 1 (high) voltage, the emissivity of the test piece is adjusted to a value between 0.5 and 1.1 as predefined in the sensor manual. The typical range of voltage used is 0 volts (low) and 5 volts (high). The emissivity table and the circuit diagram are given in Figure 1-33.

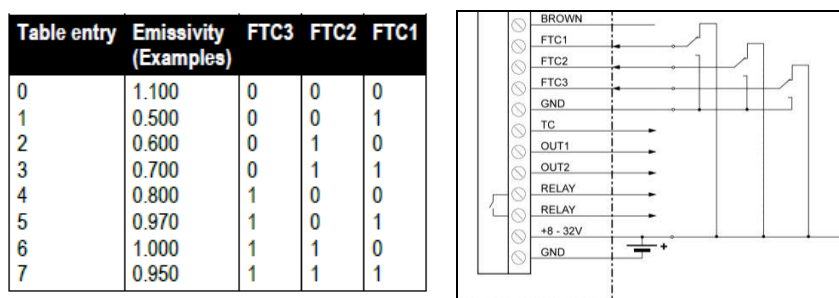


Figure 1-33. Digital selection of emissivity table (left) and circuit diagram (right).

With the new circuit, the test measurements were conducted on ambient air temperature, a glass beaker with heated coolant and a hot coffee pot as shown in Figure 1-34.

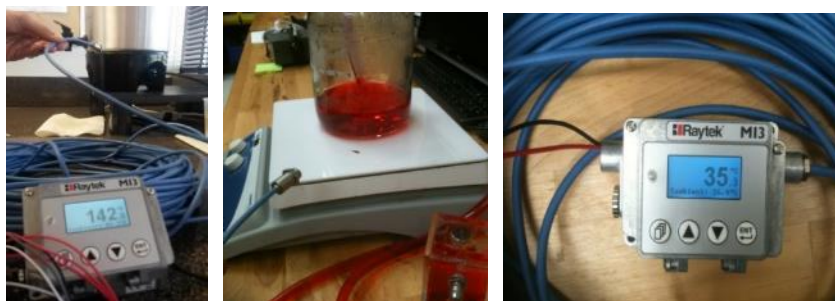


Figure 1-34. Temperature measurements a) coffee pot b) glass jar with coolant c) sensor reading for coolant test.

Currently, FIU is in the process of adjusting the sensor for ambient background temperature compensation, calibrating the emissivity for a carbon steel tank and performing bench scale tests based on the previously defined test matrix.

A poster based on this research task and titled, “Heat Transfer Calculations for the Use of an Infrared Temperature Sensor,” was presented by DOE Fellow Meilyn Planas at the WM16 student poster session.

Task 19: Pipeline Integrity and Analysis

Task 19 Overview

The objective of this task is to support the DOE and site contractors at Hanford in their effort to evaluate the integrity of waste transfer system components. This includes primary piping, encasements, and jumpers. It has been recommended that at least 5% of the buried carbon steel DSTs waste transfer line encasements be inspected. Data has been collected for a number of these system components and analyzed. Currently, different ultrasonic transducer systems are being investigated for thickness data measurement to determine the actual erosion/corrosion rates so that a reliable life expectancy of these components can be obtained. An additional objective of this task is to provide the Hanford Site with data obtained from experimental testing of the hose-in-hose transfer lines, Teflon® gaskets, EPDM O-rings, and other nonmetallic components used in their tank farm waste transfer system under simultaneous stressor exposures.

Task 19 Quarterly Progress

Subtask 19.1: Pipeline Corrosion and Erosion Evaluation

During this quarter, the investigated UT systems were down selected based on bench scale tests and the information provided by the manufacturers. A milestone document summarizing all the investigated UT systems and the final options have been submitted to the Hanford engineers and DOE (milestone 2015-P1-M19.1.1).

During the first month of the quarter, the couplant-free ultrasonic transducers from Ultran Group have been acquired, and quotation and leasing options from Innerspec Technologies have been pursued. The UT sensors from the Ultran group are couplant-free and have smaller dimensions to fit around 2-inch and 3-inch diameter pipes, which complies with the requirements of the task. These are dry coupling direct contact ultrasonic transducers (Series WD25-2) and have a nominal frequency of 2.0 MHz and an active diameter of 6.3 mm. As shown in Figure 1-35, the sensor has a right angle connection and requires an RG174/U 2M cable.

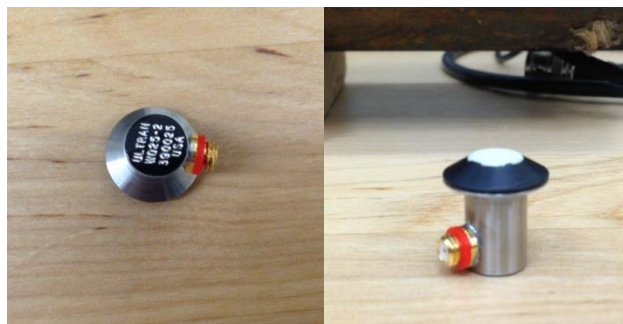


Figure 1-35. a) Ultran UT sensor a) top view b) side view.

In addition to the Ultran sensors, efforts were focused on acquiring a quote from Innerspec Technologies for their Electromagnetic Acoustic Transducer (EMAT) sensors. These sensors (called temate® BAND) can be collectively placed along the circumference of a pipe to measure thickness. A typical EMAT sensor is shown in Figure 1-36.



Figure 1-36. Innerspec Temate Band.

During the next month, time and frequency domain tests were conducted on the couplant free ultrasonic transducers from Ultran Group and the thicknesses of a carbon steel pipe were obtained. Further, evaluation and down selection of the UT sensors for bench-scale testing was pursued in consultation with site engineers.

The UT sensors utilized from Ultran were the Series WD25-2 and were used in the bench-scale test setup shown in Figure 1-37. The experimental setup consists of an oscilloscope (Tektronics TDS3034), a signal generator (BK precision 4040) and the sensors placed on the test piece (carbon steel pipe). The UT sensors have a right angle connector for RG174/U 2M cable.

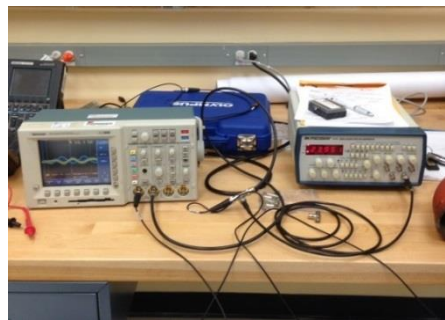


Figure 1-37. Experimental set-up.

Initial tests included testing of the signal passage through the sensors. One of the sensors was excited (frequency-20kHz) using the signal generator and the other sensor was placed in contact with the first sensor as shown in Figure 1-38a. Both sensors were connected to the oscilloscopes to measure the excitation and the received signals. As expected, it is observed that both the signals overlapped, indicating that bulk waves are produced by the sensor (Figure 1-38b).

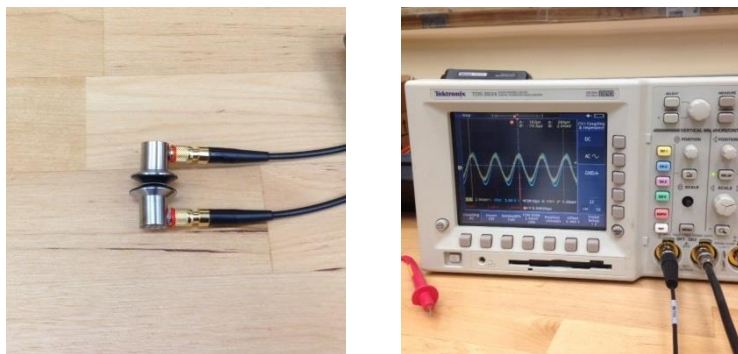


Figure 1-38. (a) Sensors in contact, (b) oscillogram.

The next test was to determine the time of flight of the signal to calculate the thickness of the pipe. Both sensors were placed next to each other. One was used to send the sound waves into the pipe (pulse) and the other was used to capture the reflected wave (echo). The arrangement is as shown in Figure 1-39. From the oscillogram in Figure 1-39b, the lag time for the waves was found to be 1.2 μs . Using this information and the velocity of sound in the material (carbon steel taken as 0.231 in/ μs), the thickness of the pipe was calculated to be approximately 0.15 in.

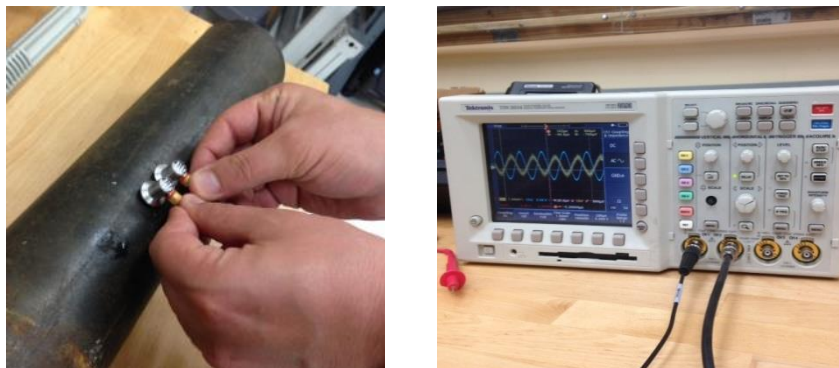


Figure 1-39. (a) Adjacent sensors (b) oscillogram.

In addition, based on the discussions with WRPS, the down selection of the UT sensors from all the investigated options was conducted. It was decided that the two viable options to be pursued are the Permasense guided wave sensors and the Ultran dry couplant sensors.

During the last month, a poster based on this research task and titled, “Stainless Steel Corrosion: Feed Properties Affecting Material Selection for LAWPS Piping at Hanford Site,” was presented by DOE Fellow John Conley at the WM16 student poster session.

Also, efforts were focused on preparing the deliverable summary document for the down selecting of the sensors (milestone 2015-P1-M19.1.1). The summary document included all of the available options for pipe thickness measurements using the ultrasonic (UT) sensors. Additionally, engineers from WRPS visited FIU during the month of March and, based on the discussions, two out of the five possible sensor systems were chosen for further investigation and testing. The two sensor systems are the Ultran mini sensors and the Permasense guided wave sensors. Due to the expense of the data acquisition systems, quotations have been obtained for leasing the Permasense UT sensor system. Currently, FIU is in the process of evaluating the leasing option and seeking a quotation from the Ultran Group to lease their system.

Subtask 19.2: Evaluation of Nonmetallic Components in the Waste Transfer System

A professional poster based on this research task and titled, “Evaluation of Nonmetallic Materials in the Waste Transfer System,” was prepared and presented at WM16. In addition a poster titled, “Nonmetallic Materials Testing for Hanford's HLW Transfer System,” was prepared and presented by DOE Fellow Anthony Fernandez at the WM16 student poster session.

This period's efforts began with repairing all leaks in the test loops that were discovered during long term trial runs. The trials were run for over 24 hours and some small leaks were discovered that were not apparent during the initial trials. After all leaks were addressed and the system ran for extended periods without any leaks, the test loop was insulated (Figure 1-40) to keep the

desired temperature of the fluid stable. Work also began on assembling the hose-in-hose transfer lines (HIHTL) blowout test apparatus including connecting a pressure transducer to the apparatus and writing a LabVIEW® code to read and record the pressure readings during the blowout tests. In the test plan, the three individual loops are documented to be run at 70°F, 130°F and 180°F, respectively; however, during the extended trial runs, it was observed that the fluid temperature increased from baseline room temperature of 70°F to 85°F due to heat from the pump and line friction.



Figure 1-40. Insulated test loop.

During the initial trial runs, which included running the aging test loop at the three experimental testing temperatures (85°F, 130°F, and 180°F), problems arose with Loop 1. Since Loop 1, will be operating at a high temperature of 180°F, and the PVC used on that loop has a maximum operating temperature of 140°F, it had to be replaced with CPVC which can handle the 180°F solution flowing through it. The HIHTL pressure testing apparatus was fabricated and a LabVIEW® code for the hose pressure testing written that has the ability to monitor the pressure inside the hose, while also recording and writing all the data to an Excel spreadsheet. The hose pressure testing will closely follow the procedures used by River Bend Transfer Systems, LLC in their hose pressure testing, so that our testing baseline testing can be validated against other tests. Below is the hose pressure testing apparatus and containment area with an unaged hose attached to the system.



Figure 1-41. HIHTL testing apparatus.

Baseline coupon tensile testing was conducted for both un-aged EPDM coupons and un-aged Garlock coupons. All procedures used for testing were derived from the ASTM standards and were recorded to provide consistency throughout all tensile testing experiments, for both EPDM and Garlock[®] material coupons. The following figure shows the un-aged EPDM coupon in the tensile testing machine before testing (left) and before rupture (right).



Figure 1-42. EPDM coupon testing.

Sample experimental data received from the un-aged EPDM coupons is shown below. The graph shows a force load curve representing the magnitude of the load versus the extension of the material.

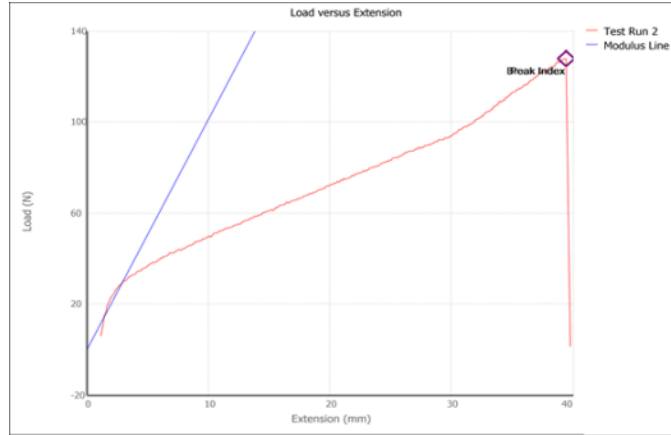


Figure 1-43. Load vs extension for EPDM.

Table 1-6 shows the average test results for peak stress, peak load, strain at break and modulus of elasticity for the un-aged EPDM coupons.

Table 1-6. Average Test Results from EPDM

Average Test Run Results - EPDM		
Display Name	Value	Unit
Peak Stress	0.002	kN/mm ²
Peak Load	0.13133	kN
Strain at Break	0.76367	mm/mm
Modulus	0.00833	kN/mm ²
Width	25	mm
Thickness	2.381	mm

Figure 1-44 shows the un-aged Garlock[®] coupon in the tensile testing machine before testing (left) and right after rupture (right).



Figure 1-44. Garlock coupon testing.

Typical experimental data obtained from the un-aged Garlock[®] coupons is shown below. The average test results for the un-aged Garlock[®] coupons is provided in Table 1-7.

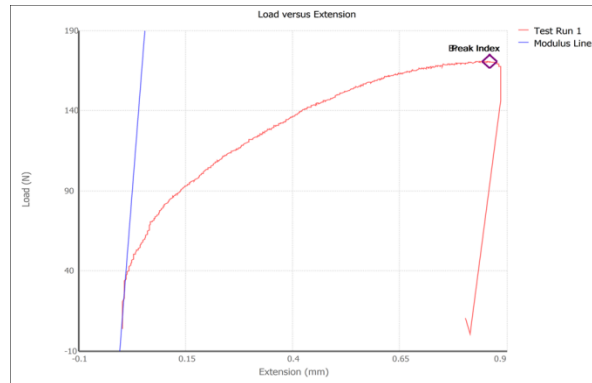


Figure 1-45. Load vs extension for Garlock[®].

Table 1-7. Average Test Results from Garlok[®] Coupons

Average Test Run Results - Garlock		
Display Name	Value	Unit
Peak Stress	0.003	kN/mm ²
Peak Load	0.17367	kN
Strain at Break	0.0167	mm/mm
Modulus	3.03967	kN/mm ²
Width	25	mm
Thickness	2.381	mm

Baseline pressure tests were conducted on hose-in-hose transfer lines (HIHTL), ethylene propylene diene monomer (EPDM) O-rings and Garlock[®] gaskets. In addition, hardness tests were conducted on EPDM and Garlock[®] material coupons.

HIHTL pressure tests involved pressurizing each test section at a constant rate until the hose ruptured. Baseline hose pressure testing was conducted on four hose specimens. The results as well as a photo of a typical failed hose specimen are shown below.

Table 1-8. Baseline HIHTL Pressure Test Results

	H-00-1	H-00-2	H-00-3	H-00-4	Average
Water Temperature (°F)	72.00	72.00	75.40	73.20	73.15
Ambient Temperature (°F)	67.00	66.00	81.00	86.00	75.00
Humidity %	37.00	36.00	67.00	60.00	50.00
Burst Pressure (psig)	2740.21	2925.95	2807.25	2747.90	2805.33
Type of Failure	Rupture	Rupture	Rupture	Rupture	N/A
Time Until Failure (s)	320.50	216.00	203.50	145.50	221.38
Start Length (in.)	29.75	30.25	30.25	30.00	30.0625
End Length (in.)	31.50	31.00	31.00	30.25	30.94
Deformation Length (in.)	1.75	0.75	0.75	0.25	0.875
Test Date	3/21/2016	3/21/2016	3/25/2016	3/25/2016	N/A

Each specimen experienced a rupture type of failure, with the average maximum pressure at 2805.33 psig. Each specimen also experienced a permanent deformation in their lengths, which averaged 0.875 inches.



Figure 1-46. Ruptured HIHTL test specimen.

The baseline O-ring pressure testing was conducted for three O-ring specimens. The test rig and the results of the testing are shown in Figure 1-47 and Table 1-9, respectively.



Figure 1-47. O-ring pressure test rig.

Table 1-9. Baseline O-ring Pressure Test Results

	O-00-1	O-00-2	O-00-3	Average
Water Temperature (°F)	73.20	77.50	76.20	75.63
Ambient Temperature (°F)	82.00	85.00	85.00	84.00
Humidity %	68.00	59.00	59.00	62.00
Holding Pressure (psig)	255.00	245.00	265.00	255.00
Pressure Maintained?	Yes	Yes	Yes	N/A
Time Until Failure (s)	N/A	N/A	N/A	N/A
Test Date	3/29/2016	3/29/2016	3/29/2016	N/A

Each specimen maintained the allotted pressure for the 5 minute time interval. The average pressure that the O-rings were maintained at was 255 psig, which was 20 psig over our original desired pressure. The change in the prescribed pressure was due to the large variations in our hand-pump.

The baseline gasket pressure testing was conducted for three gasket specimens. The test rig and the results of the testing are shown in Figure 1-48 and Table 1-10, respectively.



Figure 1-48. Gasket baseline pressure test rig.

Table 1-10. Baseline Gasket Pressure Test Results

	G-00-1	G-00-2	G-00-3	Average
Water Temperature (°F)	75.00	75.00	75.00	75.00
Ambient Temperature (°F)	79.00	78.00	78.00	78.33
Humidity %	50.00	54.00	52.00	52.00
Holding Pressure (psig)	166.75	149.89	148.30	154.98
Pressure Maintained?	Yes	Yes	Yes	N/A
Time Until Failure (s)	N/A	N/A	N/A	N/A
Test Date	4/4/2016	4/4/2016	4/4/2016	N/A

Each specimen maintained the allotted pressure for the 5 minute time interval. The average pressure that the gaskets were held at was 154.98 psig, which was only 5 psig over our desired pressure.

To assess the baseline material properties of Garlock[®], sheets of the material were obtained and coupon specimens were cut using a D412-C die. The specimens were used to determine hardness values obtained using a LECO LMV 50 Series hardness tester. To determine the material hardness, a load of 500 grams was used to create an indentation in the sample and hardness values according to the Rockwell scale and Vickers scale were obtained. Multiple measurements were taken from 3 different Garlock[®] specimens. These results and the corresponding averages are provided in Table 1-11. To obtain hardness measurements for the EPDM material, a different indenter probe is required and is currently being procured. Results for these tests will be provided when the probe is obtained.

Table 1-11. Baseline Coupon Hardness Test Results - Garlock[®] Data

Vickers	Rockwell HRB/HRC
4	54
3	54
4	54
4	54
4	54
4	54
4	54
4	54
4	54
4	54
5	54.1
5	54.1
AVERAGE VALUES	
4.09	54.02

Milestones and Deliverables

The milestones and deliverables for Project 1 for FIU Year 6 are shown on the following table. Milestone 2015-P1-M18.1.1 and its corresponding deliverable, development of a test plan for using SLIM to detect precursors to deep sludge gas release events (DSGRE's) was completed on January 22, 2016 and submitted to DOE EM. Milestone 2015-P1-M18.2.1, finalizing the design of refractory pad inspection tool, was completed on February 26, 2016 and submitted to DOE EM. Milestone 2015-P1-M18.2.3 and its corresponding deliverable, finalizing the design of the air supply line inspection tool, was completed on February 26, 2016 and submitted to DOE EM. Milestone 2015-P1-M19.1.1, down selection of alternative UT systems, was completed and the corresponding deliverable was submitted to site and DOE HQ contacts on March 11, 2016. Milestone 2015-P1-M19.2.2, complete the baseline testing on the nonmetallic materials, was completed on March 25, 2016. The corresponding deliverable was submitted to site and DOE HQ contacts on April 8, 2016.

FIU Year 6 Milestones and Deliverables for Project 1

Task	Milestone/ Deliverable	Description	Due Date	Status	OSTI
Task 17: Advanced Topics for Mixing Processes	2015-P1- M17.1.2	Complete validation of impingement correlations	05/6/2016	On Target	
	Deliverable	Draft Summary Report for Subtask 17.1.1	08/28/2016	On Target	OSTI
	Deliverable	Draft Summary Report for Subtask 17.1.2	05/6/2016	On Target	OSTI
Task 18: Technology Development and Instrumentation Evaluation	2015-P1- M18.1.1	Complete test plan for evaluating SLIM's ability to detect a precursor of DSGREs	12/18/2015	Complete	
	Deliverable	Draft Test Plan for Subtask 18.1.1	12/18/2015	Complete	OSTI
	2015-P1- M18.3.1	Complete test plan for temperature measurements using IR sensors	12/18/2015	Complete	
	2015-P1- M18.2.1	Finalize the design and construction of the refractory pad inspection tool	02/26/2016	Complete	
	2015-P1- M18.2.2	Complete engineering scale mock-up testing	08/28/2016	On Target	
	Deliverable	Draft Summary Report for Subtask 18.2.1 and 18.2.2	08/28/2016	On Target	OSTI
	2015-P1- M18.2.3	Finalize the design and construction of the air supply line inspection tool	02/26/2016	Complete	
	Deliverable	Draft Summary Report for Subtask 18.2.3	02/26/2016	Complete	OSTI

	Deliverable	Draft Summary Report for Subtask 18.3.1	07/29/2016	On Target	OSTI
Task 19: Pipeline Integrity and Analysis	2015-P1-M19.2.1	Complete test loop set up	11/20/2015	Complete	
	2015-P1-M19.1.1	Evaluate and down select alternative UT systems for bench scale testing	03/11/2016	Complete	
	Deliverable	Draft Summary document for Subtask 19.1.1	03/11/2016	Complete	OSTI
	2015-P1-M19.2.2	Complete baseline experimental testing	03/25/2016	Complete	
	Deliverable	Draft Summary Report for Subtask 19.2.2	04/8/2016	On Target	OSTI

Work Plan for Next Quarter

- Task 17:
 - FIU will continue to conduct QDNS simulations in three dimensional periodic domains. The effort will be focused in calculating the turbulent dissipation rate (TDR) during the DNS and RANS simulations of the same flow and investigate the differences between critical scalars, i.e., the TDR, shear rate and viscosity. The findings will pave the way to supply the RANS with additional information that can minimize the differences between the results of the RANS and DNS simulations. For this purpose we investigate all three regimes of the flow by using k-ε and DNS solver for laminar, transitional, and turbulent flows.
 - The results obtained from the simulation involving a curved surface jet impingement will be analyzed. The effect of different wall treatments and turbulence modeling on this simulation will be investigated. The entire study involving the applicability of Poreh’s correlation to the PJM’s will then be properly documented and submitted for publication approval.
- Task 18:
 - For the SLIM task next quarter, the remainder of the test plan will be executed with resulting images to be shared with Hanford and SRS engineers and scientists. Analysis of the data will also be completed. In terms of software, automation of the scanning of the sonar from a batch file and of the post-processing and 3D visualization of the resulting images and tank volume estimations will be tested over the next few months.
 - For the inspection tools, FIU will continue the design and manufacturing of the full scale mockup testbed. The mockup design will be extensively coordinated with WRPS, and extra care will be taken to assure a high correlation between the mockup and the proposed inspections at Hanford site.

- The peristaltic crawler will continue to be tested in existing pipelines at FIU. Some of the pipelines are corroded and have sitting water which emulates realistic conditions for the crawler to overcome. Improvements will be incorporated to the design as needed. Improvements on the instrumentation and the software infrastructure will also be incorporated. The use of a force sensitive resistor planted to the claw pads is being considered. This addition would provide gripping and sliding feedback throughout the mockup tests and inspections.
- For the miniature magnetic rover, FIU will continue to investigate design modifications to allow for sharper turns in the refractory channels. We will also investigate cable management systems for the tether. Versatility of the unit will be evaluated by testing the system in typical 3- and 4-inch diameter pipes.
- The Raytek sensor has been procured, calibrated and bench scale testing has been initiated. Additional tests will be conducted on the carbon steel tank as a mock up. A full-scale test bed resembling the actual DST's at Hanford is being fabricated at FIU-ARC, which will be used to conduct the engineering scale tests using the Raytek IR sensor. This would include various set points according to the previously specified test matrix along with the installation of thermocouples.

Task 19:

- Viable options for the UT sensor systems have been investigated and two of them have been down selected. Due to the expense of the data acquisition systems, leasing options are being investigated. Once acquired, the systems will be calibrated and tested on a full scale engineering test set up (resembling the DST's at Hanford) being fabricated at FIU-ARC.
- For the non-metallic materials task, efforts during the next quarter will include installing a pressure transducer, flow meter and a thermocouple on each of the three loops. This will allow the measurement and recording of the pressure, flow rate and temperature in each loop as requested by site personnel during a meeting at FIU. After the installation of the instruments is completed aging of the specimens will commence.

Project 2

Environmental Remediation Science and Technology

Project Description

This project will be conducted in close collaboration between FIU, Hanford Site, Savannah River Site, and the Waste Isolation Pilot Plant (WIPP) scientists and engineers in order to plan and execute research that supports the resolution of critical science and engineering needs, leading to a better understanding of the long-term behavior of contaminants in the subsurface. Research involves novel analytical methods and microscopy techniques for characterization of various mineral and microbial samples. Tasks include studies which predict the behavior and fate of radionuclides that can potentially contaminate the groundwater system in the Hanford Site 200 Area; laboratory batch and column experiments, which provide relevant data for modeling of the migration and distribution of natural organic matter injected into subsurface systems in the SRS F/H Area; laboratory experiments investigating the behavior of the actinide elements in high ionic strength systems relevant to the Waste Isolation Pilot Plant; surface water modeling of Tims Branch at SRS supported by the application of GIS technology for storage and geoprocessing of spatial and temporal data;

The following tasks are included in FIU Year 6:

Task No	Task
Task 1: Remediation Research and Technical Support for the Hanford Site	
Subtask 1.1	Sequestering uranium at the Hanford 200 Area vadose zone by in situ subsurface pH manipulation using NH ₃ gas
Subtask 1.2	Investigation of microbial-meta-autunite interactions - effect of bicarbonate and calcium ions
Subtask 1.3	Evaluation of ammonia fate and biological contributions during and after ammonia injection for uranium treatment
Task 2: Remediation Research and Technical Support for Savannah River Site	
Subtask 2.1	FIU's support for groundwater remediation at SRS F/H Area
Subtask 2.2	Monitoring of U(VI) bioreduction after ARCADIS demonstration at the SRS F-Area
Subtask 2.3	Humic acid batch sorption experiments into the SRS soil
Subtask 2.4	The synergetic effect of HA and Si on the removal of U(VI)
Subtask 2.5	Investigation of the migration and distribution of natural organic matter injected into subsurface systems
Task 3: Surface Water Modeling of Tims Branch	
Subtask.3.1	Modeling of surface water and sediment transport in the Tims Branch ecosystem
Subtask 3.2	Application of GIS technologies for hydrological modeling support
Subtask 3.3	Biota, biofilm, water and sediment sampling in Tims Branch

Task 4: Sustainability Plan for the A/M Area Groundwater Remediation System	
Subtask 4.1	Sustainable Remediation Analysis of the M1 Air Stripper
Subtask 4.2	Sustainable Remediation Support to DOE EM Student Challenge
Task 5: Remediation Research and Technical Support for WIPP	

Task 1: Remediation Research and Technical Support for the Hanford Site

Task 1 Overview

The radioactive contamination at the Hanford Site created plumes that threaten groundwater quality due to potential downward migration through the unsaturated vadose zone. FIU is supporting basic research into the sequestration of radionuclides such as uranium in the vadose zone, which is more cost effective than groundwater remediation. One technology under consideration to control U(VI) mobility in the Hanford vadose zone is a manipulation of sediment pH via ammonia gas injection to create alkaline conditions in the uranium-contaminated sediment. Another technology need for the ammonia remediation method is to investigate the potential biological and physical mechanisms associated with the fate of ammonia after injection into the unsaturated subsurface.

Task 1 Quarterly Progress

Subtask 1.1. Sequestering Uranium at the Hanford 200 Area Vadose Zone by In Situ Subsurface pH Manipulation Using NH₃ Gas

During the months of January through March, FIU conducted several isopiestic measurements of U-bearing samples. Measurements taken based on the calcium chloride standard indicated that the humidity level in the isopiestic chamber reached 87%. There is a change in slope that appears indicative of the transition from a solid to a solid + liquid system. FIU changed a crucible with the CaCl₂ standard solution due to the rusty spots on the walls of nickel crucibles.

The draft paper titled “*Characterization of U(VI)-Bearing Precipitates Produced by Ammonia Gas Injection Technology*” for the 2015 Waste Management Symposium oral presentation was completed and after minor changes based on the reviewers comments was accepted as a final version.

FIU also worked on corrections for the manuscript titled “*The effect of Si and Al concentrations on the removal of U(VI) in the alkaline conditions created by NH₃ gas*” to prepare it for submission to a peer-reviewed journal. The objective of this manuscript is to present results on uranium removal efficiencies in the alkaline synthetic porewater solutions prepared in a broad range of Si, Al, and bicarbonate concentrations typically present in field systems of the western U.S. regions and identify solid uranium-bearing phases that result from ammonia gas treatment. The manuscript was submitted to the Applied Geochemistry Journal.

FIU initiated geochemical equilibrium modeling via Geochemist's Workbench (GWB) 10.0 (Bethke, University of Illinois) software for the Ca-amended samples to predict the formation of uranium aqueous species and solid phases likely to be present as a result of NH₃ gas injections in the synthetic porewater solutions.

FIU started preparations for the sequential liquid extraction experiments to investigate the stability of precipitates created after ammonia gas injections. The protocol for the extractions follows the Jim Szecsody's protocol (Szecsody et al., 2015) for future cross-referencing of the results. Each step of the sequential extraction experiments will be conducted on samples that consist of approximately 20 mg of the precipitate mixed with 0.25 mL of liquid. The first two phases in the sequential extraction target water soluble and adsorbed/exchangeable uranium phases. The remaining four extractions define the harder to extract uranium minerals or coated surface phases. The extraction procedures consist of the following 6 steps (Szecsody et al., 2015):

1. Aqueous uranium by addition of a synthetic groundwater solution
2. Adsorbed uranium phases by 0.0144M NaHCO₃ + 0.028M Na₂CO₃ (pH 9.3, 1h)
3. 1M Na-acetate to dissolve some U-carbonates (1 h)
4. Acetic acid (pH 2.3, 5 days) to dissolve most U-carbonates and hydrated U silicates
5. 8M nitric acid (HNO₃) (95°C, 2 h) to dissolve hard-to-extract U-phases.
6. A 14mM carbonate solution at pH 9.3 (0.0144M NaHCO₃ + 0.028M Na₂CO₃) for 60 days in a parallel extraction to measure the U at long term.

The initial sequential extraction experiments will be carried out on six sample compositions. The preparation of samples is ongoing and the compositions will include silica (50 mM), aluminum (5 mM), low bicarbonate concentrations (3 mM) and high bicarbonate concentrations (50 mM), a range of calcium concentrations (0, 5 and 10 mM), and 2 ppm uranium. During this month, preparations for 12 duplicate samples were initiated. The composition of samples was previously reported in the most recent Year End Report (Lagos et al., 2015). Extractions will be conducted on samples prepared by using vacuum filtration via 0.2µm filter as well as unfiltered samples.

Sample Preparation

The sample preparation follows the same procedures reported in the Year End Report (Lagos et al., 2015). During preparation of the samples, the amount of nitric acid (HNO₃) used to adjust the sample pH and the flow rate of NH₃ gas injected were recorded. Forty (40) mL of each synthetic pore water solution were prepared and injected with NH₃ gas until the pH reached approximately 11.02. Ten (10) mL aliquots of the 40 mL synthetic pore water solutions were dispensed into 15-mL sample vials. The samples were completed by adding the appropriate volume of concentrated CaCl₂ solution (0, 100, and 200 µL), and a constant volume of UO₂(NO₃)₂ (200 µl) to reach 0 mM, 5 mM and 10 mM of Ca and 2 ppm of U(VI) in the solution mixtures. A total of 24 samples (filtered and unfiltered) were prepared. All prepared samples were left under the hood to allow the ammonia gas to evaporate and to settle any precipitate. The volume of the prepared samples was estimated to be enough to use in the future dissolution experiments.

In addition, a set of 12 duplicate 3-mL samples were prepared to be analyzed by SEM-EDS. The sample preparation follows previous procedures except that they were prepared with a uranium concentration of the 500 ppm in order to be able to observe U(VI) via EDS.

Table 2-1. Sample Preparation Calculations to Prepare 10 mL of Each Sample (50mM Si + 5mM Al + Low 3mM and High 50mM HCO₃ + 0, 5 and 10mM Ca)

#	Sample ID	HCO ₃ (mM)	Ca (mM)	Solution (μL)	Ca Injected (μL)	U Injected (μL)
UNFILTERED						
1	50Si + 5Al + 3HCO ₃ + 0Ca + 2 ppm U	3	0	9800	0	200
2	50Si + 5Al + 3HCO ₃ + 5Ca + 2 ppm U		5	9700	100	200
3	50Si + 5Al + 3HCO ₃ + 10Ca + 2 ppm U		10	9600	200	200
4	50Si + 5Al + 50HCO ₃ + 0Ca + 2 ppm U	50	0	9800	0	200
5	50Si + 5Al + 50HCO ₃ + 5Ca + 2 ppm U		5	9700	100	200
6	50Si + 5Al + 50HCO ₃ + 10Ca + 2 ppm U		10	9600	200	200
FILTERED						
7	50Si + 5Al + 3HCO ₃ + 0Ca + 2 ppm U	3	0	9800	0	200
8	50Si + 5Al + 3HCO ₃ + 5Ca + 2 ppm U		5	9700	100	200
9	50Si + 5Al + 3HCO ₃ + 10Ca + 2 ppm U		10	9600	200	200
10	50Si + 5Al + 50HCO ₃ + 0Ca + 2 ppm U	50	0	9800	0	200
11	50Si + 5Al + 50HCO ₃ + 5Ca + 2 ppm U		5	9700	100	200
12	50Si + 5Al + 50HCO ₃ + 10Ca + 2 ppm U		10	9600	200	200

Table 2-2. Sample Preparation Calculations to Prepare 3 mL of Each Sample Using a Stock Solution of U (266 mg in 5.044 mL) and (50mM Si + 5mM Al + Low 3mM and High 50mM HCO₃ + 0, 5 and 10mM Ca) For Scanned Electron Microscope (SEM) - Elemental Analysis (EDS)

Sample ID	HCO ₃ (mM)	Ca (mM)	Solution (μL)	Ca Injected (μL)	U Injected (μL)
UNFILTERED					
50Si + 5Al + 3HCO ₃ + 0Ca + 500ppm U	3	0	2971.6	0	28.4
50Si + 5Al + 3HCO ₃ + 5Ca + 500ppm U		5	2941.6	30	28.4
50Si + 5Al + 3HCO ₃ + 10Ca + 500ppm U		10	2911.6	60	28.4
50Si + 5Al + 50HCO ₃ + 0Ca + 500ppm U	50	0	2971.6	0	28.4
50Si + 5Al + 50HCO ₃ + 5Ca + 500ppm U		5	2941.6	30	28.4
50Si + 5Al + 50HCO ₃ + 10Ca + 500ppm U		10	2911.6	60	28.4
FILTERED					
50Si + 5Al + 3HCO ₃ + 0Ca + 500ppm U	3	0	2971.6	0	28.4
50Si + 5Al + 3HCO ₃ + 5Ca + 500ppm U		5	2941.6	30	28.4
50Si + 5Al + 3HCO ₃ + 10Ca + 500ppm U		10	2911.6	60	28.4
50Si + 5Al + 50HCO ₃ + 0Ca + 500ppm U	50	0	2971.6	0	28.4
50Si + 5Al + 50HCO ₃ + 5Ca + 500ppm U		5	2941.6	30	28.4
50Si + 5Al + 50HCO ₃ + 10Ca + 500ppm U		10	2911.6	60	28.4

The evaluation of scanning electron microscope imaging and energy dispersive spectroscopy data continued in order to come to a conclusion on what samples would be selected for further analysis. A viscous resin and hardener were purchased for cold mounting samples in epoxy in preparation for solid phase analysis. The radioactive nature of the samples requires that the polishing and grinding of mounted samples be completed using a facility furnished with the necessary radiation-authorized equipment. The samples, once mounted in epoxy, will be shipped to collaborators at PNNL for grinding and polishing before moving on to electron microprobe analysis. The analyses of the most recent set of samples were continued with the KPA analysis of the filtered sample supernatant solutions and DI-water rinses. The resultant data provided the concentration of uranium retained in the supernatant solutions which will in turn be used to estimate the concentration of uranium precipitated from the samples. Organized into a surface response diagram, the concentrations of uranium show a clear positive correlation with increasing bicarbonate concentration (Figure 2-1). This trend supports the assumption that low bicarbonate samples would see the most uranium in their precipitate phases.

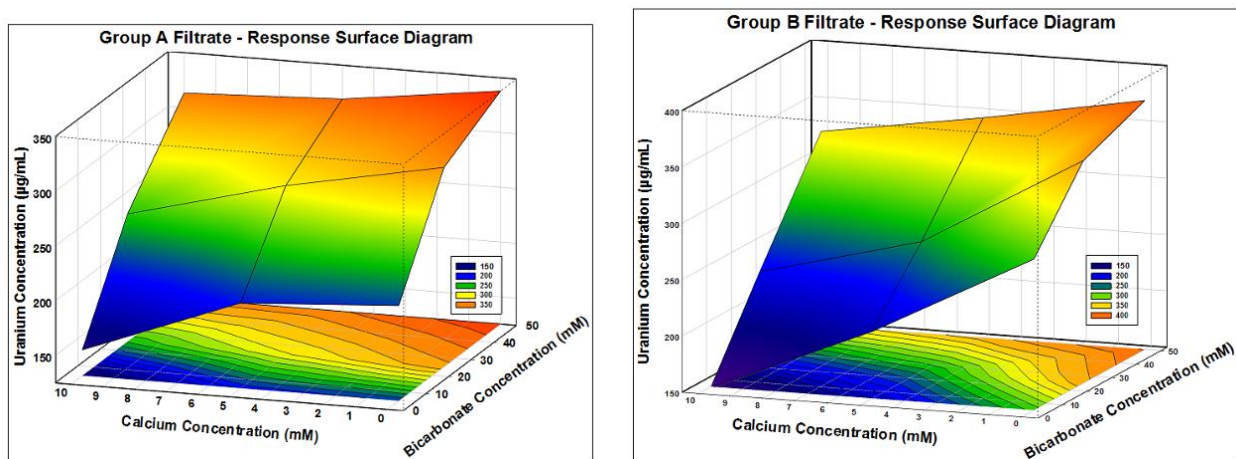


Figure 2-1. Response surface diagrams displaying filtrate solution uranium retention for the original (Group A) and duplicate (Group B) samples.

The sample rinse was intended to wash away any soluble uranium phases formed on the surface of the Group B precipitates. The KPA analysis of these solutions resulted in uranium concentrations ranging from 15 to 56 ppm (Figure 2-2). These concentrations assume no analyte is lost to the filter.

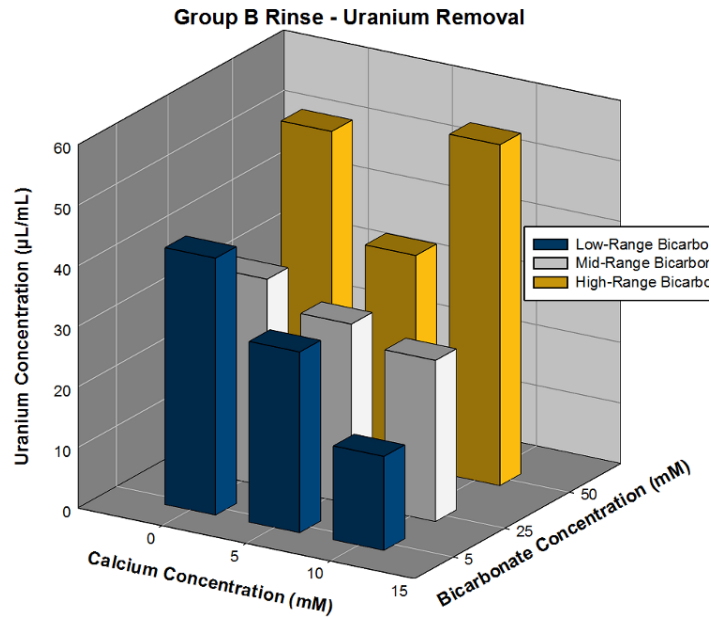


Figure 2-2. Uranium removed with the Group B rinse.

Continuing forward, the analyte concentrations and mass will be used to estimate the total uranium yield in the precipitate phase. The supernatant filtrates will be analyzed by ICP-OES to determine the quantity that has been retained that was precipitated out. Additionally, select samples will be loaded in epoxy for solid phase analysis.

In the month of March, FIU completed preparations for the sequential liquid extraction experiments to investigate the stability of precipitates created after ammonia gas injections. A total of 24 samples (duplicate filtered and unfiltered) were prepared. The protocol for the extractions will follow Jim Szecsody's protocol (Szecsody et al., 2015) for future cross-referencing of the results. The solid:solution ratio for each step of the sequential extraction experiments will be 1:15 to ensure that U measurements are within detection limits of the KPA instrument. The solid:solution ratio can be changed based on the experimental observations. The first two phases in the sequential extraction target water soluble and adsorbed/exchangeable uranium phases. Carbonate extractions using the acetic acid at pH 2.3 are based on ensuring the pH stays at 2.3 as all the carbonate in the sample dissolves. The remaining two extractions define the harder to extract uranium minerals or coated surface phases

The initial sequential extraction experiments will be carried out on six sample compositions as shown below.

50 mM Si + 5 mM Al + 3 mM HCO ₃ + 0 mM Ca + 2 ppm U
50 mM Si + 5 mM Al + 3 mM HCO ₃ + 5 mM Ca + 2 ppm U
50 mM Si + 5 mM Al + 3 mM HCO ₃ + 10 mM Ca + 2 ppm U
50 mM Si + 5 mM Al + 50 mM HCO ₃ + 0 mM Ca + 2 ppm U
50 mM Si + 5 mM Al + 50 mM HCO ₃ + 5 mM Ca + 2 ppm U
50 mM Si + 5 mM Al + 50 mM HCO ₃ + 10 mM Ca + 2 ppm U

The preparation of samples is completed; the compositions include silica (50 mM), aluminum (5 mM), low bicarbonate concentrations (3 mM) and high bicarbonate concentrations (50 mM), a range of calcium concentrations (0, 5 and 10 mM), and 2 ppm uranium. Extractions were conducted on samples prepared by using vacuum filtration with a 0.2µm filter as well as unfiltered samples after sample centrifugation.

SEM/EDS analyses were conducted on selected samples using a backscattered mode (Figure 2-3).

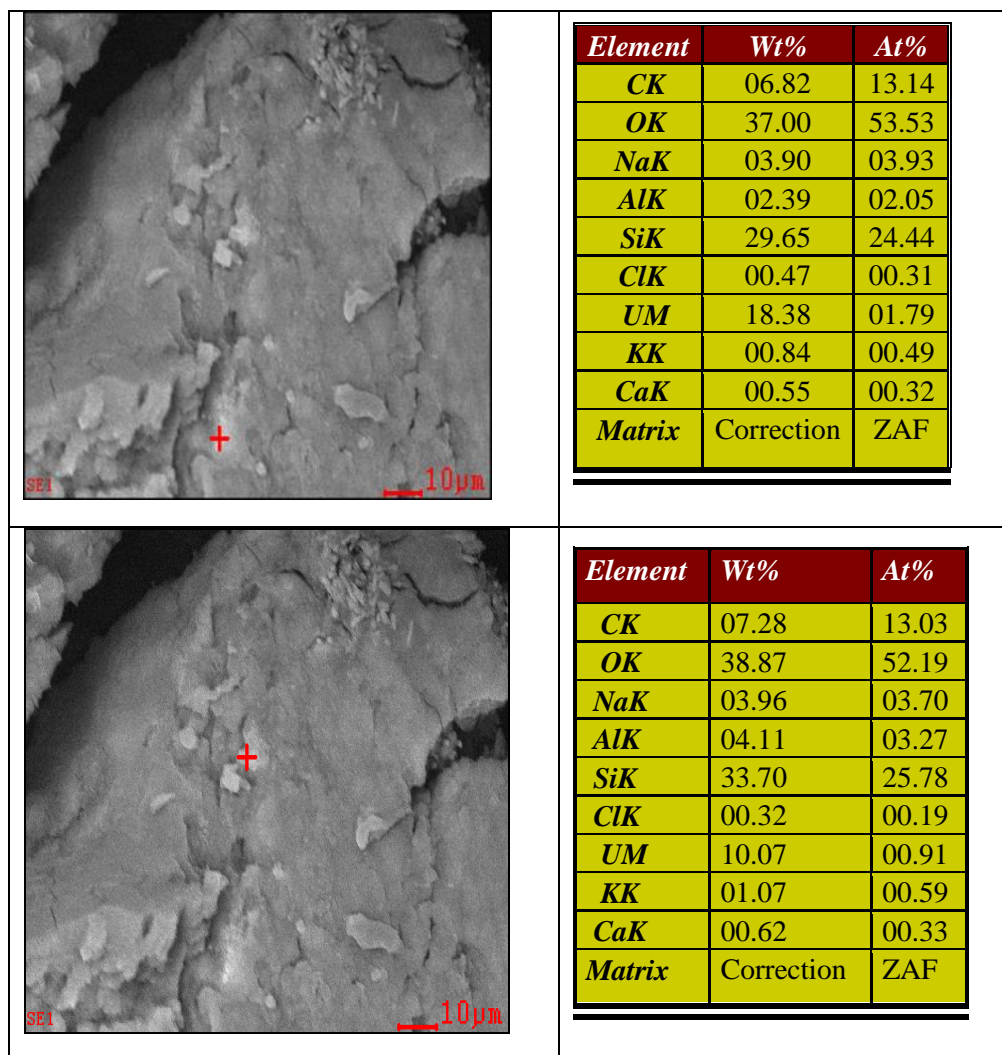


Figure 2-3. SEM/EDS analysis for samples composed of 50 mM Si + 5 mM Al + 3 mM HCO₃ + 5 mM Ca + 500 ppm of U(VI).

Analysis presents evidence that “hot” spots are high in Si and U. No crystals were observed compared to previous non-filtered sample preparation.

Sample analysis moved forward with the preparation of epoxy molds for mounting sample precipitates for further analysis. A 15 mL 2:1 mixture of resin and hardener was prepared and cured overnight to produce a cylindrical epoxy mold. A quarter inch hole was drilled through the center of the mold (Figure 2-2a), where the sample would reside and bulk of analysis would take place. Solid samples were crushed using a disposable vial, sealed with wax paper, and plastic rod

as mortar and pestle (Figure 2-5). The pulverized sample was mixed with a small volume of epoxy and mixed before being poured into the drilled out mold. This was, once again, allowed to cure at room temperature overnight (Figure 2-4b).

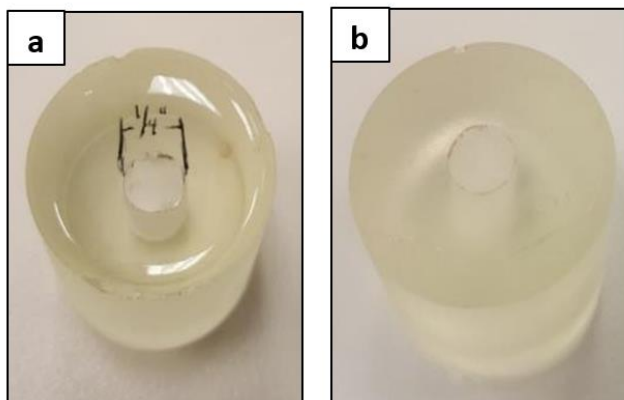


Figure 2-4. Epoxy mold before (a) and after (b) filling with resin+sample mixture.



Figure 2-5. Crushed sample precipitate.

DOE Fellow Robert Lapierre presented a poster during the Waste Management Symposia student poster competition session titled, “The characterization of uranium phases produced by the NH_3 injection remediation method under Hanford 200 area conditions,” based on the research he is conducting for the task. Robert also gave a professional oral presentation for the paper published in the conference proceedings titled, “Characterization of U(VI)-Bearing Precipitates Produced by Ammonia Gas Injection Technology into Unsaturated Sediments,” prepared by R. Lapierre, Y. Katsenovich, L. Lagos.

Subtask 1.2. Investigation on Microbial-Meta-Autunite Interactions - Effect of Bicarbonate and Calcium Ions

FIU paper titled “*The Effect of Bicarbonate on Autunite Dissolution in the Presence of Shewanella Oneidensis under Oxygen Restricted Conditions*” was accepted as-is for the publication in the WM-2016 proceedings and the authors initiated preparing a presentation for the conference.

In January 2016, FIU evaluated data on the direct visual cell counting using a hemocytometer combined with cell viability analysis using the spread plate method that was conducted for each sampling event. The initial inoculation cell density was 10^6 cells/mL (log 6 cells/mL) for all biotic samples. In bicarbonate-free samples, cell densities for the duration of the experiment showed almost no change from the initial concentration (Figure 2-6). In contrast, samples amended with 3 mM and 10 mM of bicarbonate demonstrated almost 10-14 fold increases in cell

density and values stabilized in the range of log 6.9 to log 7.3 cell/mL by the end of the experiment (Figure 2-7).

Cell viability, determined via counts of colony forming units (CFU/mL), was compared to the cell density obtained via direct cell counting. Samples containing 0 mM bicarbonate yielded an average of about 11.1% of viable cells out of a total cell density that correlates to only $1.1^5 \pm 1.0^5$ CFU/mL. In addition, viable cells showed a tendency to decrease with time. In samples amended with 3 mM and 10 mM of HCO_3^- , the ratio between viable cells and total cell density increased to 30-31%. Since the cell density in bicarbonate-amended solutions increased in average to 1.0^7 - 1.4^7 cells/mL, the quantity of viable cells was determined to be on the order of 2.2^6 - 2.3^6 CFU/mL, which is significantly higher than was observed in the bicarbonate-free solutions. The increase in total cell density and the quantity of viable cells might be an indication that the cells have acclimated to withstand uranium toxicity in the presence of bicarbonate ions. Figure 2-7 presents results for the total cell density versus viable cells for the three bicarbonate concentrations tested.

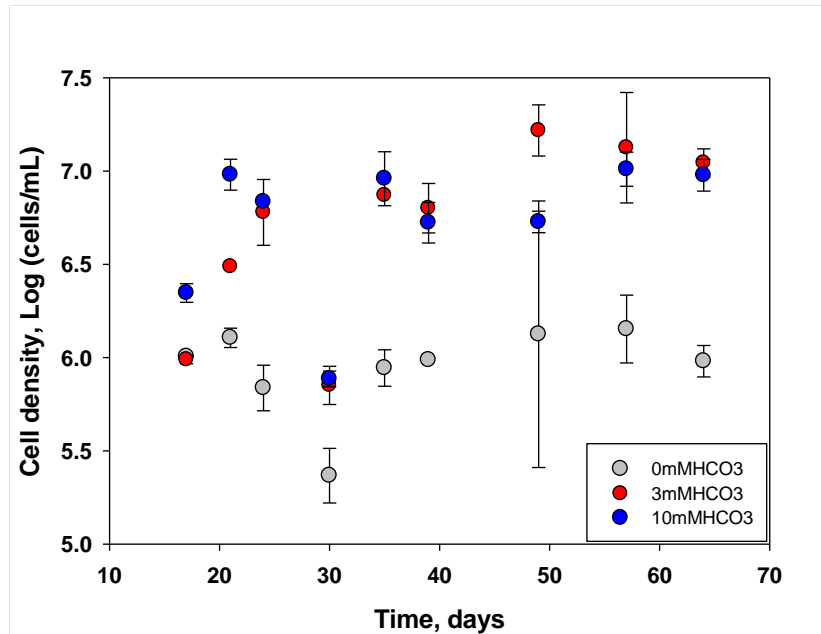


Figure 2-6. Changes in the direct cell counts for samples containing varying concentrations of bicarbonate.

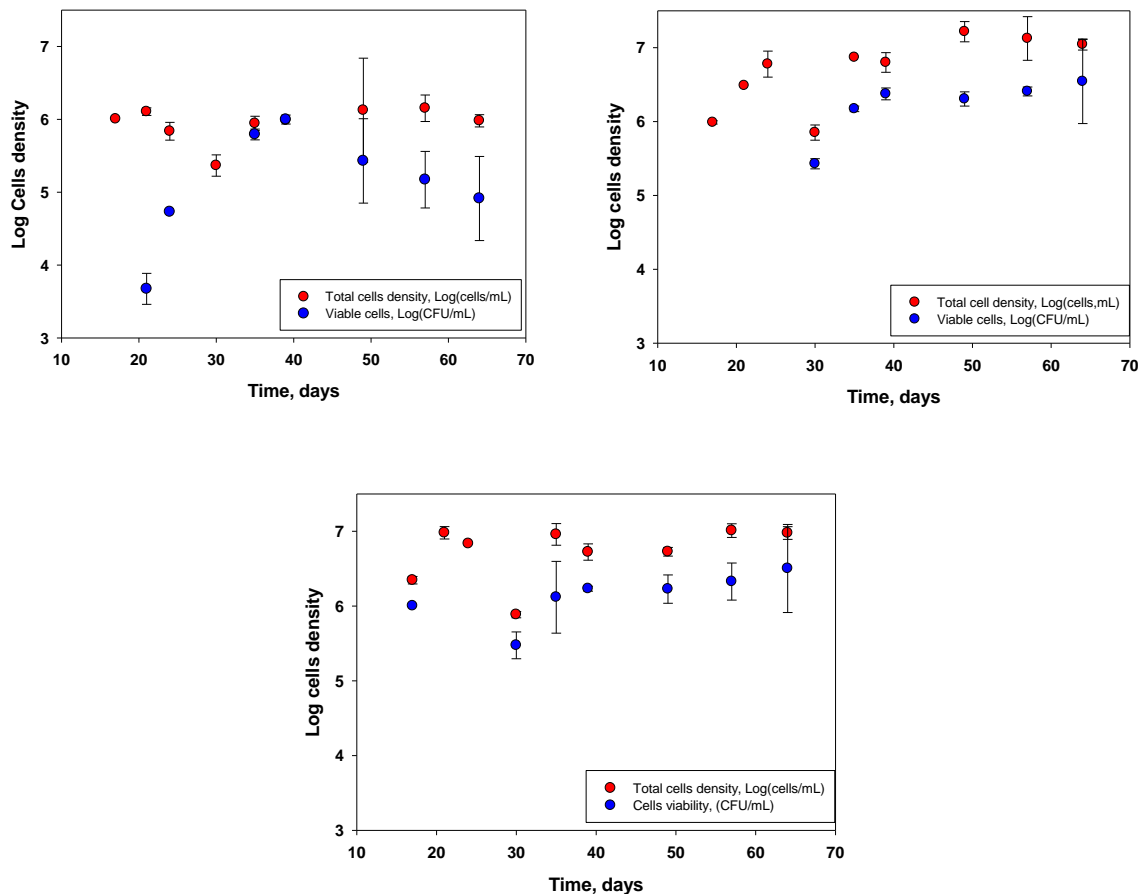


Figure 2-7. Results for the total cell density versus viable cells for a) 0 mM HCO₃⁻; b) 3 mM HCO₃⁻; c) 10 mM HCO₃⁻.

During the month of February, FIU completed a presentation titled, “The Effect of Bicarbonate on Autunite Dissolution in the Presence of *Shewanella Oneidensis* under Oxygen Restricted Conditions,” and uploaded it to the Waste Management Symposia website.

During this period, calculations were performed by means of speciation software (Visual Minteq and Hydra) to predict uranium speciation and the formation of the secondary minerals under the experimental conditions tested (Table 2-3). As can be seen, the saturation of hydroxylapatite (calcium phosphate mineral) and uranyl-phosphate minerals is predicted in all cases. Nevertheless, the elemental analysis results did not reveal a decrease in any of these elements throughout the duration of the experiment; on the contrary, uranium, calcium and phosphorous seem to be unaffected. A decrease in the concentration of these elements could be associated with the formation of secondary minerals (and bioreduction, only in the case of uranium). A possible explanation could be that the rate of release of these elements in the aqueous phase is very similar to the rate of micro-precipitation of secondary minerals, which removes these elements from the aqueous phase; hence, the apparent concentration of these elements remains the same.

**Table 2-3. Soluble and Saturated Species for All Three Conditions Studied
(bicarbonate-free samples and samples amended with 3 and 10 mM bicarbonate)**

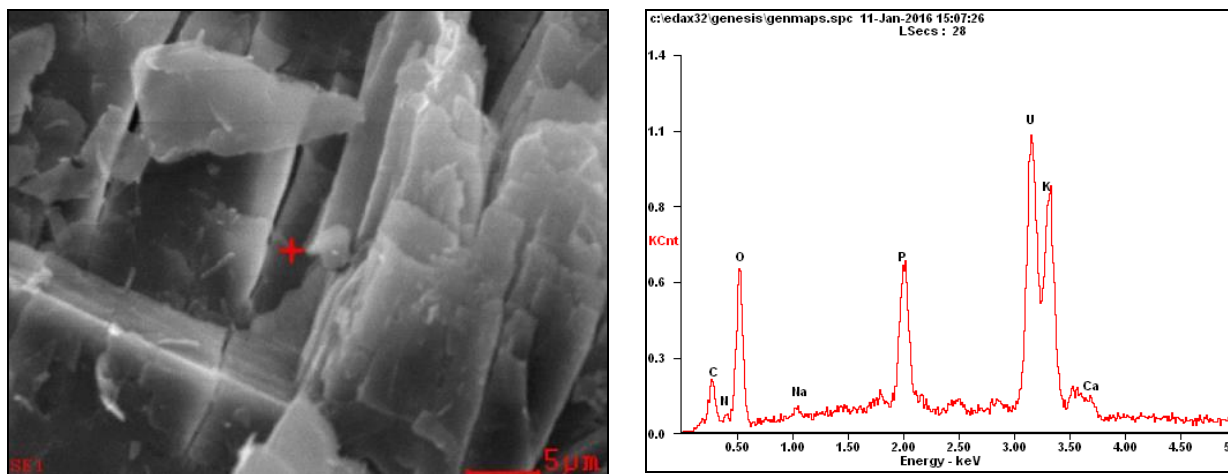
0 mM bicarbonate		3 mM bicarbonate		10 mM bicarbonate	
Soluble	Precipitates	Soluble	Precipitates	Soluble	Precipitates
20% UO ₂ HPO ₄	Hydroxylapatite	50% Ca ₂ UO ₂ (CO ₃) ₃	Hydroxylapatite	92% UO ₂ (CO ₃) ₃ ⁻⁴	Hydroxylapatite
80% UO ₂ PO ₄ ⁻	Uranyl-phosphate	44% CaUO ₂ (CO ₃) ₃ ⁻²	Uranyl-phosphate	6% CaUO ₂ (CO ₃) ₃ ⁻²	Uranyl-phosphate
	autunite	~6% negatively charged uranyl carbonate complexes	autunite		autunite

On the other hand, the soluble species are primarily negatively charged entities in the case of bicarbonate-free samples and samples that contain 10 mM bicarbonate; whereas in the case of samples amended with 3 mM bicarbonate, the negatively charged and the neutral U(VI) complexes are almost 50-50%. It has been suggested in the literature that negatively charged uranyl complexes are less bioavailable to the cells and are the least readily reducible fraction, mostly due to electrostatic repulsions between negatively charged uranyl complexes and the bacterial cell surface (Belli et al., 2015; Sheng & Fein, 2014). This scenario provides an additional potential explanation for the absence of bioreduction, especially in the case of bicarbonate-free samples and samples amended with 10 mM bicarbonate, where the majority of uranyl complexes are negatively charged. On the other hand, the point of zero charge (pzc) of autunite is 5-6 (Wellman et al., 2007), which makes the net surface charge of autunite at pH 7.5 negative. Hence, one would expect electrostatic repulsion between negatively charged bacterial surfaces and the autunite surface. Bacteria were detected on the surface of autunite in the samples amended with 3 and 10 mM bicarbonate, implying that under phosphorus-limiting conditions, bacteria may overcome the electrostatic repulsion and liberate P from uranyl mineral phases to meet metabolic needs. It is not clear though to what degree this takes place, since the amount of bacteria detected on the surface was not very high.

FIU completed a progress report on this task and sent it as a deliverable to the DOE EM HQ and PNNL site contacts on February 15, 2016.

In March 2016, FIU evaluated data from scanning electron microscopy – energy dispersion spectroscopy (SEM-EDS), in an effort to provide further understanding on the microbial-autunite interactions. Images of autunite solids taken by means of SEM revealed the destruction of autunite as a consequence of bicarbonate effect and bacterial activity (Figure 2-8). In the bicarbonate-free samples, no bacteria were observed on the autunite surface. This finding may

explain the fact that there was not any uranium release in the aqueous phase due to bacterial activity in the bicarbonate-free samples. On the other hand, bacteria were clearly observed on the mineral's surface in the case of samples amended with 3 mM and 10 mM bicarbonate (Figure 2-9). Bacteria can attach on the mineral surfaces through specific structures called extracellular polymeric substances (EPS), comprised mostly of saccharides and proteins and secondarily DNA and lipids (Donlan, 2002). Nevertheless, no extensive biofilm (covering most of the surface or creating vertical multilayer formations) was observed in these samples. The formation of an extensive film has been reported to be crucial for metal reduction by *Shewanella* and is regulated by the presence of oxygen (McLean et al., 2008; Wu et al., 2013). FIU experiments were performed in the absence of oxygen; hence, the absence of an extensive biofilm, as well as bioreduction, may be justifiable.



<i>Element</i>	<i>Wt%</i>	<i>At%</i>
<i>CK</i>	05.37	14.41
<i>NK</i>	03.83	08.83
<i>OK</i>	28.18	56.83
<i>NaK</i>	01.01	01.42
<i>PK</i>	07.04	07.33
<i>UM</i>	49.05	06.65
<i>KK</i>	04.19	03.45
<i>CaK</i>	01.34	01.08
<i>Matrix</i>	Correction	ZAF

Figure 2-8. SEM image revealing structural damage of autunite and associated elemental composition by EDS analysis.

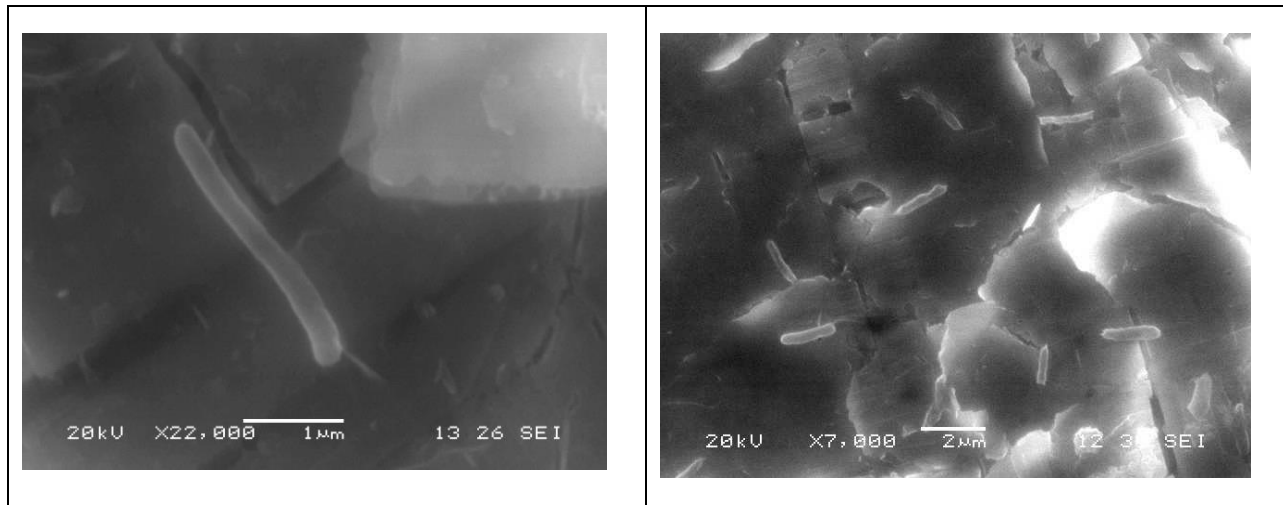


Figure 2-9. *Shewanella* cells attached to the surface of autunite.

A study by Thormann investigated the biofilm formation by *Shewanella* and reported the formation of a layer of biofilm initially until reaching full coverage of the surface and, subsequently, the formation of vertical towering biofilm structures (Thormann et al., 2004). Furthermore, acetate and lactate have been reported to be less effective stimulants for U(VI) reduction, whereas more complex organic electron donors have been directly correlated to the ability of dissimilatory metal-reducing bacteria (DMRB) to reduce U(VI) (Barlett, 2014).

The SEM photos also revealed the formation of secondary minerals, mainly uranyl phosphates and uranyl carbonates, coating the surface of autunite (Figure 2-10). These secondary minerals are a result of saturation of the aqueous phase due to the release of uranium, calcium and phosphorous under the conditions studied.

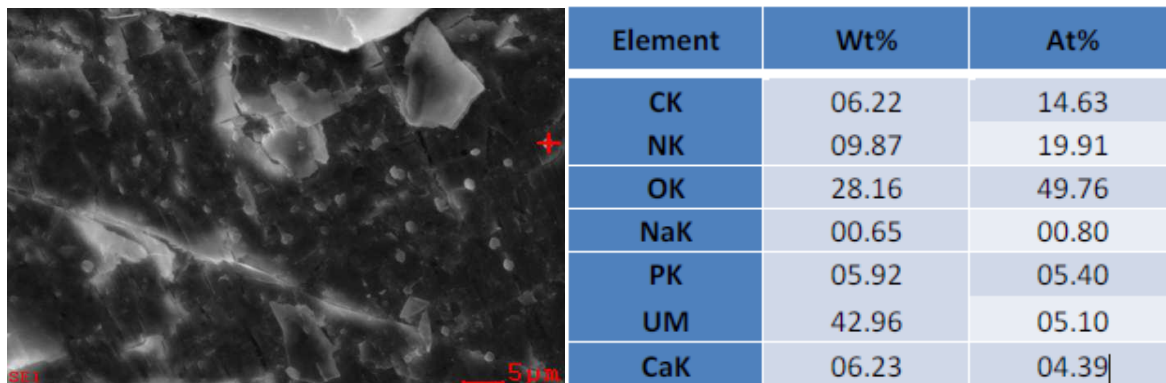


Figure 2-10. Secondary mineral particles coating on the surface of autunite and EDS analysis.

A paper titled, “The effect of bicarbonate on autunite dissolution in the presence of *Shewanella oneidensis* under oxygen restricted conditions” prepared by Drs. Y. Katsenovich, V. Anagnostopoulos, Hope Lee (PNNL), Brady Lee (PNNL), Shonali Laha (FIU-EED) and graduate student Sandra Herrera was presented in Section 10 at the WM 2016 conference.

References:

Barlett, M. 2014. Uranium reduction and microbial community development in response to stimulation with different electron donors.

Donlan, R.M. 2002. Biofilms: Microbial Life on Surfaces. in: *Emerg Infect Dis*, Vol. 8.

McLean, J.S., Pinchuk, G.E., Geydebekht, O.V., Bilskis, C.L., Zakrajsek, B.A., Hill, E.A., Saffarini, D.A., Romine, M.F., Gorby, Y.A., Fredrickson, J.K., Beliaev, A.S. 2008. Oxygen-dependent autoaggregation in *Shewanella oneidensis* MR-1. *Environmental Microbiology*, **10**(7), 1861-1876.

Thormann, K.M., Saville, R.M., Shukla, S., Pelletier, D.A., Spormann, A.M. 2004. Initial Phases of Biofilm Formation in *Shewanella oneidensis* MR-1. *Journal of Bacteriology*, **186**(23), 8096-8104.

Wu, C., Cheng, Y.-Y., Yin, H., Song, X.-N., Li, W.-W., Zhou, X.-X., Zhao, L.-P., Tian, L.-J., Han, J.-C., Yu, H.-Q. 2013. Oxygen promotes biofilm formation of *Shewanella putrefaciens* CN32 through a diguanylate cyclase and an adhesin. *Scientific Reports*, **3**, 1945.

Subtask 1.3. Evaluation of Ammonia Fate and Biological Contributions During and After Ammonia Injection for Uranium Treatment

Subtask 1.3.1: Investigation of NH₃ partitioning in relevant Hanford minerals and synthetic porewater

During the months of January through March, batch experiments continued investigating the effects of pH increase by either NaOH or NH₄OH on uranium sorption and kaolinite/illite/montmorillonite mineral dissolution. Data was presented for both synthetic porewater and similar ionic strength in NaCl for samples equilibrated at pH 7.5 to mimic the natural groundwater at Hanford and then increased to pH 11.5 by either NaOH or NH₄OH. These batch samples follow the protocols outlined in the October and November 2015 monthly reports. It should be noted that uranium removal from the aqueous phase is represented by apparent K_d values which, in this system, likely represent both sorption and precipitation processes.

Sequential extractions were also begun on kaolinite and batch experiments were continued to investigate the effects of pH increase by either NaOH or NH₄OH on uranium sorption and illite and montmorillonite mineral dissolution in NaCl electrolyte. The batch samples prepared for sequential extractions were initially equilibrated for >30 days. The initial equilibrium sorption and mineral dissolution results are presented below. However, extraction steps 1 to 4 have also been completed and are awaiting analysis. In addition, aqueous U speciation modeling was begun using Visual Minteq and is presented below (Figures 2-3 and 2-4) for the initial aqueous components for both synthetic porewater and NaCl background electrolyte.

In addition, the student research poster entitled, “A comparison of NH₄OH and NaOH treatments of uranium immobilization in the presence of kaolinite,” was presented at Waste Management 2016 and an abstract was submitted for the Fall National American Chemical Society meeting for August 21-26, 2016 entitled, “Investigation of NH₃(g) Treatment of the Immobilization of Uranium in the Presence of Pure Minerals.”

Batch Experiments: NaOH vs. NH₄OH Treatment

Figures 2-11 to 2-13 show results from batch experiments for 5 g/L kaolinite, illite or montmorillonite and 500 ppb U in the presence of a synthetic porewater described in the November monthly report (total ionic strength 7.2 mM). Figure 2-11 represents apparent K_d values in mL/g for uranium and Figures 2-12 and 2-13 represent elemental dissolution of pure minerals at pH ~ 11.5. In the data presented, the pH of the batch samples is raised by either 2.5 M NH₄OH or 2.5 M NaClO₄ + 0.025 M NaOH. The NaOH + NaCl solution is used to add a similar base power with equivalent ionic strength changes to the weak base NH₄OH.

In the presence of the synthetic porewater, the removal of U from the aqueous phase increases with pH as shown by the increase in apparent K_d partitioning coefficients in the December monthly report for kaolinite. A similar trend is followed for illite and montmorillonite. However, the data for pH 7.5 has not yet been finalized. In Figure 2-11, the apparent K_d for pH ~11.5 in synthetic porewater is shown for quartz (100 g/L), kaolinite (5 g/L), illite (5 g/L) and montmorillonite (5 g/L). Further, the K_d values appear to be greater for the NH₄OH treatment for each of the minerals considered with the exception of quartz. However, statistical comparison is still in progress.

Figures 2-12 and 2-13 show the dissolution of the minerals as the pH is increased by either NaOH or NH₄OH. Si dissolution appears to increase more for the NaOH treatment than NH₄OH as the pH is increased. Because Si is likely dissolving as silicic acid (H₄SiO₄), it is possible that the differences are due to ionic strength dominated by molecular versus charged species. Further, the aqueous Al and Si dissolution appear to be correlated. It must be noted that the percent dissolution likely represents multiple processes (i.e., dissolution, precipitation and complexation). However, this is under further investigation through aqueous speciation modeling.

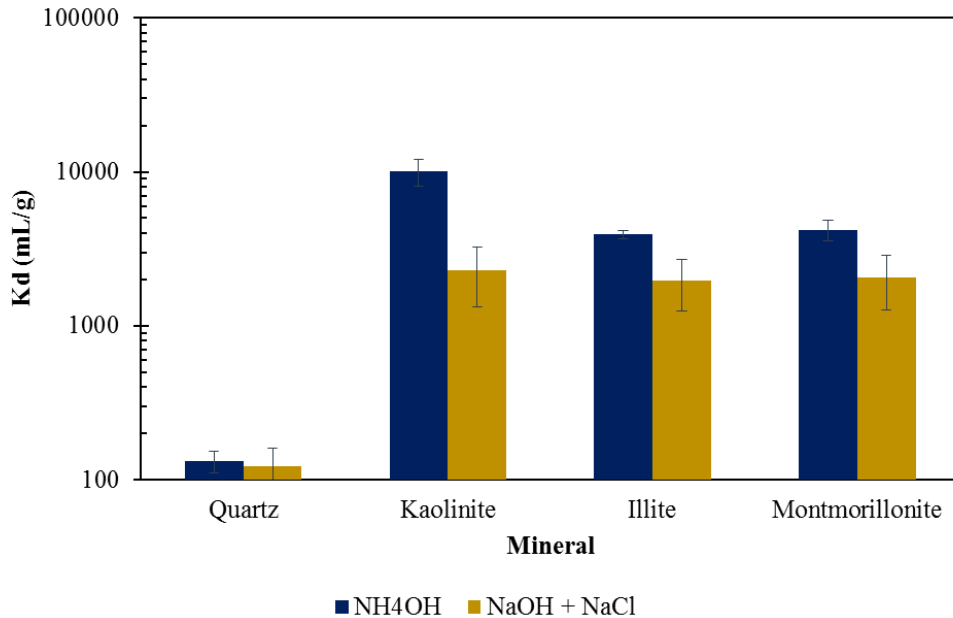


Figure 2-11. Apparent K_d (mL/g) for U (500 ppb) removal in the presence of kaolinite (5 g/L), quartz (100g/L), illite (5 g/L) or montmorillonite (5 g/L) in synthetic porewater at variable pH via adjustment with either NaOH (yellow) or NH₄OH (blue)

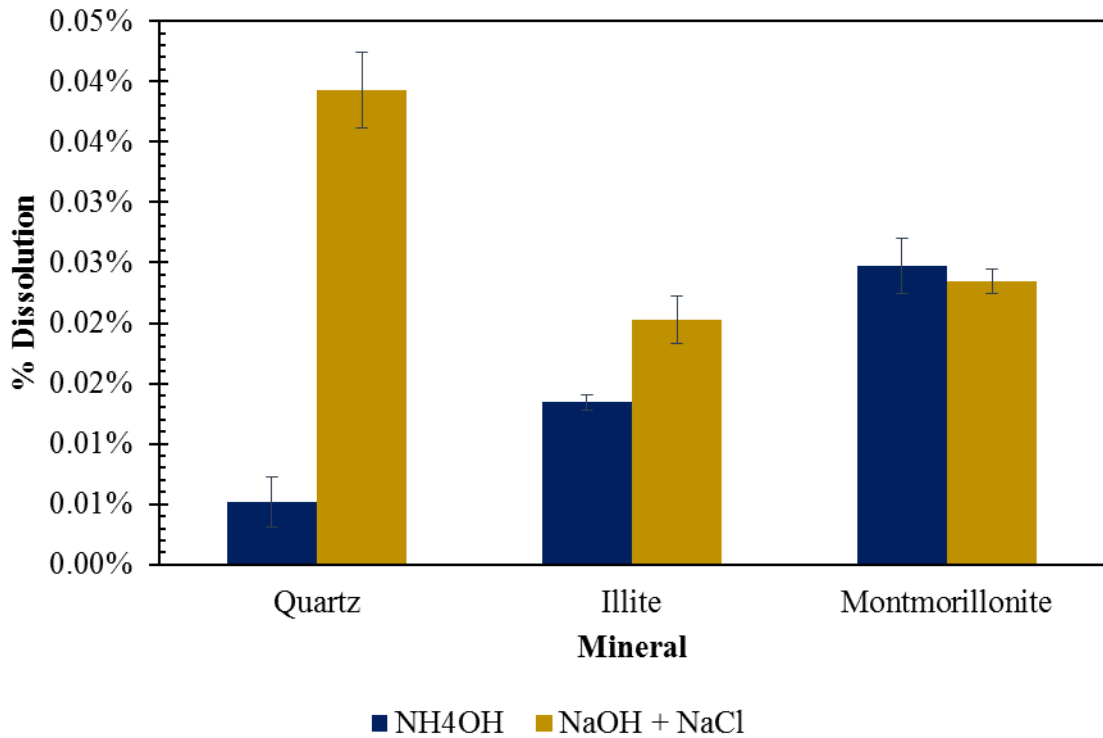
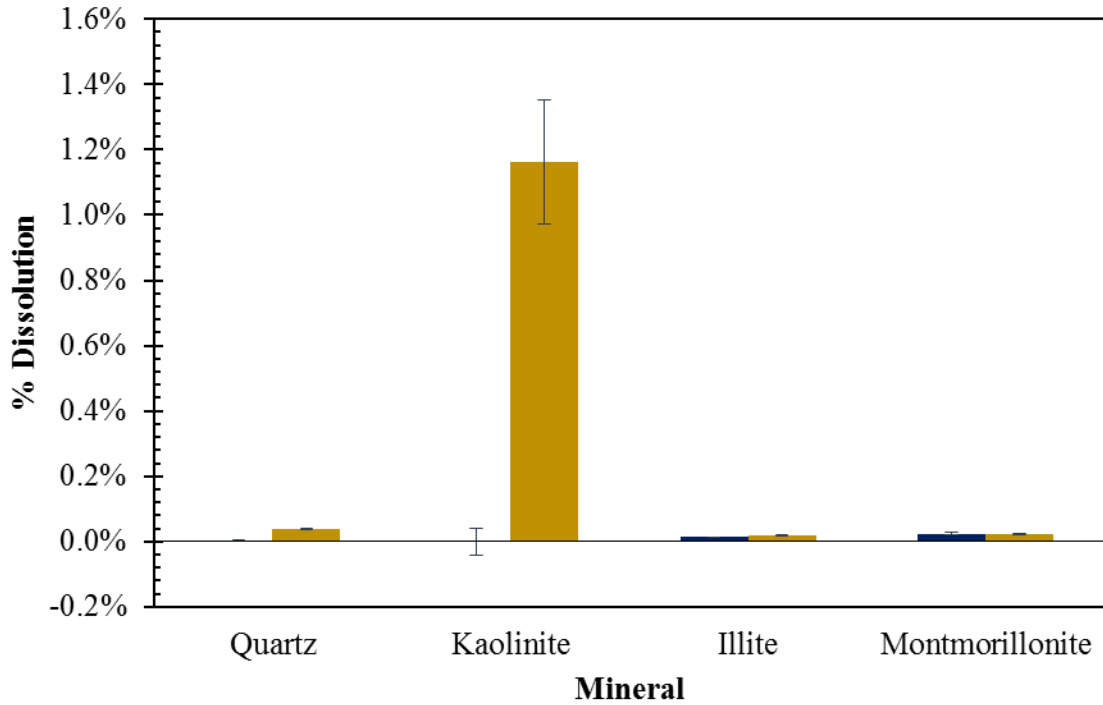


Figure 2-12. Elemental dissolution of Si from quartz (100 g/L), kaolinite (5 g/L), illite (5 g/L) and montmorillonite (5 g/L) at pH ~ 11.5 with adjustment via NaOH or NH4OH, top – all minerals included, and bottom – kaolinite removed for comparison

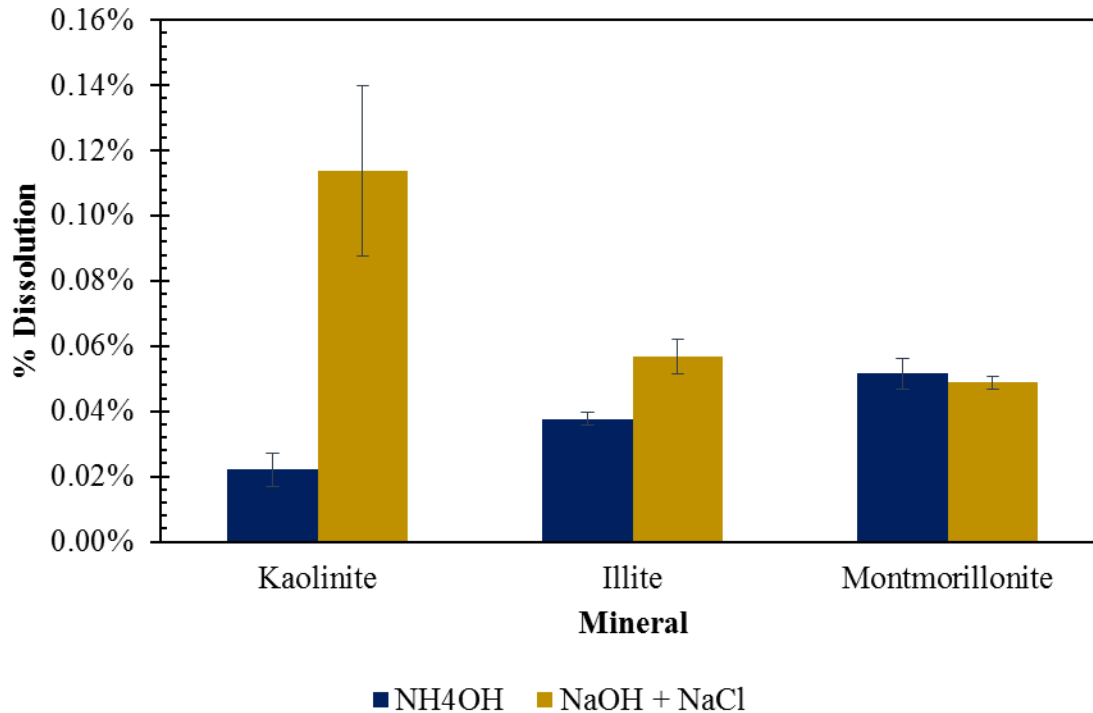


Figure 2-13. Elemental dissolution of Al from kaolinite, illite and montmorillonite each at 5 g/L at pH ~ 11.5 via NaOH or NH₄OH

Aqueous Speciation Modeling via Visual Minteq

Preliminary speciation is presented for U in 0.007 M NaCl (based on the initial ionic strength) in Figure 2-14. It is important to note that the major aqueous species observed in modeling for the NaCl electrolyte is $\text{UO}_2(\text{CO}_3)_3^{4-}$ at pH 11.5. This speciation may change; however, the additional ionic strength from mineral dissolution and pH adjustment with either NaOH or NH_4OH are accounted for in the model. Furthermore, speciation is much more complex at pH 7.5 with five different species having >5% of the fraction. UO_2CO_3 and $\text{UO}_2(\text{CO}_3)_2^{2-}$ are the major species with 27% and 48% of the aqueous fraction, respectively.

Preliminary speciation is presented for U in synthetic porewater in Figure 2-14. At pH 11.5, the major species present is $\text{UO}_2(\text{CO}_3)_3^{4-}$ (99.8%) as in the NaCl system. However, $\text{CaUO}_2(\text{CO}_3)_3^{2-}$ also makes up ~0.2% of the species at elevated pH in the present of synthetic porewater. The speciation at pH 7.5 is also complex with four different species having >1% abundance, including: $\text{Ca}_2\text{UO}_2(\text{CO}_3)_3$ at 65%, $\text{CaUO}_2(\text{CO}_3)_3^{2-}$ at 29.1%, $\text{UO}_2(\text{CO}_3)_2^{2-}$ at 3% and UO_2CO_3 at 1.7%. These neutral and negatively charged U species will greatly impact U sorption as they are less likely to sorb to the negatively charged kaolinite mineral.

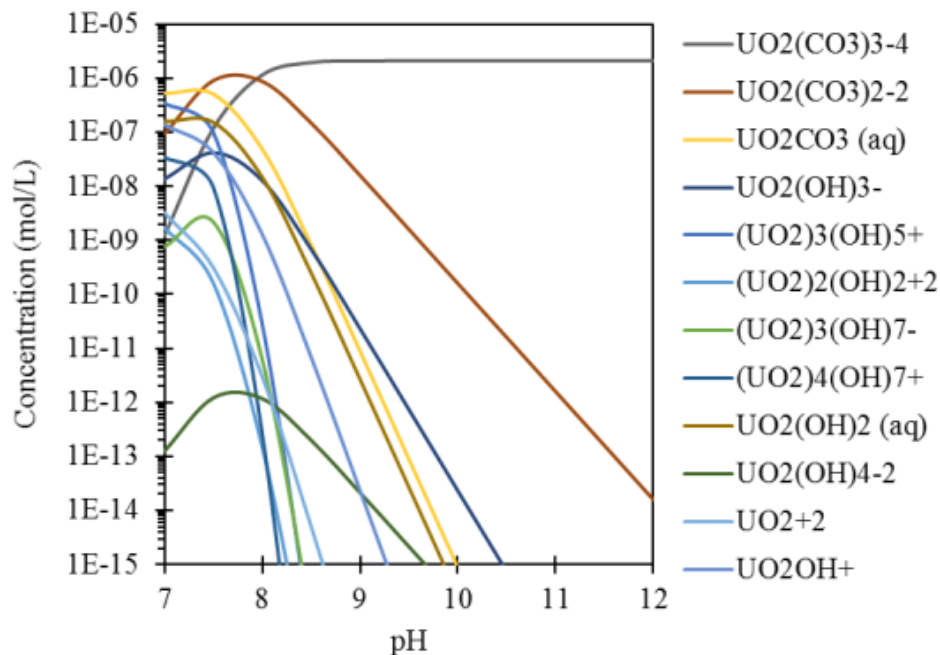


Figure 2-14. Aqueous U speciation in 500 ppb U, 0.007 M NaCl solution in the presence of 0.00038 atm partial pressure of CO₂ (natural atmospheric) as modeled via Visual Minteq.

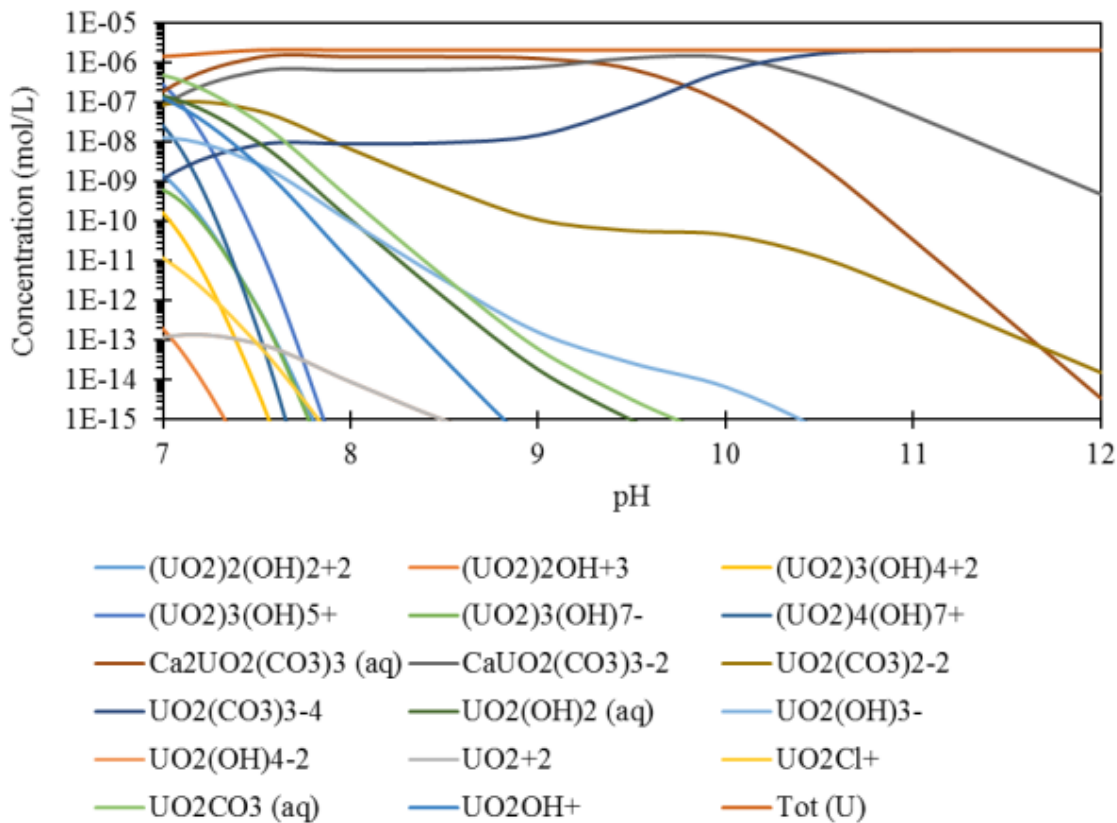


Figure 2-15. Aqueous U speciation in 500 ppb U in synthetic porewater solution in the presence of 0.00038 atm partial pressure of CO₂ (natural atmospheric) as modeled via Visual Minteq.

Sequential Extraction Preparation

Batch samples were prepared in triplicate in the presence of either synthetic porewater or 0.007 M NaCl, 530±17 ppb U, and 20.0±0.4 g/L kaolinite. The total volume was approximately 50 mL with one gram of kaolinite to have a sufficient mass for sequential extractions. Control samples were prepared at neutral pH (Table 2-4) and equilibrated for 32 days. Samples treated with either 2.5 M NH₄OH or 2.5 M NaCl + 0.025 M NaOH were equilibrated for 35 days. Following this period, the aqueous phase was removed after centrifugation (5000 rpm for 30 min.) and analyzed by KPA (U) and ICP-MS (Al and Si) in 1% HNO₃. All error bars are based on the error of the triplicate samples as this is larger than the instrumental error.

Table 2-4. Summary of Equilibrium pH for Batch Experiments at 20 g/L Kaolinite in the Presence of 500 ppb Uranium

Sample ID	pH
NaCl-NH ₄ OH	11.69±0.02
NaCl-NaOH	11.53±0.03
Synpore-NH ₄ OH	11.44±0.01
Synpore-NaOH	11.50±0.04
Synpore-Initial	7.47±0.08
NaCl-Initial	6.71±0.05

Figures 2-16 and 2-17 represent the equilibrium apparent partitioning coefficient for uranium and aqueous concentrations of aluminum and silicon, respectively. In addition, the K_d's are summarized in Table 2-5 for synthetic porewater and NaCl. The K_d's measured prior to sequential extractions with >30 days of equilibration and 20 g/L kaolinite are compared with previous batch sorption K_d's measured in 5 g/L kaolinite after three days of equilibration. These data are in excellent agreement as discussed below.

Table 2-5. Apparent K_d Partitioning Coefficients (mL/g) for Previous Batch Sorption Experiments and Batch Experiments Prepared for Sequential Extraction

Sample ID	>30 days, 20 g/L kaolinite	3 days, 5 g/L kaolinite
NaCl-NH ₄ OH	313±26	210±20
NaCl-NaOH	53330±550	56430±5140
Synpore-NH ₄ OH	3560±90	10030±1970
Synpore-NaOH	2670±250	2280±950
Synpore-Initial	25±4	25±7
NaCl-Initial	1510±550	1650±290

Note: NaCl-NaOH K_d's are based on detection limits and will be re-analyzed due to Cl⁻ interference on the KPA

The data for the control at neutral pH in synthetic porewater is within the error of previous batch data presented (25±7 mL/g in previous 5 g/L batch experiments and 25±4 g/L in current 20 g/L batch experiments for sequential extraction). In addition, the NaOH treatment with synthetic porewater is also in excellent agreement with previous batch experiments (2280±950 mL/g versus 2670±250 mL/g). However, the NH₄OH treatment in synthetic porewater measured a lower K_d (3560±90 for 20 g/L kaolinite with 35 day equilibration versus 10030±1970 mL/g for 5 g/L kaolinite with 3 day equilibration). Therefore, it is likely that the NH₄OH was not at

equilibrium after three days or that some U re-entered the aqueous phase over time. However, there is still slightly more removal of U from the system with treatment with NH₄OH versus NaOH with both equilibration periods.

The data for 7 mM NaCl also agree well with previous batch experiments. It is notable that these experiments represent data collected by two independent scientists, still with exceptional agreement. Moreover, it is important to observe that the system is clearly at equilibrium within three days of mixing. However, it must be noted that the NaCl – NaOH samples will be re-analyzed due to interferences with Cl⁻ on the KPA. The K_d's currently reported are based on analytical detection limits.

The initial synthetic porewater samples represent the lowest removal of uranium from the aqueous phase as expected based on previous batch experiments. This is likely due to the formation of uranyl carbonate species as predicted by speciation modeling presented in the February monthly report. Further, treatment by either NaOH or NH₄OH represent a significant removal of uranium from the aqueous phase for synthetic porewater. The initial NaCl data is likely not in equilibrium with atmospheric CO₂ and, therefore, carbonate species play a smaller role in complexation.

Although the aqueous Si and Al concentrations cannot be explicitly compared to previous measurements due to the different solids loadings, they are similar and present some interesting results. The aqueous Si measurements are all significantly lower than the reported solubility for Si without the presence of other metal cations. A review compiled by Iler in his text “The Chemistry of Silica” reports solubility between 60 – 130 ppm (Iler 1979). Further, previous works have measured a decrease in solubility when Al or Fe are present in the aqueous phase. Soluble Al has been shown to reduce solubility to <10 ppm (Iler 1973, Iler 1979). In addition, up to 2 ppm Si have been measured in equilibrium with mica and kaolin and up to 10 ppm with montmorillonite (Iler 1979). All measurements here are below 30 ppm. Without the inclusion of the NaCl – initial and NaCl – NH₄OH data which have considerable scatter, all Si measurements are below 11 ppm (Figure 2-17).

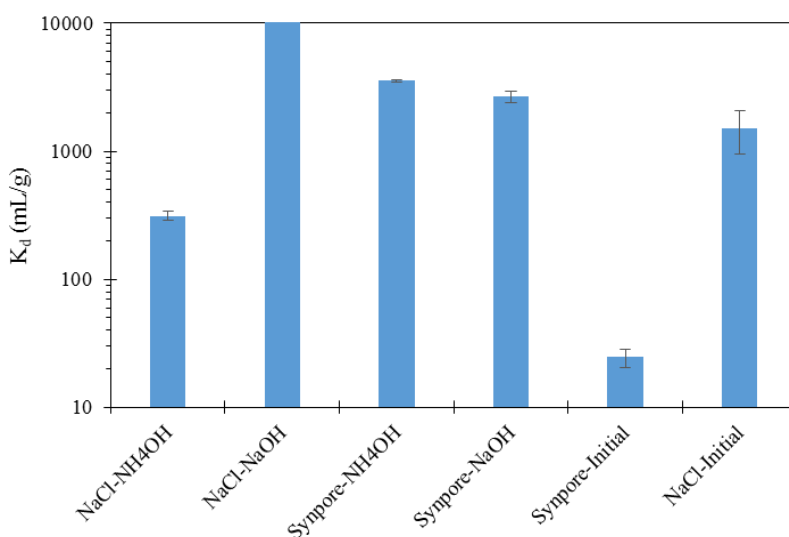


Figure 2-16. Equilibrium sorption (>30 days) for 500 ppb U in the presence of 20 g/L kaolinite with synthetic porewater or 0.007 M NaCl.

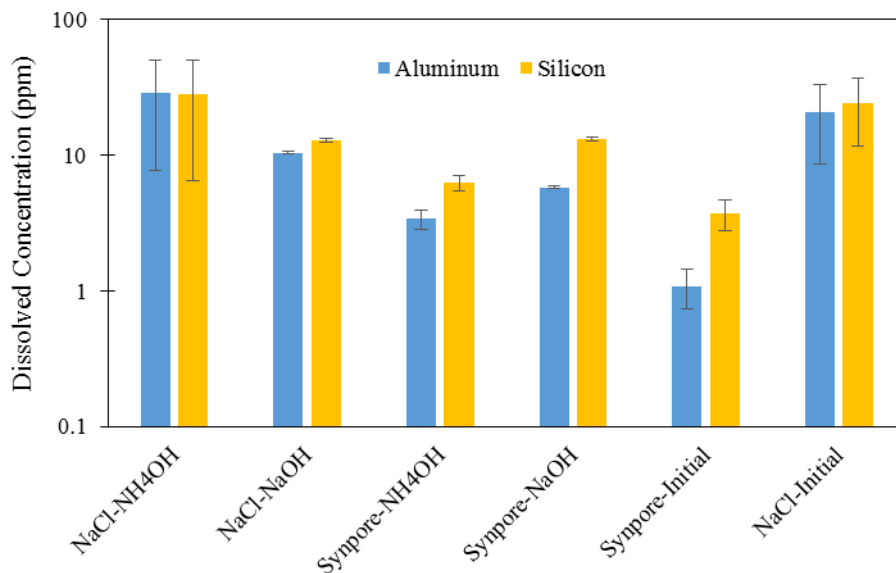


Figure 2-17. Aqueous Si and Al at equilibrium (>30 days) with 0.007 M NaCl or synthetic porewater.

Future Experiments:

Ongoing Batch Experiments

BET surface area analysis will be completed on each of the minerals being used in these batch experiments to allow for normalization of apparent K_d values to surface area for more appropriate comparison. In addition, ammonia analysis through the use of an ammonia gas sensing electrode is ongoing for current samples. Statistical comparison through t-testing will be completed to compare the NaOH and NH₄OH treatments. Following the experiments with kaolinite in NaCl, equivalent batch experiments with quartz (ongoing), illite (ongoing), montmorillonite and natural Hanford sediments will be completed for comparison.

Sequential Extractions

To further characterize the sorption/desorption and precipitation/dissolution processes occurring in these batch experiments, sequential extraction methods were designed based on previous work. The goal of these experiments is to gather information on the availability of uranium through the NaOH and NH₄OH treatments. Steps 1 – 4 extractions were completed on 20 g/L kaolinite suspensions equilibrated at pH 7.5 in synthetic porewater or NaCl and pH 11.5 in synthetic porewater or NaCl as adjusted by NaOH or NH₄OH. The final extraction step and data analysis will be completed in the next quarter.

A five step extraction procedure (Table 2-6) was used for the following four operationally defined phases: (1) water soluble, (2) exchangeable, (3) some carbonates, (4) remaining carbonates/acid soluble, and (5) residual. The first three fractions will be considered as the *available* fraction of uranium. It should be noted that because of the operational definition of these steps, the procedure is more properly defined as a fractionation scheme (Filgueiras et al., 2002). Steps 1 – 4 as described in Table 2-6 below are completed. However, analysis for U by KPA and Al/Si by ICP-OES is currently ongoing. In addition, a wash step between each step

after step 1 was utilized based on previous work with 5 mL of MilliQ H₂O (>18 MΩ-cm) mixed for ~30 seconds and then centrifuged (Tessier, Campbell et al. 1979, Clark, Johnson et al. 1996, Lee, Yoon et al. 2004, Beltrán, de la Rosa et al. 2010).

Table 2-6. Sequential Extraction Methodology

Operationally-defined Fraction	Extraction Conditions	References
Aqueous	Synthetic porewater	(Clark, Johnson et al. 1996, Szecsody, Truex et al. 2010, Szecsody, Truex et al. 2012)
Adsorbed/Exchangeable	1 M MgNO ₃ at pH 7 for 16 hours	(Tessier, Campbell et al. 1979, Clark, Johnson et al. 1996, Serkiz, Johnson et al. 2007, Alam and Cheng 2014)
Some Carbonates	1 M Sodium Acetate adjusted to pH 5 with Acetic Acid for 1 hour	(Tessier, Campbell et al. 1979, Beltrán, de la Rosa et al. 2010, Szecsody, Truex et al. 2010, Szecsody, Truex et al. 2012)
Remaining Carbonates	1.45 M Acetic Acid at pH 2.3 for 5 days	(Szecsody, Truex et al. 2010, Szecsody, Truex et al. 2012)
Residual	8 M HNO ₃ @ 95°C for 2 hours	(Szecsody, Truex et al. 2010, Szecsody, Truex et al. 2012)

Note: 5 mL DDI H₂O wash was completed after each step to remove residual extraction solutions and a 1:40 solid to liquid ratio was used for each extraction step

References:

1. Alam, M. S. and T. Cheng (2014). "Uranium release from sediment to groundwater: Influence of water chemistry and insights into release mechanisms." Journal of Contaminant Hydrology **164**: 72-87.
2. Beltrán, R., J. de la Rosa, J. Santos, M. Beltrán and J. Gomez-Ariza (2010). "Heavy metal mobility assessment in sediments from the Odiel River (Iberian Pyritic Belt) using sequential extraction." Environmental Earth Sciences **61**(7): 1493-1503.
3. Clark, S. B., W. H. Johnson, M. A. Malek, S. M. Serkiz and T. G. Hinton (1996). "A Comparison of Sequential Extraction Techniques to Estimate Geochemical Controls on the Mobility of Fission Product, Actinide, and Heavy Metal Contaminants in Soils." Radiochimica Acta **74**: 173-179.
4. Iler, R. (1973). "Effect of adsorbed alumina on the solubility of amorphous silica in water." Journal of Colloid and Interface Science **43**(2): 399-408.

5. Iler, R. K. (1979). "The chemistry of silica: solubility, polymerization, colloid and surface properties, and biochemistry." Canada: John Wiley & Sons Inc.
6. Lee, M. H., Y. Y. Yoon, S. B. Clark and S. E. Glover (2004). "Distribution and geochemical association of actinides in a contaminated soil as a function of grain size." Radiochimica Acta **92**(9-11): 671-675.
7. Serkiz, S. M., W. H. Johnson, L. M. J. Wile and S. B. Clark (2007). "Environmental availability of uranium in an acidic plume at the Savannah River Site." Vadose Zone Journal **6**(2): 354-362.
8. Szecsody, J. E., M. J. Truex, L. Zhong, N. Qafoku, M. D. Williams, J. P. McKinley, Z. Wang, J. Bargar, D. K. Faurie and C. T. Resch (2010). Remediation of Uranium in the Hanford Vadose Zone Using Ammonia Gas: FY 2010 Laboratory-Scale Experiments, Pacific Northwest National Laboratory (PNNL), Richland, WA (US), Environmental Molecular Sciences Laboratory (EMSL).
9. Szecsody, J. E., M. J. Truex, M. J. Zhong, T. C. Johnson, N. P. Qafoku, M. D. Williams, W. J. Greenwood, E. L. Wallin, J. D. Bargar and D. K. Faurie (2012). "Geochemical and Geophysical Changes during Ammonia Gas Treatment of Vadose Zone Sediments for Uranium Remediation." Vadose Zone Journal: 1-13.
10. Tessier, A., P. G. Campbell and M. Bisson (1979). "Sequential extraction procedure for the speciation of particulate trace metals." Analytical chemistry **51**(7): 844-851.

Subtask 1.3.3: The influence of microbial activity on the corresponding electrical geophysical response after ammonia injections in the vadose zone

FIU has continued reviewing literature pertaining to the feasibility of using the spectral induced polarization geophysical method (SIP) for detecting presence of microbes. This review is set to be finished by March.

A new DOE Fellow, Alejandro Garcia, was assigned to security and safety training before traveling to Pacific Northwest National Labs for a 10-week spring 2016 internship. Preparations for the trip are in a progress and FIU is in discussion with PNNL to finalize Alejandro Garcia's scope of work during the internship.

In February, DOE fellow Alejandro Garcia began a 10-week spring 2016 internship at PNNL. Preparations have begun for the column experiments related to the spectral induced polarization (SIP) signatures of microbial activity designed to remediate uranium-contaminated vadose zone sediment.

In March, DOE fellow Alejandro Garcia was continuing his 10-week spring 2016 internship at PNNL. Preparations have begun for the column experiments related to the spectral induced polarization (SIP) signatures of microbial activity designed to remediate uranium-contaminated vadose zone sediment. Initial planning at PNNL has designated the construction of six columns with varying constituents: 1) a control, 2) injected with 3 mM HCO₃, 3) injected with a carbon source, 4) injected with 3 mM HCO₃ + a carbon source, 5) injected with a carbon source + inoculum, and 6) injected with 3 mM HCO₃ + a carbon source + inoculum. This approach would allow the analysis of the effects of various variables on the SIP response, so that the microbial

response can be isolated. Columns are being set up using a clear PVC pipe with holes drilled on the sides and large opaque PVC end caps on either end. Each column will have a coiled Ag/AgCl current electrode on either end, 2 or 3 potential electrodes equidistant on the side and 4 sample ports. Each electrode will be composed of a silver wire encased in agar gel, which is then situated within a PVC nipple. Some electrical equipment was ordered; however, as it was not usable for SIP, replacement equipment is being obtained. Initial testing may use a large SIP unit similar to the one being used in existing columns. Media solutions for bacteria culturing were prepared in aerobic conditions within a standard lab hood designated for work with radioactive materials. The cultures were capped and left to sit for ~1-2 weeks before transferring; the conditions within bottles could be described as oxygen restricted. Future plans include completing the construction of the columns as well as the microbe culture, initiating some initial measurements and shipping the equipment and columns to ARC at FIU to continue the experiments.

Task 2: Remediation Research and Technical Support for Savannah River Site

Task 2 Overview

The acidic nature of the historic waste solutions received by the F/H Area seepage basins caused the mobilization of metals and radionuclides, resulting in contaminated groundwater plumes. FIU is performing basic research for the identification of alternative alkaline solutions that can amend the pH and not exhibit significant limitations, including a base solution of dissolved silica and the application of humic substances. Another line of research is focusing on the evaluation of microcosms mimicking the enhanced anaerobic reductive precipitation (EARP) remediation method previously tested at SRS F/H Area.

Task 2 Quarterly Progress

Subtask 2.1. FIU's Support for Groundwater Remediation at SRS F/H –Area

The objective of the experiments conducted during month of January was to investigate the influence of the ionic strength on the U(VI) binding on SRS sediment from F/H area under circumneutral conditions. The experiments were conducted by bringing 400 mg of SRS soil of mean particle diameter $0.18 < d < 2 \text{ mm}$ in contact with 20 mL of SRS synthetic groundwater pH 3.5 bearing 500 ppb of U(VI). 70 ppm of sodium silicate was added to achieve circumneutral conditions and then different quantities from stock solutions of CaCl_2 and NaClO_4 were added in order to achieve the desired electrolyte concentrations. The concentrations of CaCl_2 and NaClO_4 were 0.001, 0.01 and 0.1 M. Control samples (no addition of electrolyte) were also studied, which already contained a concentration of CaCl_2 10^{-5} M. After 24h, aliquots were isolated from the supernatant and the residual concentration of U(VI) in the supernatant was determined by means of KPA. All experiments were performed in triplicate and the results are presented in Figure 2-18.

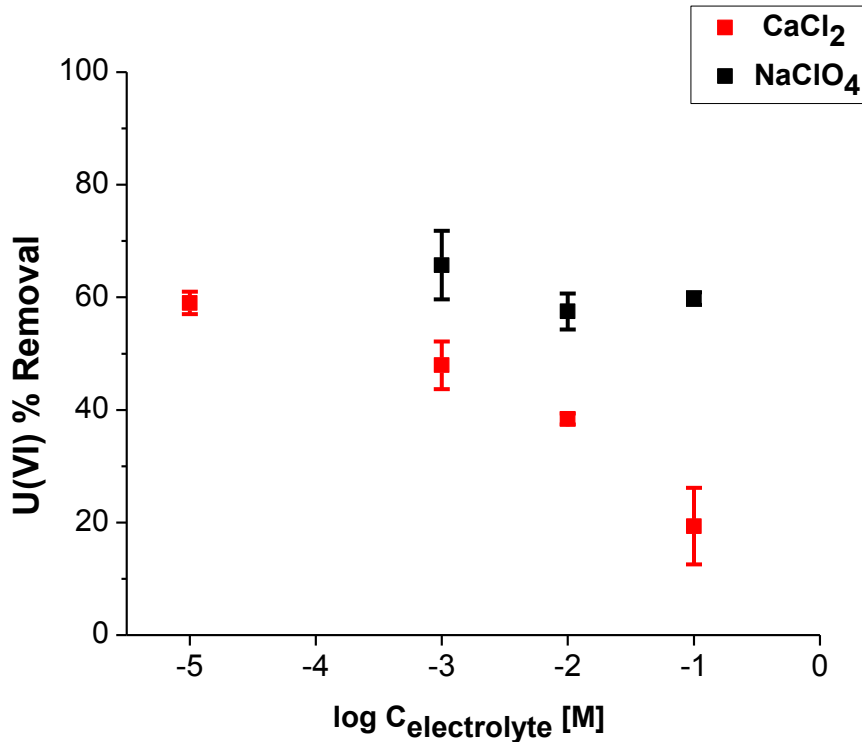


Figure 2-18. U(VI) per cent removal as a function of electrolyte concentration using CaCl₂ and NaClO₄ (x-axis is in logarithmic scale). Error bars represent relative standard deviation.

The retention of cations from mineral surfaces is frequently described by the surface complexation model. Surface complexation involves the formation of direct bonds between metal cations and surface –OH groups and/or O atoms and comprises of two different types of complexes: the outer-sphere complexes and the inner-sphere complexes (Wu et al., 1999). In the case of inner-sphere complexation, the ions are bound directly to the surface site (Figure 2-19). On the other hand, in outer-sphere complexation, the ion is presumed to bind to the surface site by chemical bonds without losing the hydration shell, meaning that the water molecule is located between the ion and binding site (Figure 2-19). The distance to the surface is larger and the bond strength is weaker in comparison to inner-sphere complexation (Worch, 2015).

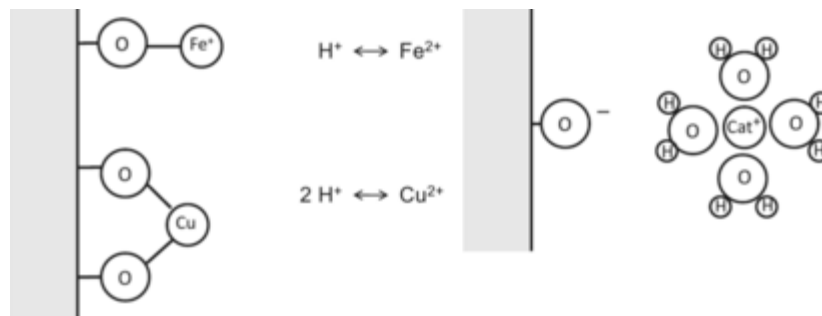


Figure 2-19. Example of inner-sphere complexation (left) and outer-sphere complexation (right), as adapted by Sigg and Stumm, Aquatic Chemistry [3].

Outer-sphere complexation takes place in the double layer (as opposed to inner-sphere complexation, which takes place on the surface), where an excess of counter-ions are located, neutralizing surface charge. The double layer decreases with ionic strength (electrolyte concentration) increase and hence, outer-sphere complexes are presumed to be susceptible to coulombic interactions (Sherwood Lollar, 2005). Ions that form outer-sphere complexes exhibit reduced sorption with ionic strength increase whereas ions that form inner-sphere complexes are usually not affected by the fluctuation of ionic strength (Bachmaf & Merkel, 2010). The removal of U(VI) by SRS soil remained unaffected when ionic strength was adjusted with the addition of NaClO₄, implying that U(VI) removal under the conditions studied may be mainly attributed to the formation of inner-sphere complexes. NaClO₄ was chosen because it is an inert electrolyte: it exhibits practically no complexation with metals present in the aqueous form and the sorption of ClO₄⁻ on oxide surfaces is minimal (Morales et al., 2011; Zebardast et al., 2014). Similar results were reported by Guo et al. (Guo et al., 2009) who found that the sorption of U(VI) on goethite was insensitive to the fluctuation of ionic strength, adjusted with NaCl.

On the other hand, removal decreases significantly with the increase of calcium chloride concentration. The speciation of the soluble U(VI) species under the conditions studied is presented at Table 2-7 (10⁻⁵ M CaCl₂ is the concentration of SRS synthetic groundwater, without any further addition of calcium chloride).

Table 2-7. Speciation of U(VI) Soluble Species for All the Calcium Concentrations Studied, as provided by Visual Minteq.

CaCl₂ concentration (M)			
10⁻⁵	10⁻³	10⁻²	0.1
47.3% (UO ₂) ₃ (OH) ₅ ⁺	46.9% (UO ₂) ₃ (OH) ₅ ⁺	44.5% (UO ₂) ₃ (OH) ₅ ⁺	21.7% (UO ₂) ₃ (OH) ₅ ⁺
14.5 % UO ₂ OH ⁺	14.8 % UO ₂ OH ⁺	15.6 % UO ₂ OH ⁺	13.5% UO ₂ OH ⁺
4.1% (UO ₂) ₄ (OH) ₇ ⁺	4.0% (UO ₂) ₄ (OH) ₇ ⁺	3.6% (UO ₂) ₄ (OH) ₇ ⁺	1.3% (UO ₂) ₄ (OH) ₇ ⁺
7.8% UO ₂ H ₃ SiO ₄ ⁺	8.0% UO ₂ H ₃ SiO ₄ ⁺	8.4% UO ₂ H ₃ SiO ₄ ⁺	7.7% UO ₂ H ₃ SiO ₄ ⁺
18.7 % UO ₂ CO ₃	18.4 % UO ₂ CO ₃	17.3 % UO ₂ CO ₃	12.3 % UO ₂ CO ₃
5.6 % UO ₂ (OH) ₂	5.5 % UO ₂ (OH) ₂	5.2 % UO ₂ (OH) ₂	3.7 % UO ₂ (OH) ₂
		1.9 % Ca ₂ UO ₂ (CO ₃) ₃	34.4 % Ca ₂ UO ₂ (CO ₃) ₃

The speciation remains practically the same for the range of 10^{-5} - 10^{-2} M of calcium chloride; hence, the decrease in the uranium removal may not be associated with speciation changes. A possible explanation is the competition of calcium ions and uranium complexes for the same or neighboring binding sites, resulting in a reduced uranium sorption. The uptake of calcium by goethite has been documented in literature and it has been found that calcium binds on goethite both as an outer- and inner-sphere complex (Rahnemaie et al., 2006; Rietra et al., 2001) based on the following scheme $=\text{SO}-\text{Ca}^+$ (Sverjensky, 2006), where S stands for the solid surface and O is the oxygen atom. Goethite may constitute only a small fraction of SRS soil; nevertheless, it is very reactive towards metal cations in the solution. Taking into consideration the results of Guo et al. (Guo et al., 2009), who showed that when ionic strength is adjusted with NaCl, U(VI) sorption on goethite remains the same, it is concluded that calcium plays an important role in inhibiting U(VI) sorption on SRS soil in circumneutral conditions. As calcium concentration increases (0.1M), the decrease in U(VI) sorption is even more sharp (from 40% down to 18%), perhaps due to the formation of $\text{Ca}_2\text{UO}_2(\text{CO}_3)_3$, which may not be available for further complexation by the binding sites.

In the month of February, batch experiments were performed to investigate the kinetic pattern of U(VI) retention by different SRS soil fractions. Two sets of samples were produced: the first set was comprised of controls and samples that contained SRS soil fraction $d < 63 \mu\text{m}$, the second set included controls and samples that contained SRS soil fraction $63 \mu\text{m} < d < 180 \mu\text{m}$, and both sets were amended with 500 ppb U (VI), spiked with 70 ppm of sodium silicate (SS), and pH adjusted to circumneutral conditions. All experiments were conducted in triplicate and the standard deviation was calculated. The samples equilibrated for a period of 2 days on a platform shaker at 125 rpm. Aliquots were extracted from each sample at different time intervals over the equilibration period and analyzed by KPA to determine the U (VI) concentration in the supernatant.

Results obtained from previous experiments suggest a correlation between the iron composition of the SRS soil and U (VI) removal. To understand this relationship, scanning electron microscopy with energy dispersive X-ray spectroscopy (SEM/EDS) was used to conduct elemental analysis of the different SRS soil fractions. The results are shown in Table 2-8, which displays the U (VI) % removal and the different Fe, Al, and Si concentrations in mg/g. Images obtained from SEM are displayed in Figure 2-20.

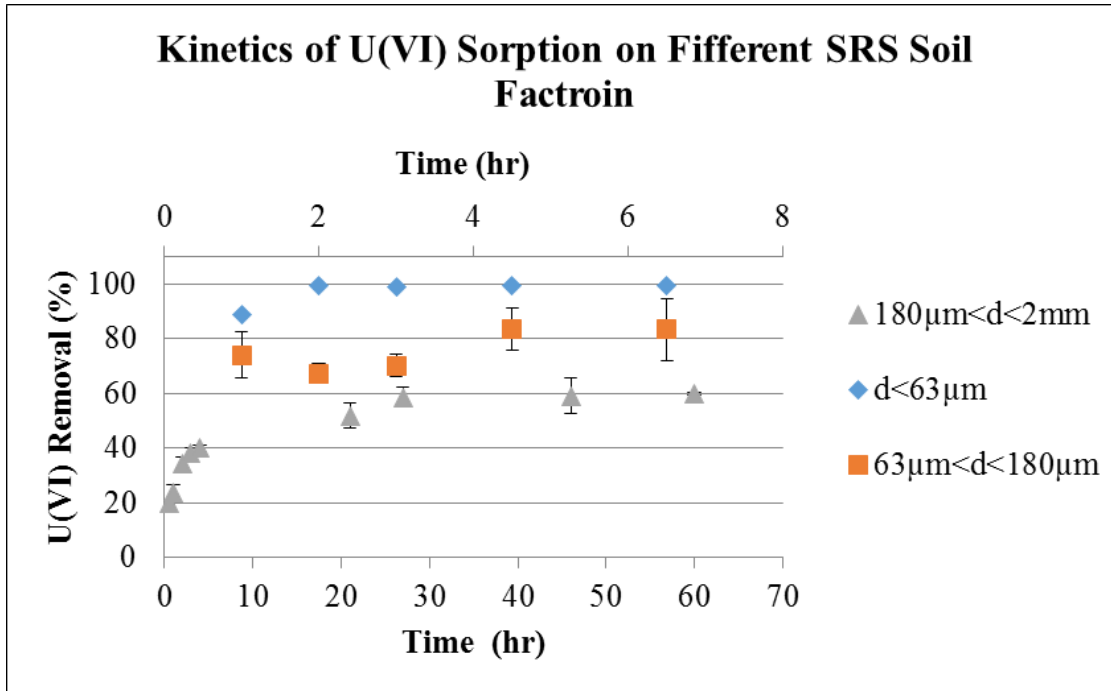


Figure 2-20. U (VI) percentage removal as a function of time for different SRS soil fraction, pH 6.5.

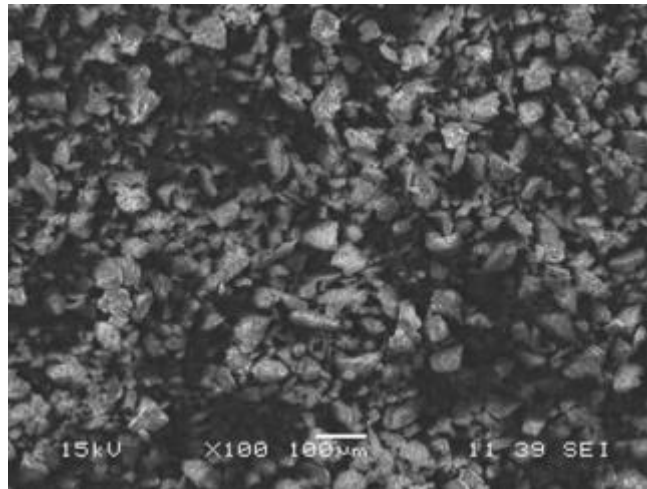


Figure 2-21. SRS soil fraction: d < 63µm morphology obtained by means of SEM/EDS.

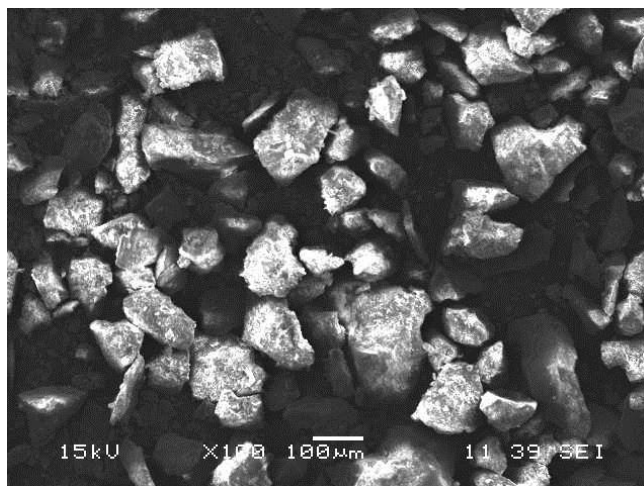


Figure 2-22. SRS soil fraction: $63\mu\text{m} < d < 180\mu\text{m}$ morphology obtained by means of SEM/EDS.

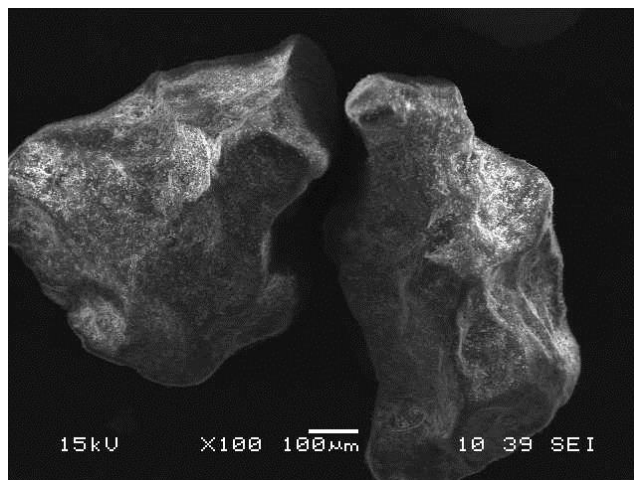


Figure 2-23. SRS soil fraction: $180\mu\text{m} < d < 2\text{mm}$ morphology obtained by means of SEM/EDS.

Table 2-8. U (VI) Percent Removed from the SRS Soil Fractions and the Fe, Al, and Si Concentrations

SRS Soil Fraction	U(VI) % Removed	[Fe] (mg/g)	[Al] (mg/g)	[Si] (mg/g)
$d < 63\mu\text{m}$	99 ± 0.2	89 ± 2	72 ± 4	396 ± 3
$63\mu\text{m} < d < 180\mu\text{m}$	79 ± 8	70 ± 11	71 ± 5	389 ± 4
$180\mu\text{m} < d < 2\text{mm}$	59 ± 1	40 ± 4	54 ± 13	416 ± 37

Figure 2-21 illustrates the kinetics results for the finer fractions of the SRS soil, which displays considerably greater removal of U (VI). The finer fractions reach equilibrium at about 1 hour. Previous kinetics experiments with fraction $180\mu\text{m} < d < 2\text{mm}$ showed that the equilibrium was reached at 10 hours and only $59 \pm 1\%$ of the U(VI) was removed. Figure 2-21 shows the morphology of the fractions $d < 63\mu\text{m}$, where finer particulate clay-like sediment is observed, whereas Figures 2-22 and 2-23 show the morphology of the $63\mu\text{m} < d < 180\mu\text{m}$ fraction which more closely resembles rock. While quartz, which is the most abundant mineral in the SRS soil,

remains constant in all fractions, a clear trend can be observed between the Fe content and the U(VI) removal. Results suggest that goethite is the most reactive mineral phase in the SRS soil. Possible reasons contributing to higher U(VI) % removal is the increase in surface area due to the higher content of goethite particles.

During the month of March, desorption experiments were conducted using a mixture of pure minerals mimicking SRS F/H Area composition: quartz, and a mixture of quartz and kaolinite (95% quartz and 5% kaolinite). For comparison reasons, desorption experiments were performed on SRS background soil (180µm<d<2mm). Understanding the SRS geochemical soil composition, and its contributions to the U (VI) sorption processes, can lead to a greater grasp of the longevity of the remediation technology.

Three different batch sets were created: the first was comprised of 0.2 g of quartz, the second contained a blend of 95% quartz and 5% kaolinite (total mass 0.2 g), and the third contained 0.2 g of SRS background soil (comprising mostly of quartz, kaolinite, and goethite), respectively. Ten (10) ml of synthetic SRS groundwater spiked with 500 ppb U (VI) and sodium silicate was added (70 ppm) in order to adjust the pH to circumneutral conditions. The mixture was left for 24 hours to equilibrate and, after the equilibration, aliquots were taken and analyzed by means of KPA to determine residual U (VI) concentration. Subsequently, the supernatant was then removed and 10 ml of synthetic SRS groundwater was reintroduced. The new mixture was left to equilibrate for another 24 hours and the U(VI) concentration released in the aqueous phase was determined by means of KPA. All experiments were conducted in triplicate.

Table 2-9. U(VI) Removal by Each Set, Followed by the Percentage of U(VI) Released in the Aqueous Phase, as a Result of Contact with SRS Synthetic Groundwater

Soil Type	U(VI) % Sorbed	U(VI) % Desorbed
Quartz	16±2	109±13
Quartz and Kaolinite	22±1	99±12
Quartz, Kaolinite, Goethite (SRS soil, 180 µm<d<2 mm)	59±6	61±5

The results indicate that when the mineral mixture is comprised of quartz and kaolinite, the amount of uranium removed is much lower compared to the mixture of SRS background soil, suggesting that goethite is the most reactive mineral phase towards U(VI) under circumneutral conditions. Furthermore, the amount of U(VI) sorbed is quantitatively released in the aqueous phase upon contact with SRS synthetic groundwater in the case of quartz and quartz and kaolinite mixtures. On the other hand, desorption was significantly less in the experiments with SRS background soil, which contains goethite as well, indicating that goethite contributes to stronger binding of U(VI). Possible reasons contributing to higher U (VI) sorption and lower desorption may be the higher surface area provided by goethite particles, as well as Fe-U(VI) interactions.

References:

- Bachmaf, S., Merkel, B.J. 2010. Sorption of uranium(VI) at the clay mineral–water interface. *Environmental Earth Sciences*, **63**(5), 925-934.
- Barlett, M. 2014. Uranium reduction and microbial community development in response to stimulation with different electron donors.
- Belli, K.M., DiChristina, T.J., Van Cappellen, P., Taillefert, M. 2015. Effects of aqueous uranyl speciation on the kinetics of microbial uranium reduction. *Geochimica et Cosmochimica Acta*, **157**, 109-124.
- Donlan, R.M. 2002. Biofilms: Microbial Life on Surfaces. in: *Emerg Infect Dis*, Vol. 8.
- Guo, Z., Li, Y., Wu, W. 2009. Sorption of U(VI) on goethite: Effects of pH, ionic strength, phosphate, carbonate and fulvic acid. *Applied Radiation and Isotopes*, **67**(6), 996-1000.
- McLean, J.S., Pinchuk, G.E., Geydebekht, O.V., Bilskis, C.L., Zakrajsek, B.A., Hill, E.A., Saffarini, D.A., Romine, M.F., Gorby, Y.A., Fredrickson, J.K., Beliaev, A.S. 2008. Oxygen-dependent autoaggregation in *Shewanella oneidensis* MR-1. *Environmental Microbiology*, **10**(7), 1861-1876.
- Morales, J.W., Galleguillos, H.c.R., Hernández-Luis, F., Rodríguez-Raposo, R. 2011. Activity Coefficients of NaClO₄ in Aqueous Solution. *Journal of Chemical & Engineering Data*, **56**(8), 3449-3453.
- Rahnemaie, R., Hiemstra, T., van Riemsdijk, W.H. 2006. Inner- and outer-sphere complexation of ions at the goethite-solution interface. *Journal of Colloid and Interface Science*, **297**(2), 379-388.
- Rietra, R.P.J.J., Hiemstra, T., van Riemsdijk, W.H. 2001. Interaction between Calcium and Phosphate Adsorption on Goethite. *Environmental Science & Technology*, **35**(16), 3369-3374.
- Sheng, L., Fein, J.B. 2014. Uranium Reduction by *Shewanella oneidensis* MR-1 as a Function of NaHCO₃ Concentration: Surface Complexation Control of Reduction Kinetics. *Environmental Science & Technology*, **48**(7), 3768-3775.
- Sherwood Lollar, B. 2005. *Environmental Geochemistry*. Elsevier Science, Italy.
- Sigg, L., Stumm, W. 2011. *Aquatic Chemistry*. Vdf Hochschulverlag, Zurich.
- Sverjensky, D.A. 2006. Prediction of the speciation of alkaline earths adsorbed on mineral surfaces in salt solutions. *Geochimica et Cosmochimica Acta*, **70**(10), 2427-2453.
- Thormann, K.M., Saville, R.M., Shukla, S., Pelletier, D.A., Spormann, A.M. 2004. Initial Phases of Biofilm Formation in *Shewanella oneidensis* MR-1. *Journal of Bacteriology*, **186**(23), 8096-8104.

Wellman, D.M., Gunderson, K.M., Icenhower, J.P., Forrester, S.W. 2007. Dissolution kinetics of synthetic and natural meta-autunite minerals, $X_3-n(n)+[(UO_2)(PO_4)]_2 \cdot xH_2O$, under acidic conditions. *Geochemistry, Geophysics, Geosystems*, **8**(11), n/a-n/a.

Worch, E. 2015. *Hydrochemistry: Basic Concepts and Exercises*. De Gruyter, Berlin, Germany.

Wu, C., Cheng, Y.-Y., Yin, H., Song, X.-N., Li, W.-W., Zhou, X.-X., Zhao, L.-P., Tian, L.-J., Han, J.-C., Yu, H.-Q. 2013. Oxygen promotes biofilm formation of *Shewanella putrefaciens* CN32 through a diguanylate cyclase and an adhesin. *Scientific Reports*, **3**, 1945.

Wu, J., Laird, D., Thomson, M. 1999. Sorption and desorption of copper on soil clay components. *Journal of Environmental Quality*, **28**, 334-338.

Zebardast, H.R., Pawlik, M., Rogak, S., Asselin, E. 2014. Potentiometric titration of hematite and magnetite at elevated temperatures using a ZrO₂-based pH probe. *Colloids and Surfaces A: Physicochemical and Engineering Aspects*, **444**, 144-152.

Subtask 2.2. Monitoring of U(VI) Bioreduction after ARCADIS Demonstration at F-Area

Data suggested that there is no sulfate reduction in any of the batches augmented with sulfate and the concentration remained on the level of 500 ppm as originally added to the initial solutions (518-542±14.5 ppm). This might explain why XRD analysis hasn't revealed the formation of pyrite phases. FIU is drafting a paper to summarize the results of the experiments and is collecting all of the information needed to conduct speciation modeling of the microcosm experiment using the Geochemist Workbench software.

Speciation modeling was conducted via Geochemist Workbench (GWB) software. Aqueous speciation and saturation indexes of solid phases are presented in Figure 2-24.

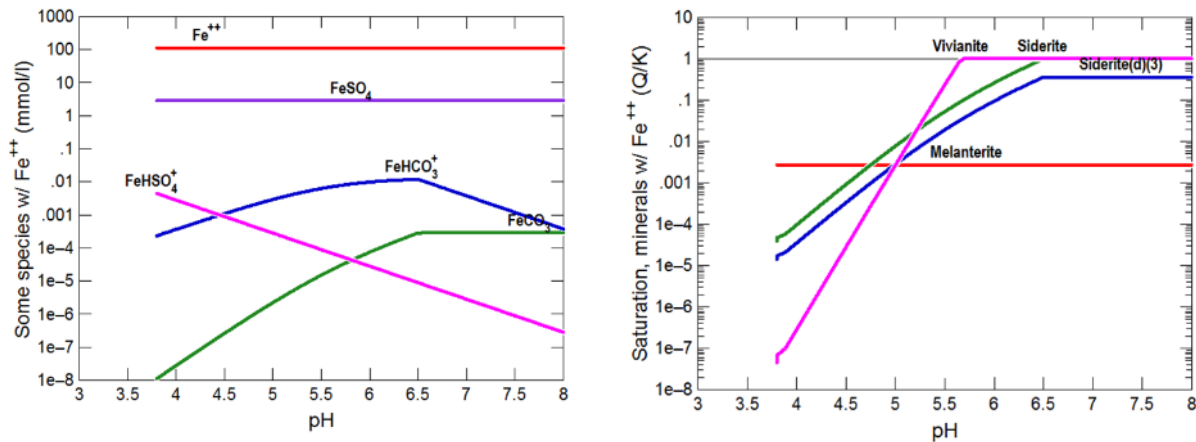


Figure 2-24. Speciation modeling results for conditions mimicking the enhanced anaerobic reductive precipitation (EARP) remediation method previously tested at SRS F/H Area.

Speciation modeling suggested that the formation of siderite is observed at pH ~7. The concentration and weight percentage of siderite is very small. No pyrite formation was observed at any pH tested. Most likely, at acidic pH, ferrous iron will be easily flushed out from the treatment zone since there is no formation of reduced iron solid phases. FIU is continuing to draft a manuscript to publish a summary of the results on the application of this technology for the SRS environmental conditions.

Subtask 2.3: Sorption Properties of Humate Injected into the Subsurface System

During the months of January through March, the desorption experiment of HumaK at different pH values was completed. Initially, the supernatant of the samples was replaced with deionized water at different pH values (from 4 to 8). pH of the samples was adjusted, and samples were homogenized by a vortex mixer. Samples were placed on a platform shaker for five days. During that period of time, pH was checked and adjusted daily by adding either 0.1 M HCl or 0.1 M NaOH. After five days, the samples were centrifuged for 30 min at 2700 rpm. The concentration of HumaK in the supernatant was analyzed by means of UV-vis spectrophotometry. The results of this experiment are presented in the figure below.

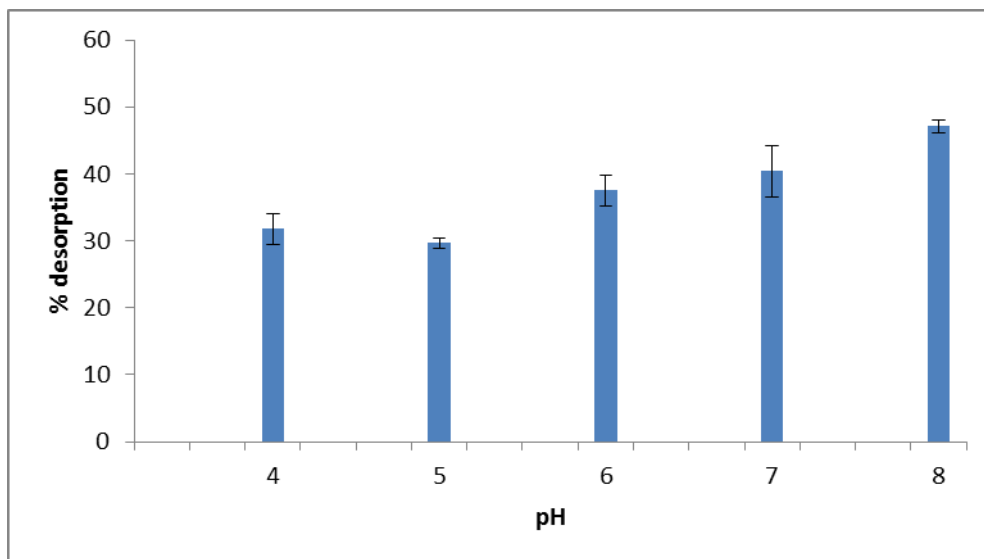


Figure 2-25. Percent desorption versus pH.

From the results, it can be seen that when the pH of the solution is increased, the extent of desorption is increased. The reason for this is that as the pH is increased, there is a decrease of the positive charges at the surface of the sediment that may attract electrostatically the humic molecules. Another possibility is the detaching of the carboxylic and phenolic groups of humic molecules from the surface through a fast exchange with hydroxyl ions. Also, with the increase of pH, there is an increase of the negative charges of the humic substances due to the deprotonation of the carboxyl groups and other functional groups, and this leads to mutual repulsion of humic molecules adsorbed at the surface, enhancing the desorption. All of these factors lead to a net repulsion and to fast movement of the humic molecules away from the surface of the sediments. It is important to notice that the remaining humic substances adsorbed in the sediment are irreversibly adsorbed, probably because these molecules were adsorbed chemically.

The results from this task were presented at the Waste Management Symposia. Hansell Gonzalez, a DOE Fellow, presented a poster titled, “Study of an Unrefined Humate Solution as a Possible Remediation Method for Groundwater Contamination,” in the student poster session. In addition, a professional poster for Waste Management 2016 titled, “Study of an Unrefined Humate Solution as a Possible Remediation Method for Groundwater Contamination,” was completed and presented at the conference. It presents results on the ongoing study of HumaK to provide a detailed characterization of SRS sediments and HumaK, which elucidates the mechanism of HumaK sorption onto SRS aquifer sediments after injection. This poster presents results for the scanning electron microscope with energy dispersive x-ray spectroscopy analysis that were used to investigate the surface morphology and elemental composition of SRS sediments and HumaK. In addition, the data analysis presents data on the results of Fourier transform infrared spectroscopy for the identification of functional groups present in HumaK and SRS sediments (Figure 2-26), and the results of the potentiometric titrations to investigate the acido-basic properties of both materials. Also, the FTIR spectra of HumaK and SRS sediments were reprocessed by using Spekwin32 software. This software allows peak identification, peak labeling, and simultaneously compares the results to known spectra.

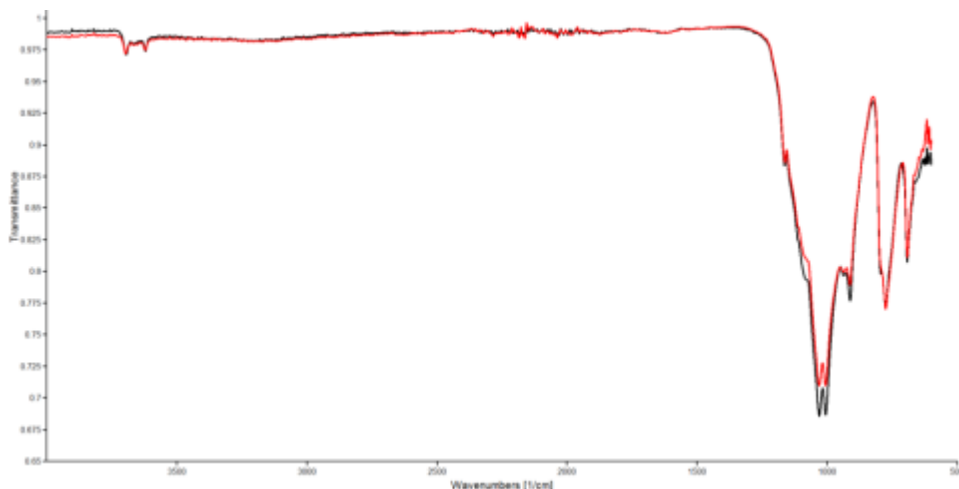


Figure 2-26. FTIR spectra of SRS sediments before adsorption (black line) and after adsorption of HumaK (red line).

By using this software, the spectrum of SRS sediments before the adsorption of HumaK (black line) was compared to the spectrum obtained after the adsorption of HumaK (red line). It is clearly seen that there is a decrease in the peak intensity around the 1000 cm^{-1} region after adsorption of HumaK. This suggests that there was probably a chemical bond formation between the binding sites of the sediment and the functional groups of HumaK.

Work continued on the draft of the manuscript in the Results and Discussion sections (specifically, the part that addresses the effect of pH). This manuscript summarizes all the experimental work done with Huma-K as a low-cost remediation method for acidic groundwater contaminated with uranium and provides discussion on the effect of pH in Huma-K sorption onto SRS sediments, supported with a literature review.

Subtask 2.4. The Synergistic Effect of HA and Si on the Removal of U(VI)

FIU initiated synergy experiments with 30 ppm of humic acid: a fresh stock solutions of 30 ppm humic acid and 3.5 mM of silica were prepared. Triplicate samples of batches containing HA, Si, sediment and uranium at pH 3 and pH 4 were prepared by mixing known amount of various constituents except uranium as shown in Table 2-10 and Table 2-12. Uranium was added prior to pH adjustment and precautions were taken to add the appropriate amount of DIW so that the addition of the acid/base results in a total volume of approximately 20 ml. pH of the samples was adjusted with 0.01M HCl or 0.1M NaOH to desired pH and the samples were placed on a platform shaker. pH of the samples was measured daily and adjusted if different from the original pH (Table 2-11 and Table 2-13). The batches are currently being prepared for KPA analysis, and the data for pH 3 and 4 will be recorded once collected.

Table 2-10. Sample Matrix of 30 ppm HA Batch Samples with amount of acid/base added to achieve pH 3

pH 3 Adjusted Set		Constituents							
		SiO ₂	Humic Acid (HA)	Sediments	Uranium U (VI)	Vol of acid/base	DIW	pH	
		ml	ml	mg	ml	ml	ml	Initial	Final
Batch No. 2	2.1	2.1	6	0	0.01	1.80	10.50	4.35	3.03
	2.2					1.75	10.50	4.31	3.01
	2.3					1.80	10.45	4.52	3.03
Batch No. 3	3.1	0	6	0	0.01	1.60	12.75	4.12	3.03
	3.2					1.65	12.75	4.33	3.01
	3.3					1.60	12.80	4.24	3.03
Batch No. 5	5.1	2.1	6	400	0.01	2.16	10.85	4.41	2.96
	5.2					2.23	10.60	4.18	2.97
	5.3					4.39	10.60	4.30	2.98
Batch No. 6	6.1	0	6	400	0.01	3.28	12.39	4.32	2.98
	6.2					3.00	12.59	4.36	2.97
	6.3					2.80	12.69	4.31	3.01

Table 2-11. Change in pH of Samples over Time for pH 3 Batches

Sample #		pH						
		Day 1	Day 2	Day 3	Day 4	Day 5	Day 6	Day 7
Batch No. 2	2.1	4.35	3.07	3.02	3.14	3.11	3.03	3.03
	2.2	4.31	3.04	3.06	3.07	3.08	3.01	3.01
	2.3	4.52	2.99	3.13	3.05	3.09	3.03	3.03
Batch No. 3	3.1	4.12	3.08	3.10	3.07	3.03	3.03	3.03
	3.2	4.33	3.06	3.06	3.06	3.06	3.06	3.06
	3.3	4.24	3.09	3.05	3.07	3.03	3.03	3.03
Batch No. 5	5.1	4.41	3.16	3.15	2.96	2.96	2.96	2.96
	5.2	4.18	3.12	3.06	3.08	2.91	2.91	2.91
	5.3	4.30	3.14	2.88	3.24	2.68	2.68	2.68
Batch No. 6	6.1	4.32	3.22	3.06	3.23	2.73	2.73	2.73
	6.2	4.36	3.20	3.09	3.19	2.78	2.78	2.78
	6.3	4.31	3.21	3.09	3.18	2.80	2.80	2.80

Table 2-12. Sample Matrix of pH 4 Batch Samples

pH 4 Adjusted Set		Constituents							
		SiO ₂	Humic Acid (HA)	Sediments	Uranium U (VI)	Vol of acid/base	DIW	pH	
		ml	ml	mg	ml	ml	ml	Initial	Final
Batch No. 2	2.1	2.1	6	0	0.01	1.04	11.25	4.68	4.28
	2.2					1.51	11.25	4.72	4.04
	2.3					0.23	11.25	4.56	4.03
Batch No. 3	3.1	0	6	0	0.01	0.30	13.25	4.59	4.04
	3.2					0.20	13.25	4.51	3.88
	3.3					0.20	13.25	4.55	4.00
Batch No. 5	5.1	2.1	6	400	0.01	0.25	11.20	4.72	4.03
	5.2					0.25	11.20	4.66	4.00
	5.3					0.23	11.20	4.59	4.06
Batch No. 6	6.1	0	6	400	0.01	0.26	13.25	5.29	4.07
	6.2					0.25	13.25	4.75	3.96
	6.3					0.26	13.25	4.69	4.01

Table 2-13. Change in pH of Samples

Sample #		pH						
		Day 1	Day 2	Day 3	Day 4	Day 5	Day 6	Day 7
Batch No. 2	2.1	4.68	4.11	4.13	4.18	4.23	4.67	4.28
	2.2	4.72	9.15	4.06	4.12	4.02	4.06	4.04
	2.3	4.56	4.40	4.01	4.00	4.01	3.93	4.03
Batch No. 3	3.1	4.59	4.30	4.05	4.01	4.17	3.99	4.04
	3.2	4.51	4.24	4.04	3.98	4.04	4.07	3.98
	3.3	4.55	4.30	4.05	4.00	4.03	4.02	4.00
Batch No. 5	5.1	4.72	4.13	4.07	4.05	4.02	4.03	4.03
	5.2	4.66	4.21	4.05	4.04	4.02	4.00	4.00
	5.3	4.59	4.22	4.06	4.05	4.08	4.06	4.06
Batch No. 6	6.1	5.29	4.03	4.03	4.07	4.11	4.07	4.07
	6.2	4.75	4.18	4.06	4.11	3.96	3.96	3.96
	6.3	4.69	4.16	4.05	4.12	4.01	4.01	4.01

The research for this task was presented at WM2016 as a poster titled, “Synergetic Interactions between Uranium, Humic Acid, Silica Colloids and SRS Sediments at Variable pH,” in session 71A Posters: Environmental Remediation Analysis, Technology and Treatment Systems at Waste Management Symposia 2016. **This poster won the Best in Track #7 poster presentation and is eligible to win the “Best of 2016 Conference Poster Presentation” award.**

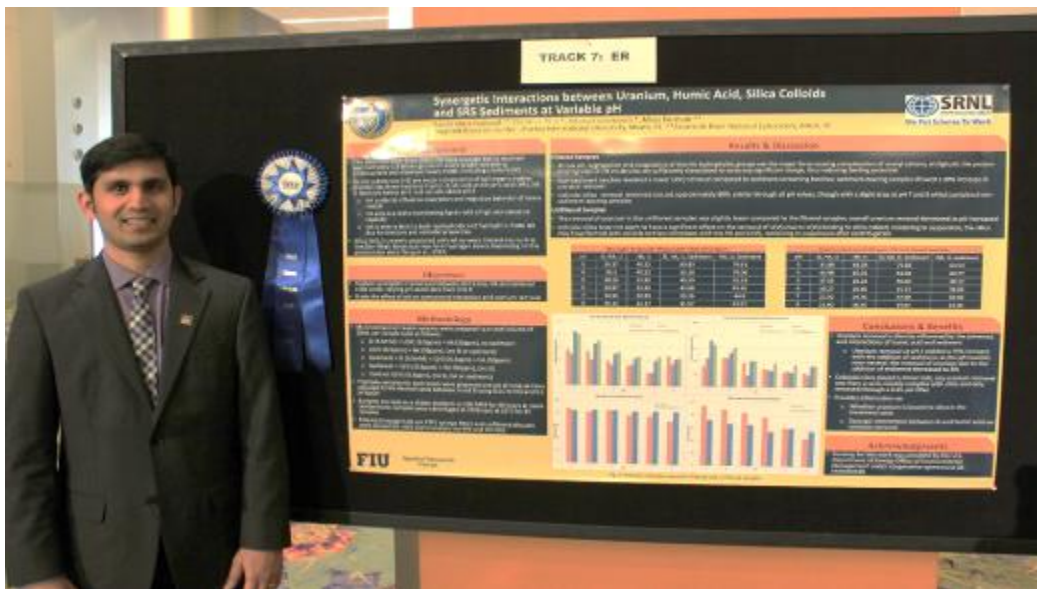


Figure 2-27. WM poster presented by Dr. Ravi Gudavalli that was awarded best in track #7.

FIU continued preparation of samples for analysis via KPA and ICP to measure the concentration of uranium and silica, respectively. In addition, a draft progress report summarizing the accomplishments under this task was initiated. DOE Fellow Alexis Smoot prepared a poster based on this research to be presented at the Life Sciences South Florida STEM Undergraduate Research Symposium at Broward College on April 2, 2016.

Subtask 2.5. Investigation of the Migration and Distribution of Natural Organic Matter Injected into Subsurface Systems

The work completed for this task will assemble, integrate, and develop a practical and implementable approach to quantify and simulate potential natural organic matter (NOM, such as humic and fulvic acids, humate, etc.) deployment scenarios over the range of conditions at DOE sites. Initial laboratory experiments and an initial set of simplified models have been developed at SRNL. Under this task, additional batch and column studies and testing will be conducted at FIU to provide the transport parameters for an extension of the current model scenarios. The following was accomplished during the quarter of January 2016 - March 2016:

1. Columns 1 & 2 were dismantled and several soil samples were collected for SEM-EDS and TOC analyses. Results of the EDS analysis of the Column 1 samples were reported in the last quarterly report.
2. Approximately 1.5 grams of soil from various sections of the two columns was oven dried and ground to obtain fine particles. Samples were sent to FIU's Southeast Environmental Research Center (SERC) for TOC analysis to get quantitative data of humic acid retained in the columns.
3. A proposed experimental procedure was developed to be submitted to the FIU Radiation Control Committee for approval as uranium will now be used in the column studies
4. Humate injection scenarios were updated to include 0.5 PV of Huma-K as opposed to 1 PV previously used. These scenarios will help identify optimum Huma-K concentrations and flow rates to be used in the column experiments. After discussing with SRNL collaborators, 10,000 ppm of Huma-K at 2 ml/min was chosen.

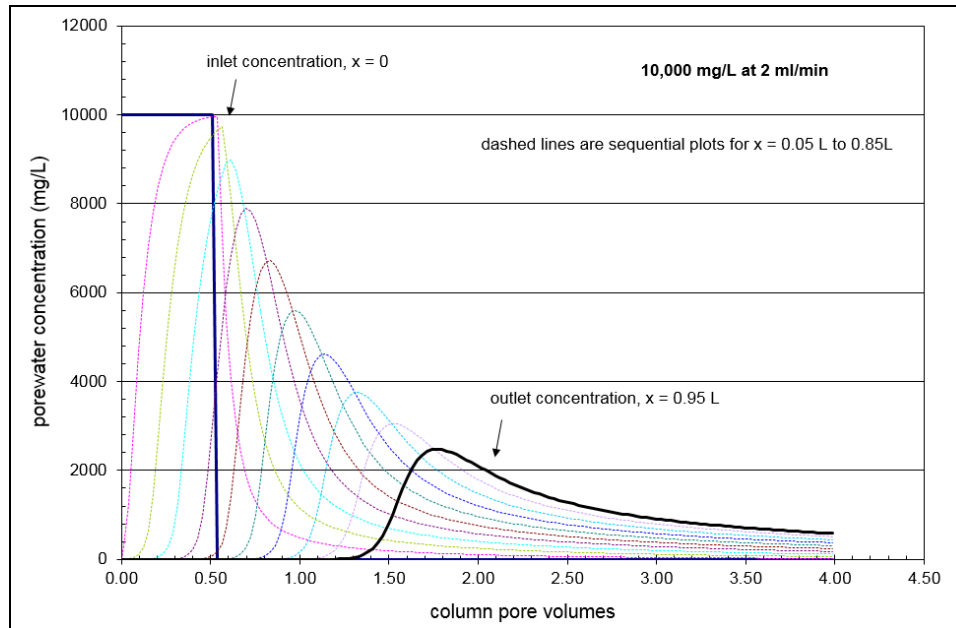


Figure 2-28. Humate injection scenario for 10,000 mg/L at 2 ml/min.

5. A poster entitled, "Migration and Distribution of Natural Organic Matter Injected into Subsurface Systems," that is based on this research was presented in poster session 71B: Environmental Remediation Analysis, Technology and Treatment Systems at the 2016 Waste Management Symposium.

Migration and Distribution of Natural Organic Matter Injected into Subsurface Systems at F/H Area at Savannah River Site

Ravi Gudavalli, Kiara Pazan, Miles Denham, Brian Looney

Applied Research Center, Florida International University, Miami, FL, Savannah River National Laboratory, Aiken, SC

Background

- The Savannah River Site's F/H Area seepage basins received approximately 1.8 billion gallons of low level acidic waste solutions containing dissolved metals and radionuclides
- Significant quantities of uranium isotopes, iodine-129, Tc-99, and tritium migrated into the groundwater, creating an acidic plume with a pH between 3 and 5.5
- Studies have shown humate to be a potential approach for controlling mobility of contaminants as U is expected to sorb strongly onto humate-loaded sediments at mildly acidic pH
- Huma-K is an unfractionated humic substance high in humic and fulvic compounds, made from Leonardite, an organic-rich mineral formed due to decomposition by microorganisms

Objectives

- To evaluate the potential use of Huma-K to enhance attenuation of uranium in the acidic F-Area aquifer
- To study the migration and distribution of Huma-K injected into subsurface systems via column experiments
- Obtain sorption and desorption parameters under different pH levels

Materials and Methods

Soil Characterization of SRS's F-Area soil

- Bulk Density: 1.33 g/cm³
- Porosity: 0.495
- Particle Density: 2.65 g/cm³
- Soil pH: 4.06

Humate Injection Scenarios: A Langmuir model was used to simulate and observe breakthrough curves to determine optimal Huma-K concentration and flow rate

Results and Discussion

Bromide Tracer Tests:

- A conservative bromide tracer was injected to determine the column's pore volume (PV) and transport parameters

Column	Recovery (%)	PV (mL)	Variance, σ^2	P_0	Retardation Factor	K_d (L/kg)
1	98.2559	85.80	107.24	33.3	1.35	0.13
2	100.511	74.12	63.34	42.35	1.46	0.17

Sorption/ Desorption of Huma-K:

- 1 PV of 5000 ppm of Huma-K with adjusted pH 9 was injected into preconditioned columns of pH 3.5 and 5, followed by 4 PV of artificial groundwater (AGW)
- Effluent samples were collected at regular intervals and HA concentrations were measured using a UV-VIS spectrophotometer

➢ Breakthrough curves show most humate injected was retained until after 1.5 PV of AGW, where concentration peaked at 6000 ppm and 5700 ppm for Columns 1 and 2, respectively (Fig. 7)

- A possible explanation is the precipitation/re-dissolution of humate as it moves through the column

Results and Discussion (Cont.)

- Column 1 had a stronger pH gradient. After initial injection, pH is low and humate has precipitated and significantly sorbed. As AGW flows through, it dissolves precipitated HA and desorbs HA. Thus, there is higher concentration of HA eluting from Column 2 than Column 1 in 2nd PV.
- The high 5000 ppm HA concentration may have the buffering capacity to bind more protons in solution and raise pH faster for Column 1 because of the strong pH gradient

Column	pH		Humic Acid		
	Initial	Final	Injected (mg)	Recovered (mg)	Retained (mg)
1	3.72	6.46	576.03	457.14	118.89
2	4.77	7.08	521.52	350.06	171.46

Benefits

- Understand the sorption of humic acid onto SRS sediments and its effectiveness on uranium mobility in the subsurface
- The research will provide coupling between flow and transport of the contaminant in the subsurface and will investigate the spatial and temporal changes within the subsurface to simulate the response of the system after injection of humate.

Conclusions

- Overall, more HA was retained in column 2, which was preconditioned with a pH 5 AGW solution, than in column 1, which had pH 3.5. The increase in pH increased in the retention of HA by 180 mg per kg of soil. The results were different than expected due to the unanticipated effects of precipitation and dissolution because of mechanical and physicochemical factors.

Future Work

- Perform total organic carbon (TOC) analysis for sediments from columns to estimate the distribution of Huma-K.
- Inject uranium into the soil columns to study the effect of sorbed humic acid on the mobility of uranium through porous media.

Acknowledgements

- This research is sponsored by the U.S. Department of Energy Office of Environmental Management under cooperative agreement # DE-EM000598.

Figure 2-29. Poster presented at waste management symposium 2016 on migration and distribution of humic acid

6. TOC analysis was performed with 10 mg of a finely ground sample of soil from each column. Sample concentrations were below the detection limit. The analysis will be repeated with 40 mg soil samples to overcome the detection limit.
7. Testing and calibration of the new pump to be used in the column experiments was initiated. The tubing used only achieved a 0.86 ml/min flow rate. New tubing was obtained to achieve the required 2 ml/min flowrate.
8. DOE Fellow Sarah Bird supporting this task prepared a poster based on this research at the Life Sciences South Florida STEM Undergraduate Research Symposium to be held at Broward College on April 2, 2016.

Task 3: Surface Water Modeling of Tims Branch

Task 3 Overview

This task will perform modeling of surface water, and solute/sediment transport specifically for mercury and tin in Tims Branch at the Savannah River Site (SRS). This site has been impacted by 60 years of anthropogenic events associated with discharges from process and laboratory facilities. Tims Branch provides a unique opportunity to study complex systems science in a full-scale ecosystem that has experienced controlled step changes in boundary conditions. The task effort includes developing and testing a full ecosystem model for a relatively well defined system in which all of the local mercury inputs were effectively eliminated via two remediation actions (2000 and 2007). Further, discharge of inorganic tin (as small micro-particles and nanoparticles) was initiated in 2007 as a step function with high quality records on the quantity and timing of the release. The principal objectives are to apply geographical information systems and stream/ecosystem modeling tools to the Tims Branch system to examine the response of the system to historical discharges and environmental management remediation actions.

Task 3 Quarterly Progress

Subtask 3.1. Modeling of Surface Water and Sediment Transport in the Tims Branch Ecosystem

- Following the implementation of the overland flow module, further development of the MIKE SHE surface water model of the Tims Branch watershed continued in January with focus on completion of milestone 2015-P2-M3, “Complete input of MIKE SHE model configuration parameters for simulation of evapotranspiration (Subtask 3.1),” due 2/29/16. Dr. Mahmoudi and her students are reviewing and preparing the configuration parameters required by the MIKE SHE model for simulation of evapotranspiration.
- Delineation of the cross sections of Tims Branch using ArcGIS has also continued to progress with the aid of DOE Fellow Christopher Strand, for input into MIKE 11 to develop the stream network.
- In parallel, the search for groundwater timeseries data to develop the groundwater table for the MIKE SHE model continued for the next phase of development of the MIKE SHE model.

- FIU also continued developing the SWAT model to assess the annual and seasonal distribution and characteristics of hydrological processes in the Tims Branch watershed. He has set up the hydrologic response units (HRUs) and input the required soil and hydrological parameters. He is currently trying to calibrate the SWAT model using various algorithms to minimize the gap between observed and simulated results.
- FIU has reforecasted the milestones and deliverables associated with the SRS surface water modeling of Tims Branch task forward one month through the end of this performance year, as shown in the FIU Performance Year 6 Milestones and Deliverables for Project 2 table below, due to technical difficulties related to a server failure at ARC during the last week of January 2016, which caused the loss of many of the data files being developed in support of this research task. Data recovery efforts were pursued but failed to salvage the lost files. The reforecast dates will allow the research team the time needed to regenerate the missing data files and complete the proposed tasks. As such, milestone 2015-P2-M3, complete input of MIKE SHE model configuration parameters for simulation of evapotranspiration (Subtask 3.1), which was due on February 29, 2016 was reforecast to March 31, 2016.
- With assistance from the ARC information technology team, a plan has been devised going forward to avoid any similar issues from arising. All data associated with this task will be moved to a shared folder on an FIU Engineering Information Center (EIC) server which will be backed up regularly on an automatic basis. Technical support for this server will be provided, as needed, from the FIU Department of Engineering and Computing. The shared folder will have access restricted to the ARC research team supporting this task.
- The month of February was focused upon retrieval of lost input parameters required for model development.
- Efforts in February were also geared towards the completion of posters related to this research to be presented at the 2016 Waste Management Symposia in both the professional and student tracks during the week of March 6-10, 2016.
- FIU worked on regenerating several data files required for model development that were lost due to a server failure at ARC during the last week of January 2016. Despite this setback, FIU was able to complete milestone 2015-P2-M3, complete input of MIKE SHE model configuration parameters for simulation of evapotranspiration (ET) (Subtask 3.1), by the reforecast due date of March 31, 2016. An email was sent to SRNL and DOE HQ personnel to mark the completion of this milestone and provide a brief update on the progress of the model development.
- The following provides details of the ET module setup:
 1. The ET module was developed using two methods: Richards Equation and Two Layer Evapotranspiration/Unsaturated Zone (ET/UZ).
 2. Two methods were used in module development: (a) uniform data of reference ET, Leaf Area Index, and Root Depth; and (b) station-based timeseries which requires timeseries of reference ET, and station-based rainfall records.
 3. Timeseries of rainfall records were acquired from the SRS database.

4. Station-based timeseries of rainfall data from various stations within South Carolina were obtained to generate rainfall grids in MIKE SHE. This data was processed prior to input into the relevant MIKE SHE module.
5. Station-based timeseries of reference ET was acquired from stations within Aiken County near SRS. This data was processed in accordance with MIKE SHE requirements.
6. Table 2-14 shows some of the parameters used in the ET module. These values are based on numerical stability criteria and experimental measurements reported in the literature:

Table 2-14. ET Module Parameters

Parameter	Value	Units
Detention Storage	2.5	mm
Surface-Subsurface Leakage Coefficient	0.0001	1/sec
Reference Evapotranspiration	2.22	mm/day
Leaf Area Index	1.3 – 6.3	m ² / m ²
Root Depth	0.0 – 4000	mm

7. Simulation of overland flow in MIKE SHE requires both ET and UZ modules to be fully developed and active. The UZ module will be completed by the next milestone due on April 29, 2016. Meanwhile the FIU hydrology team at ARC will continue with the model development and data assimilation.
- Several posters related to this research were also presented at the 2016 Waste Management Symposia in both the professional and student tracks during the week of March 6-10, 2016.

Subtask 3.2. Application of GIS Technologies for Hydrological Modeling Support

- DOE Fellow Natalia Duque developed a GIS shapefile to represent the initial water depth in the Tims Branch watershed and has been working on developing an ArcGIS ModelBuilder process flow model to automate this process so it can be used in future for other areas.
- In addition, FIU began conducting a literature review to assist in an analysis of the possible hydrological impact of land use/land cover change in the Tims Branch watershed using an integration of remote sensing, GIS, statistical methods and hydrological modeling. Some of the documents currently under review include:
 1. Butt, A., Shabbir, R., Ahmad, S. S., & Aziz, N. (2015). Land use change mapping and analysis using Remote Sensing and GIS: A case study of Simly watershed, Islamabad, Pakistan. *The Egyptian Journal of Remote Sensing and Space Science*, 18(2), 251-259. doi:http://dx.doi.org/10.1016/j.ejrs.2015.07.003
 2. Hegazy, I. R., & Kaloop, M. R. (2015). Monitoring urban growth and land use change detection with GIS and remote sensing techniques in Daqahlia governorate Egypt.

3. Horn, S. Using a GIS to determine how different types of land cover have changed over time in the State of Connecticut.
 4. Jasrotia, A. S., & Kumar, A. (2014). Groundwater Quality Mapping Based on the Geographical Information System (GIS) of Jammu District, Jammu and Kashmir India. *Journal of Spatial Hydrology*, 12(1).
 5. Petchprayoon, P., Blanken, P. D., Ekkawatpanit, C., & Hussein, K. (2010). - Hydrological impacts of land use/land cover change in a large river basin in central–northern Thailand. - 30(- 13), - 1930.
 6. Rawat, J. S., & Kumar, M. (2015). Monitoring land use/cover change using remote sensing and GIS techniques: A case study of Hawalbagh block, district Almora, Uttarakhand, India. *The Egyptian Journal of Remote Sensing and Space Science*, 18(1), 77-84. doi:<http://dx.doi.org/10.1016/j.ejrs.2015.02.002>
- Due to the server failure resulting in the loss of data as described above, the month of February was dedicated to retrieving and compiling original data files and redeveloping ArcGIS ModelBuilder process flow models to assist with the automation and batch processing of several of the data files required for hydrological model development, and to speed up the data regeneration process.
 - Efforts were also geared towards the completion of posters related to this research to be presented at the 2016 Waste Management Symposia in both the professional and student tracks during the week of March 6-10, 2016.
 - FIU spent the month of March continuing to retrieve and compile original data files that were lost due to the server failure as mentioned above, to support the modeling work and development of the evapotranspiration module. The ArcGIS ModelBuilder process flow models were regenerated and applied to automate and batch process several of the required input parameters and to speed up the data regeneration process.
 - Posters related to this subtask were also presented at the 2016 Waste Management Symposia in both the professional and student tracks during the week of March 6-10, 2016.

Subtask 3.3. Biota, Biofilm, Water and Sediment Sampling in Tims Branch

A conference call was held between FIU and Dr. John Seaman from SREL on January 27, 2016 to follow up on the collaborative efforts to conduct sampling and collect measurements of environmental parameters in Tims Branch to support the hydrological model development. An ISCO system was purchased by SREL which was received in late December 2015. The unit is equipped with a velocity meter and geochemical probes and will be deployed in Tims Branch just below Steed Pond. Sediment and water samples will be collected periodically while field measurements such as pH, ORP, temperature, flow velocity, etc. will be transmitted via a wireless network to facilitate the download of real-time data. The data collected will be shared with FIU to assist with model calibration. Furthermore, Dr. Seaman has agreed to support FIU's research by collecting additional water and sediment samples for tin analysis.

For FIU to calibrate the hydrological model, timeseries data such as stream flow velocity and other relevant parameters at various locations along Tims Branch will be very useful. As such,

FIU will coordinate with SREL to collect additional in-situ data parameters using hand-held field measurement devices. Dr. Mahmoudi will identify/map out key points along the Tims Branch stream for data collection and coordinate with Dr. Seaman with respect to the parameters required, the frequency of data collection and who will collect the data. FIU anticipates student support for this effort during the DOE Fellows 2016 summer internships stationed at SRS/SRNL. Dr. Seaman has joined the monthly conference calls between FIU and DOE-HQ (EM-12/EM-13) and SRS/SRNL points of contact in order to maintain communication and encourage dialogue related to the sampling and data collection required to support model development.

Task 4: Sustainability Plan for the A/M Area Groundwater Remediation System

Task 4 Overview

The research and analysis performed under this task is being performed to support DOE EM-13 (Office of D&D and Facilities Engineering) under the direction of Mr. Albes Gaona, program lead for DOE's Sustainable Remediation Program. This task and associated research was completed and a draft report submitted on 12/18/15.

Subtask 4.1. Sustainable Remediation Analysis of the M1 Air Stripper

The goal of the SRS M Area groundwater remediation system is to provide hydraulic containment of the contaminated groundwater. The focus of FIU's analysis for improved sustainability of the M Area groundwater remediation system is to provide analyses and recommendations for improving the electro-mechanical components and operations of this remediation system (e.g., air stripper, pumps). These improvements should result in a more sustainable system that saves energy, cuts greenhouse gas emissions, and saves financial and other resources.

- This task was completed and a technical report submitted to DOE and SRNL on Dec. 18, 2015 entitled, "A Sustainability Analysis for the M1 Air Stripper and Pumps of the M Area Groundwater Remediation System at the Savannah River Site." In addition, DOE Fellow Yoel Rotterman presented a student poster at the Waste Management Symposium (March 6-10, 2016) based upon data and analyses in this report.
- No additional effort is planned on this task.

Task 5: Remediation Research and Technical Support for WIPP

Task 5 Overview

This new task is in collaboration with research scientists Donald Reed and Timothy Dittrich in support of Los Alamos National Laboratory's field office in Carlsbad, New Mexico. This research center has been tasked with conducting experiments in the laboratory to better understand the science behind deep geologic repositories for the disposal of nuclear waste. The majority of their work is conducted in high ionic strength systems relevant to the Waste Isolation Pilot Plant (WIPP) located nearby. WIPP is currently the only licensed repository for the disposal of transuranic (TRU) defense waste in the world. However, the facility is not currently operating following an airborne release from a waste drum which failed to contain waste following an exothermic reaction of the waste. This was due to incompatibility of mixed waste received from LANL (organic adsorbent mixed with nitrate salt waste). The off-site releases of

$^{239/240}\text{Pu}$ and ^{241}Am detected were only slightly above background and were still below public exposure limits. However, FIU-ARC is now initiating a new task to support the basic research efforts requested to update risk assessments for the WIPP site as it moves towards restarting operations.

The objective of this task is to support LANL researchers in the basic science research required to address concerns in risk assessment models for the re-opening of the WIPP site for acceptance of defense waste.

Task 5 Quarterly Progress

During the month of January, plans for Dr. Hilary Emerson to travel to Los Alamos National Lab's Carlsbad Environmental Monitoring and Research Center (CEMRC) Carlsbad facilities were finalized with collaborators at Los Alamos, including travel, housing and radiation worker training. Dates of travel were February 15 to April 8, 2016.

Characterization was begun for the mineral samples received from WIPP at FIU on February 2, 2016, including X-ray diffraction (XRD), scanning electron microscopy (SEM) with energy dispersive spectroscopy (EDS), and BET surface area analysis. The samples received were clean (non-radioactive) rock and clay mineral samples from near the WIPP site. The rock samples were crushed in a percussion mortar and pestle, sieved and washed prior to being sent to FIU ARC for analysis. Analysis was begun on the three highest priority samples including: 1) Culebra formation, 355-500 μm size fraction; 2) Magenta formation, 355-500 μm size fraction; and 3) residual clay fines. The first two fractions were the highest priority as they are the ideal size fraction for the planned column experiments and minerals of interest to the WIPP. The clay fraction is of interest in the event that batch experiments are conducted during the FIU ARC guest appointment at Carlsbad Environmental Monitoring & Research Center (CEMRC).

The Culebra formation is consistent with dolomite based on the SEM EDS and XRD as shown in Figures 2-30 and 2-31. Further, the EDS analysis did not show significant impurities although analysis of more locations will be required to be statistically significant. The Magenta formation was more complex with significant impurities observed in the EDS [Mg (15-49%), Al (2-15%) and Si (66-4%), S (0-46%), Fe, per Figures 2-32 and 2-33] and an XRD pattern that was not consistent with dolomite. Additional work will be required to properly index the XRD spectra with the PDF library. Although the XRD pattern for the residual clay sample has not yet been indexed, the EDS analysis (Figure 2-34) of several locations shows that the minerals are largely composed of Mg, Al and Si with some locations having several atomic percent of Fe.

Element	Wt%	At%
CK	10.55	19.97
OK	28.08	39.92
MgK	14.35	13.43
CaK	47.02	26.68

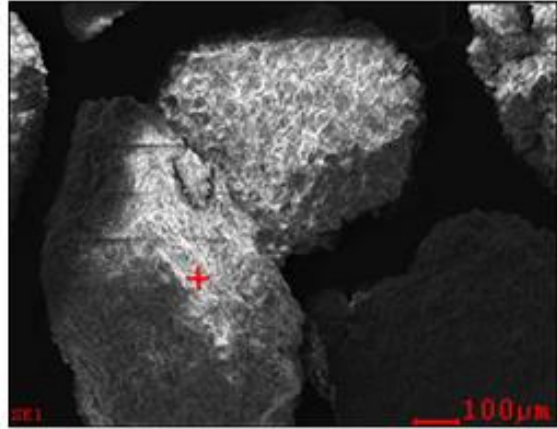


Figure 2-30. Representative SEM EDX analysis of Culebra formation, 355-500 μm size fraction, consistent with dolomite.

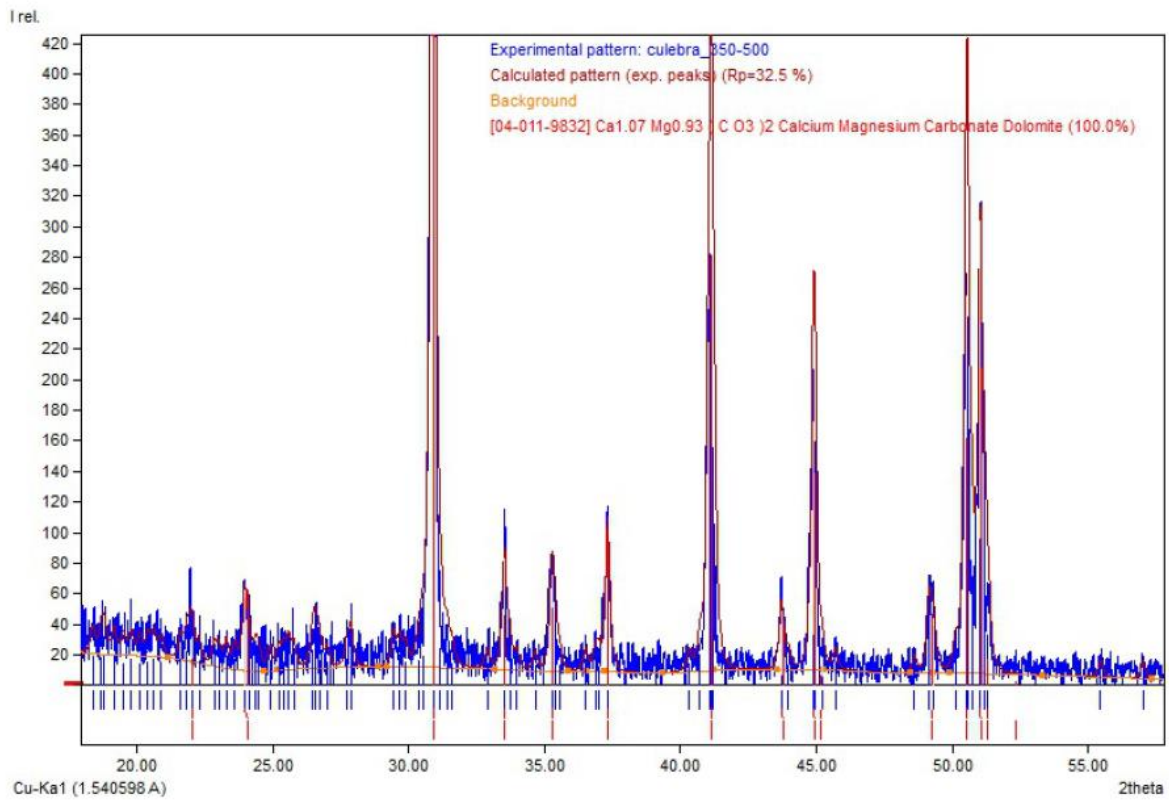


Figure 2-31. XRD spectra with reference spectra from Culebra formation, 355-500 μm size fraction for dolomite (Match! Software).

Element	Wt%	At%
NaK	00.40	00.63
MgK	00.38	00.57
AlK	00.21	00.28
SiK	00.54	00.70
SK	41.09	46.21
CaK	57.38	51.62

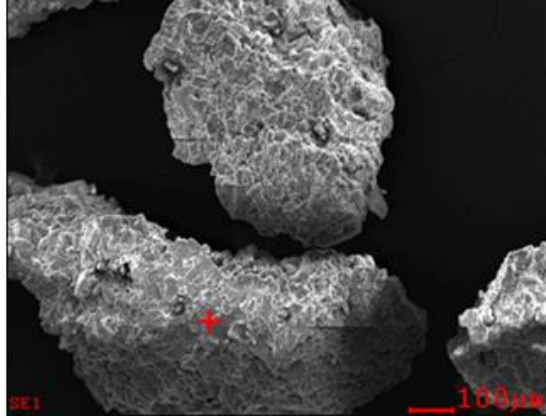


Figure 2-32. SEM EDS spectra of Magenta formation, 355-500 μm size fraction, with S impurities (JEOL 6330F FEG-SEM with EDS) [Note: C and O excluded from EDS].

Element	Wt%	At%
NaK	00.11	00.13
MgK	12.71	14.91
AlK	10.32	10.91
SiK	65.38	66.40
KK	01.90	01.39
CaK	06.77	04.82
FeK	02.82	01.44

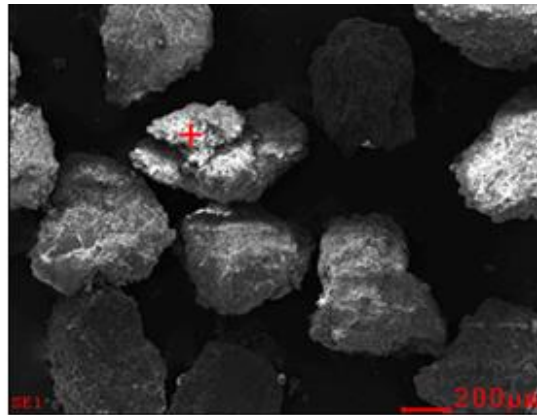


Figure 2-33. SEM EDS spectra of Magenta formation, 355-500 μm size fraction, with Al/Si impurities consistent with clay minerals (JEOL 6330F FEG-SEM with EDS) [Note: C and O excluded from EDS].

Element	Wt%	At%
NaK	01.54	01.94
MgK	26.90	31.96
AlK	15.19	16.26
SiK	40.19	41.34
ClK	01.29	01.05
KK	04.43	03.27
FeK	03.82	01.98

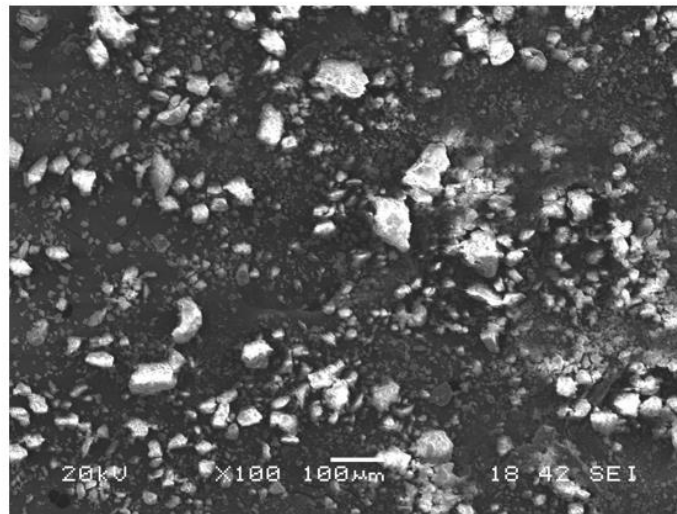
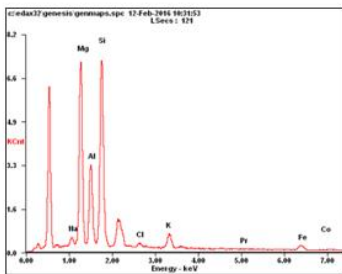


Figure 2-14. Representative SEM EDS spectra of residual clay materials (JEOL 6330F FEG-SEM with EDS), major elements include Mg, Al and Si [Note: C and O are excluded from EDS].

Hilary Emerson (FIU ARC) arrived in Carlsbad on February 14, 2016, to begin the collaborative work with Timothy Dittrich and Don Reed of the CEMRC Actinide Chemistry and Repository Science Program (ACRSP). She has completed the requirements to begin working in the facilities, including: bioassay, whole body and lung count and required health and safety training (including Radiation Worker II). In addition, batch sorption experiments for Nd(III) to dolomite [5 g/L, 25 g/L and 100 g/L] at variable ionic strength [0.01 M NaCl to 1.0 M NaCl] and mini column experiments were initiated beginning with equilibration of the dolomite (Culebra formation 355 – 500 μm).

Based on several lessons learned discussed below from the initial scoping experiments and speciation modeling via Visual Minteq, all current and future experiments are to be completed at 20 ppb Nd(III) and in the presence of a 3 mM NaHCO_3 buffer. Further, in addition to the scoping experiments outlined above, results are presented for 0.1 M ionic strength [0.003 M NaHCO_3 + 0.097 M NaCl] and 20 ppb Nd(III) for a long-term mini column experiment and additional kinetic batch experiments at 5 g/L of dolomite in triplicate.

Preliminary Batch Experiments

Preliminary results for batch experiments for 150 ppb Nd(III) in 0.01 and 1.0 M NaCl in the presence of 5, 25 and 100 g/L dolomite are presented in Figure 2-34. These experiments were conducted in duplicate and error bars represent the standard deviation of the duplicates. The aqueous phase was analyzed by inductively coupled plasma mass spectrometer (Agilent 7900, ICP-MS) following centrifugation for 20 minutes at 8000 rpm.

The initial target pH for these experiments was pH 7.5. However, the dolomite solid quickly buffered the system to a pH of 9.21 ± 0.06 and 9.43 ± 0.06 for the 0.01 and 1.0 M NaCl solutions, respectively. Therefore, the experimental controls (no dolomite) were not representative due to the pH fluctuations and the increase in aqueous carbonate due to mineral dissolution. Further, the recovery for Nd in the blanks is <30% and were not accounted for in K_d calculations in Figure 2-34. In addition, it is likely that the aqueous phase was not in equilibrium with atmospheric carbonate. Because initial experiments were designed for pH 7.5 and assumed equilibration with the atmosphere for initial solubility estimates, it is likely that precipitation also occurred in batch experiments in the presence of dolomite.

Figures 2-34 to 2-36 present the Nd(III) aqueous speciation and solubility in equilibrium with atmospheric carbonate (Figure 2-34) and without carbonate (Figure 2-35). Further, the total aqueous solubility is compared in Figure 2-36. Based on these simulations, a solubility of 190 – 9000 ppb is predicted at pH 7.5 and 0.2 – 360 ppb for pH 9.5 (with the lower range without carbonate and the upper range with carbonate present).

Based on these simulations and experiments, additional batch experiments will be conducted with 20 ppb Nd(III) at pH 8 – 8.5 with 3 mM NaHCO_3 to reach near the aqueous concentrations of bicarbonate in equilibrium with the atmosphere and increase the buffering capacity of suspensions to allow for a more stable pH throughout experiments. This is based on Figure 2-37 for 0.1 M NaCl. However, simulations were run for other ionic strengths (0.001 – 1 M NaCl) with similar results.

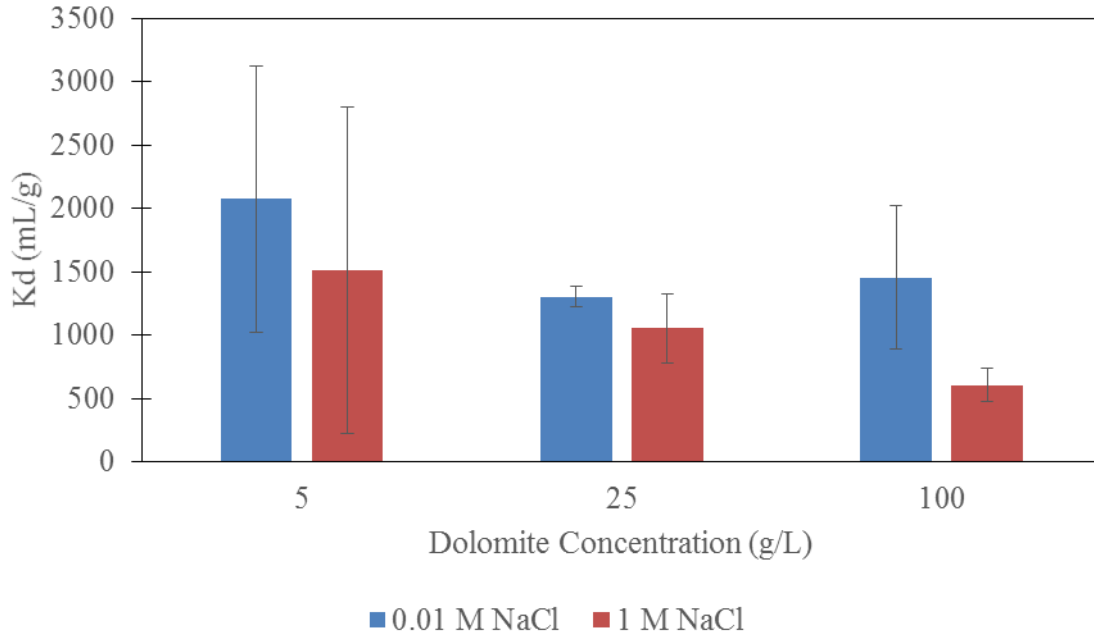


Figure 2-34 Results from batch sorption experiments in the presence of 150 ppb Nd(III) as a comparison of partitioning coefficients, Kd's (mL/g) with respect to dolomite concentration (g/L).

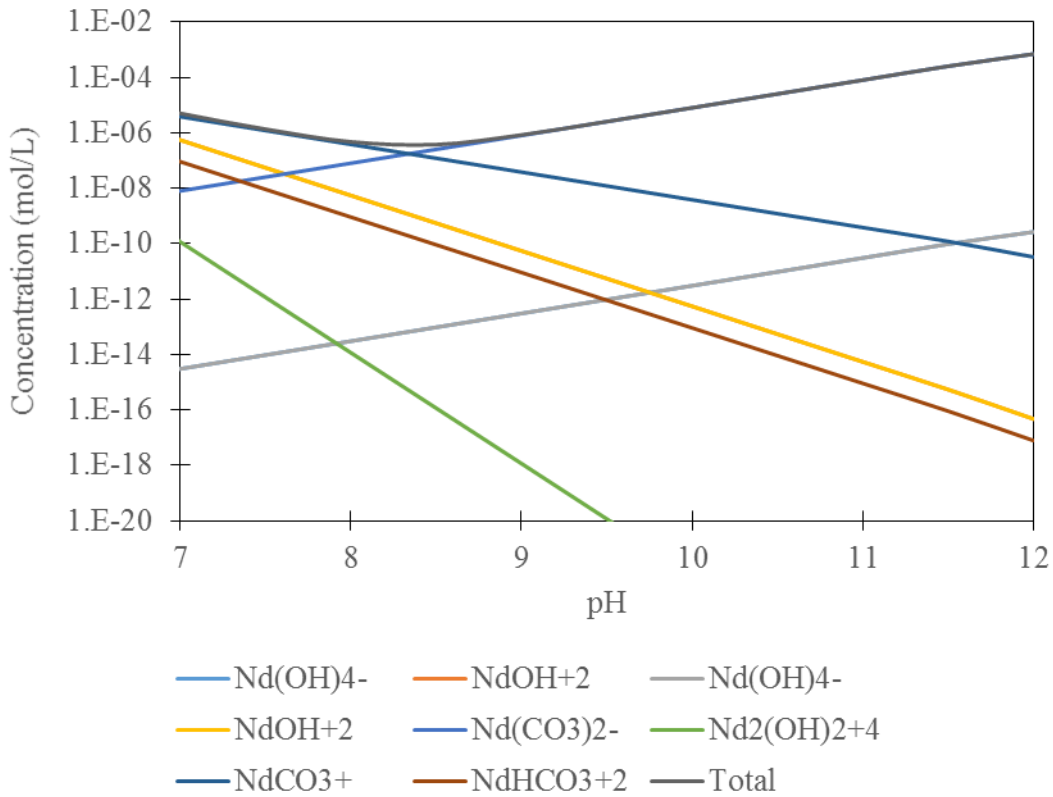


Figure 2-35. Aqueous speciation and solubility (total) with respect to pH for Nd(III) in 0.01 M NaCl in the presence of atmospheric carbonate.

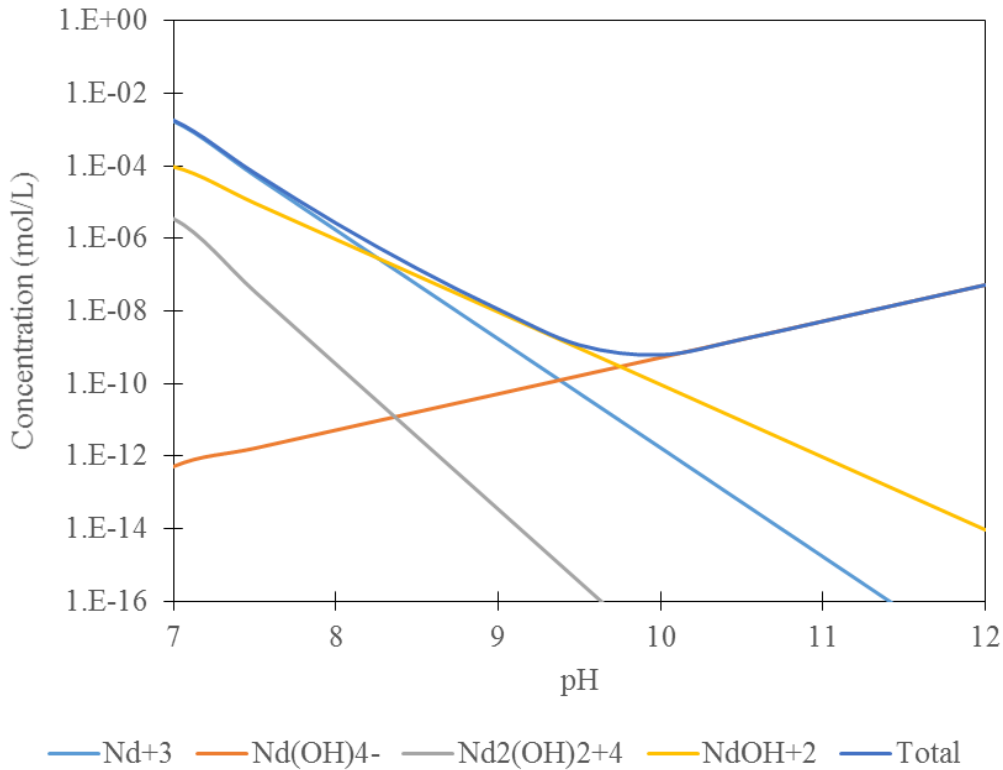


Figure 2-36. Aqueous speciation and solubility (total) with respect to pH for Nd(III) in 0.01 M NaCl in the absence of carbonate.

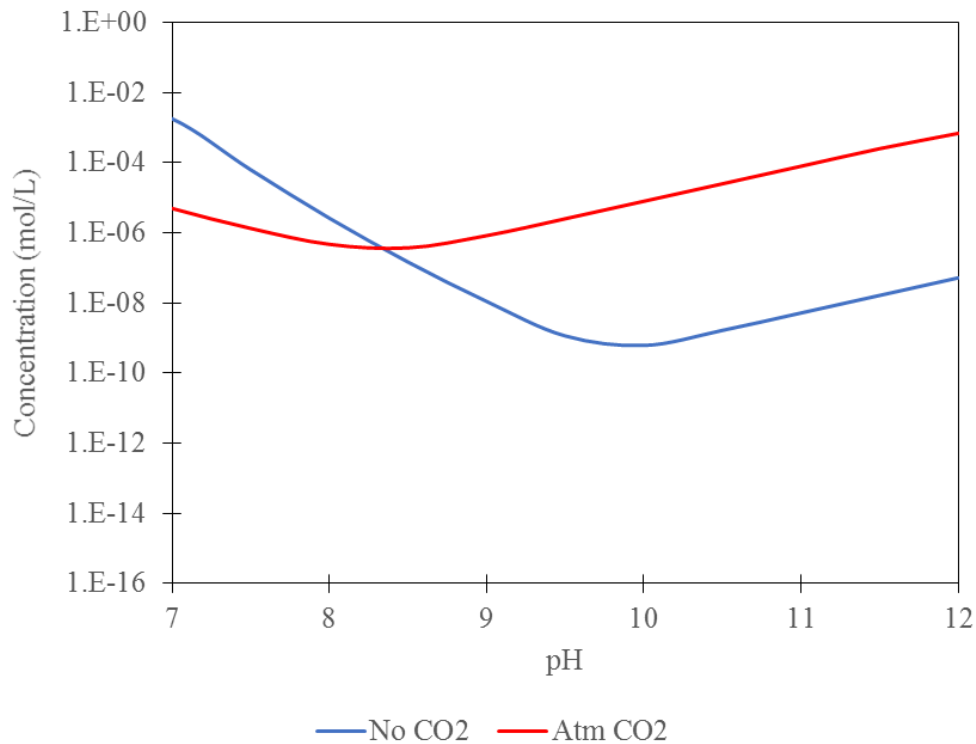


Figure 2-37. A comparison of solubility of Nd(III) in 0.01 M NaCl in equilibrium with the presence (red) and absence of atmospheric CO₂(g) (blue).

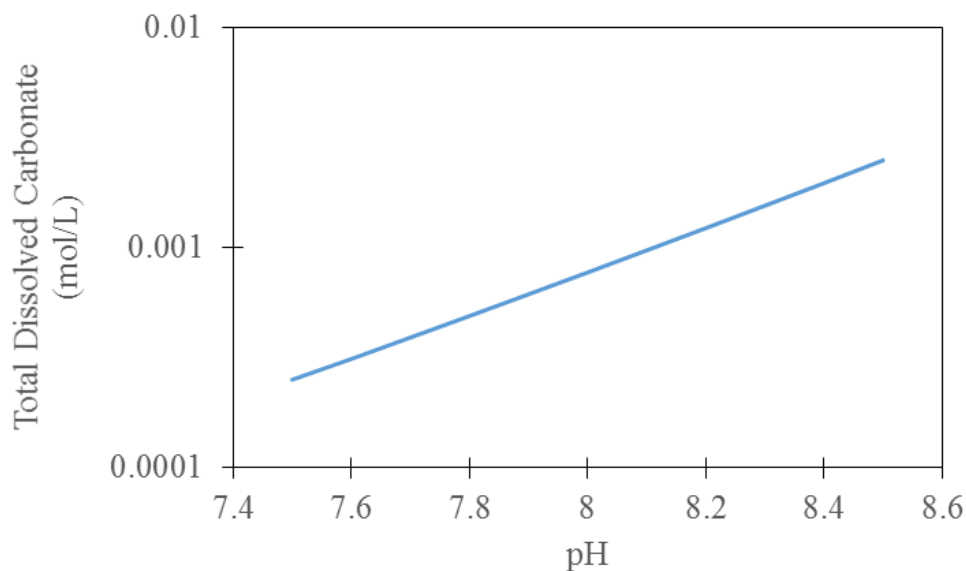


Figure 2-38. Total dissolved carbonate with respect to pH in equilibrium with the atmosphere and in the presence of 0.1 M NaCl.

Preliminary Column Experiments

The initial column was designed based on previous work by Dittrich and Reimus (2015). It was designed with a small size and pore volume to allow for injection of large volumes of solution over a relatively short period of time in order to estimate the retardation of strongly sorbing contaminants. The initial column was 1 cm in length with 1 gram of dolomite and a porosity of approximately 0.32 (based on mass). Further, the experimental conditions for the initial column were 100 ppb Nd(III) in 0.01 M NaCl and a target pH of 8.5.

There was considerable fluctuation in the effluent pH (7.96 ± 0.34). These pH fluctuations were likely due to the low buffering capacity of NaCl and disequilibrium with atmospheric carbonate. In addition, there was some variability in stock measurements pulled from the syringes and bottles over time and likely precipitates in the stock solutions which were fairly stable in suspension. Over the length of the experiments (approximately two weeks), the stock suspensions in bottles were measured at $84 \pm 9\%$ of the initial and in syringes were measured at $70 \pm 10\%$. Therefore, there were some losses of Nd(III) due to sorption to walls and/or precipitation.

However, significant losses were recorded following filtration through a 0.5 mL 30k MWCO filter (Amicon EMD Millipore) and were repeatable with different methods as illustrated in Figures 2-39 and 2-40. In Figure 2-39, the stock suspension was filtered through the same filter sequentially with reproducible results. Then, in Figure 2-40, the stock suspension was filtered through different filters following different pre-equilibration procedures: (1) no pre-wetting, (2) pre-wetting with 0.01 M NaCl, and (3) pre-wetting with the 0.01 M NaCl – 100 ppb Nd(III) stock. Each of these also produced similar results, although previous researchers have often incorporated pre-treatment steps of filters to allow for equilibration of filters with the aqueous phase and filling of any available sorption sites on filters. However, these steps are not necessary for these filters. It should be noted that filtration of acidified Nd(III) stock solutions was within

error of the initial solutions. These filtration steps show that Nd(III) is either adsorbing to filter material or removing precipitated Nd(III) or a combination of both. To ultimately check for sorption to filters, stock solutions will be filtered sequentially through new filters.

After running the preliminary column experiment for approximately three weeks (and nearly 800 pore volumes), the experiment was suspended. The breakthrough data is summarized in Figure 2-41. It should be noted that the steep drop in Nd(III) breakthrough near 700 pore volumes is the point where injection of 100 ppb Nd(III) in 0.01 M NaCl was suspended and 0.01 M NaCl injection was begun (without Nd). It is significant that approximately 15% of the Nd(III) spike was present in the effluent for the majority of the column experiment. It is likely that these concentrations represent mobile Nd colloids. However, filtration data was not collected and current work is ongoing to understand if the effluent concentrations may represent dissolved or colloidal Nd(III). Further, near 775 pore volumes, 0.007 M NaCl + 0.003 M NaHCO₃ was injected into the column and appeared to mobilize slightly more Nd than 0.01 M NaCl.

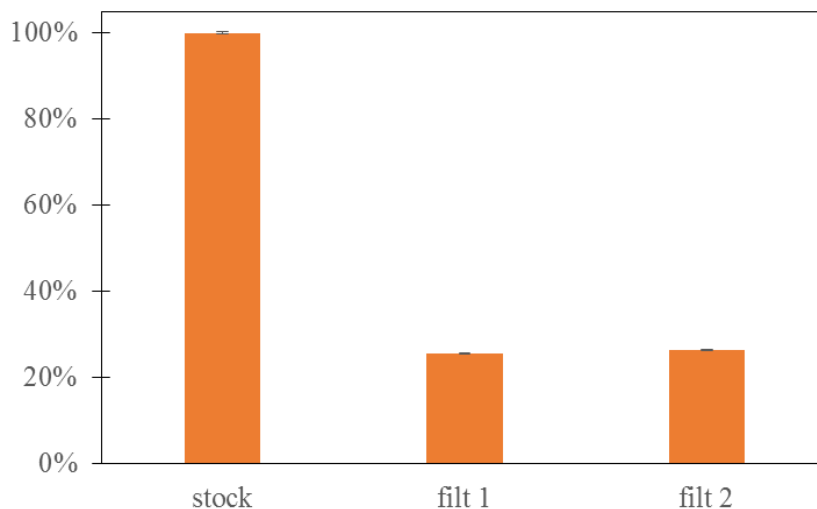


Figure 2-39. Results from sequential filtration of the preliminary column spike solution [100 ppb Nd, 0.01 M NaCl] through 30k MWCO filters.

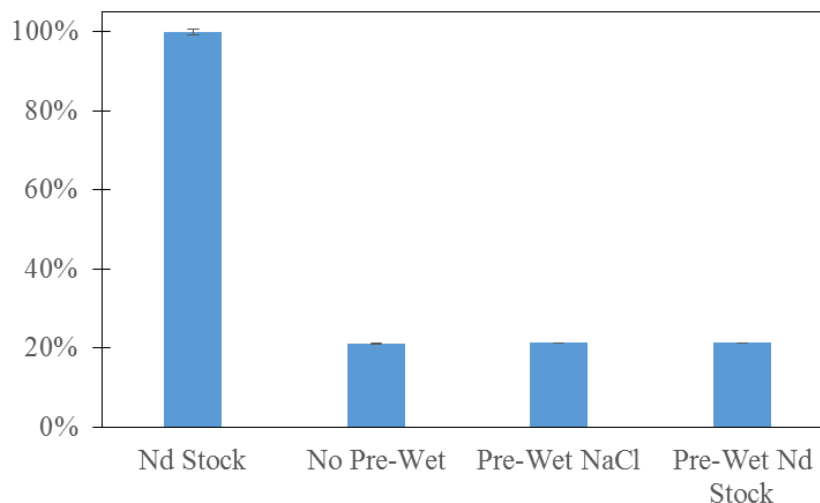


Figure 2-40. Results from filtration of the preliminary column spike solution [100 ppb Nd, 0.01 M NaCl] through 30k MWCO filters with different pre-equilibration procedures.

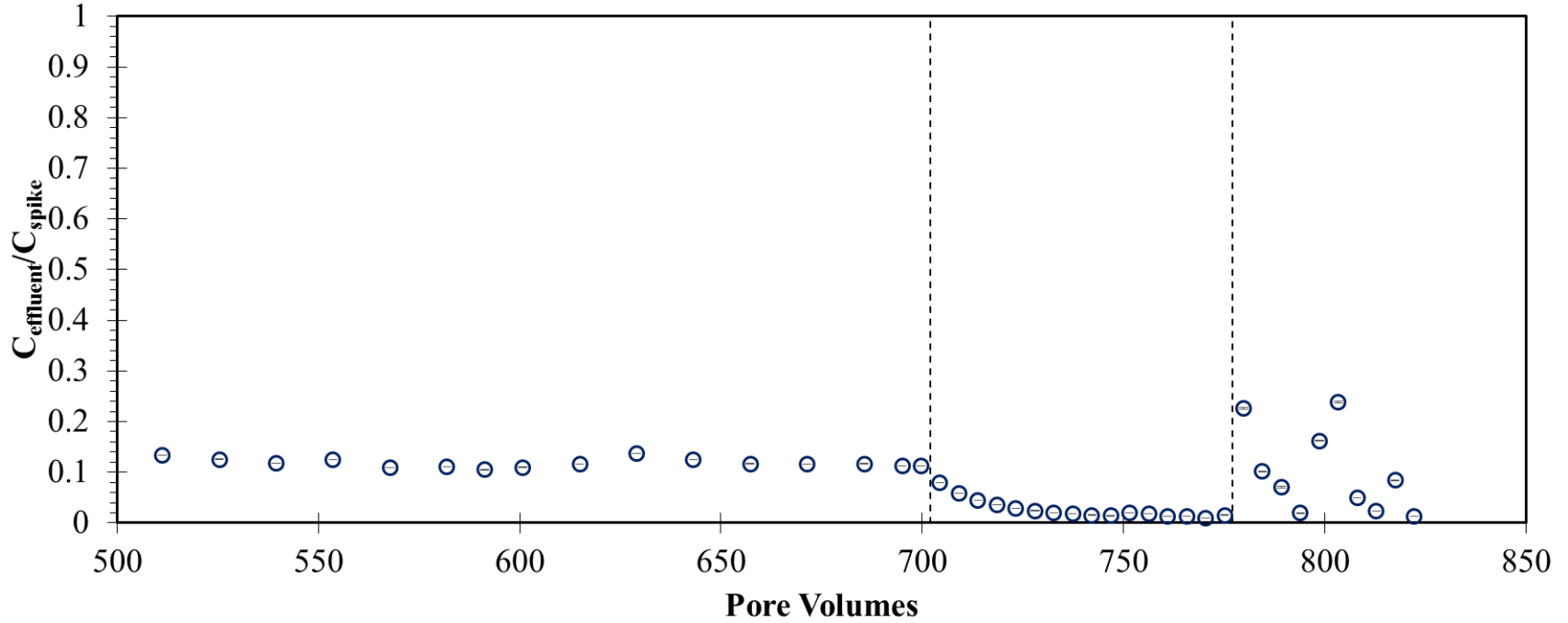


Figure 2-41. Breakthrough results from the preliminary column experiment [100 ppb Nd, 0.01 M NaCl], Note: injection of 0.01 M NaCl without Nd was begun near 700 pore volumes and 0.007 M NaCl + 0.003 M NaHCO₃ near 775 pore volumes as shown by dotted lines.

Lessons Learned

Based on the preliminary batch and column experiments and aqueous speciation modeling, the following changes have been made to collect more reliable and environmentally relevant data:

1. All experiments will be conducted at 20 ppb Nd(III) or lower.
2. All experiments will be conducted in the presence of 3 mM NaHCO₃.
3. Care will be taken to ensure that spike solutions are stable with respect to pH and Nd(III) concentration prior to injection into columns or batch experiments.

Batch Experiments

Batch kinetics experiments at 0.01 and 0.1 M total ionic strength (3 mM NaHCO₃ + NaCl) are currently in progress with 20 ppb Nd and a long-term mini column experiment is in progress with 0.1 M total ionic strength (3 mM NaHCO₃ + 0.097 NaCl). Samples are planned to be collected up to 7 days (10,080 minutes). However, preliminary data shows that sorption is strong and fast (Figure 2-42)

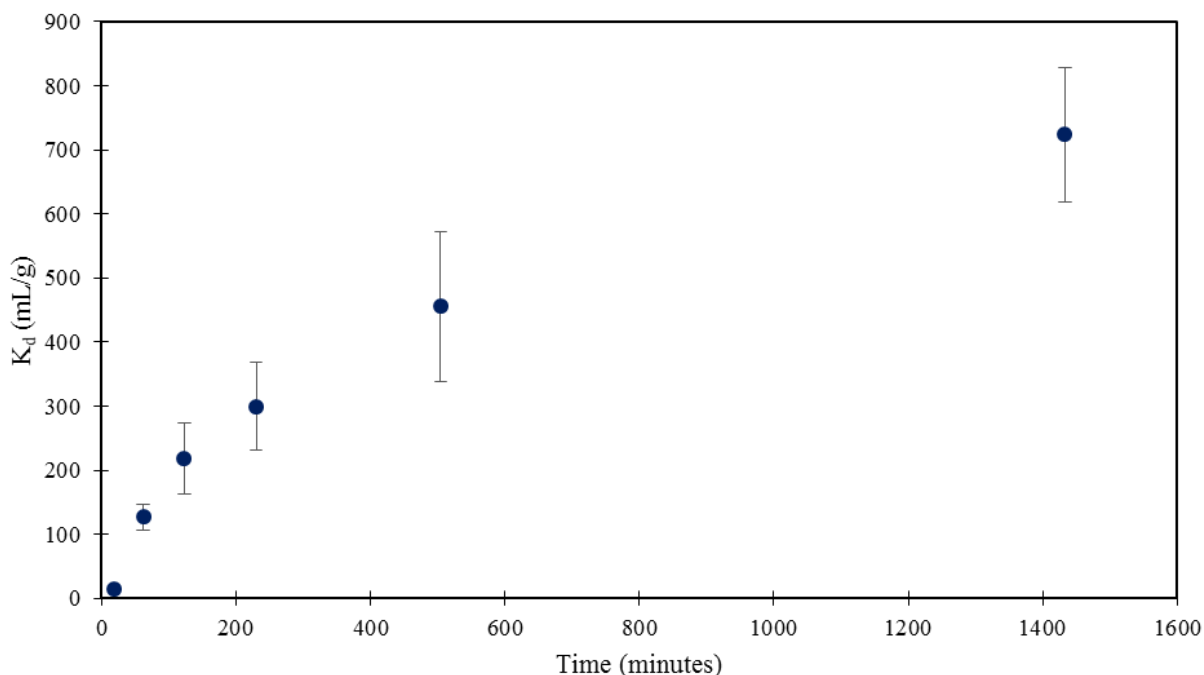


Figure 2-42. Initially 20 ppb Nd(III) partitioning in the presence of 5 g/L dolomite with respect to time at pH 8.59±0.07 in 0.007 M NaCl + 0.003 M NaHCO₃.

Mini Column Experiments

A long-term mini column with 0.1 M total ionic strength and 20 ppb Nd(III) continuous injection at 1.5 mL/hr is currently in progress (Figure 2-43). More than 1200 pore volumes have been pushed through the column without saturation of the column. The columns are 1 cm in length and contain approximately one gram of dolomite with a porosity of ~0.32. Therefore, if breakthrough had occurred at 1280 pore volumes, the K_d for Nd(III) as calculated by the mini

columns would be 140 mL/g. Therefore, based on the K_d 's reported for the batch experiments, we should not have reached the breakthrough point for the columns.

This is based on equation 1 below where θ =porosity, ρ =bulk density of dolomite and K_d =equilibrium partition coefficient for Nd. The retardation factor (R) is generally described as equivalent to the ratio of groundwater velocity to the contaminant velocity. Further, this ratio can be related to the number of pore volumes in the column in the same manner because a conservative tracer should move through the column with the flow of groundwater or after one pore volume. Therefore, the retardation factor can also be considered equivalent to the number of pore volumes that must go through the column before breakthrough of the contaminant.

$$R = 1 + \frac{\rho B}{\theta} K_d \quad \text{Eqn. 1}$$

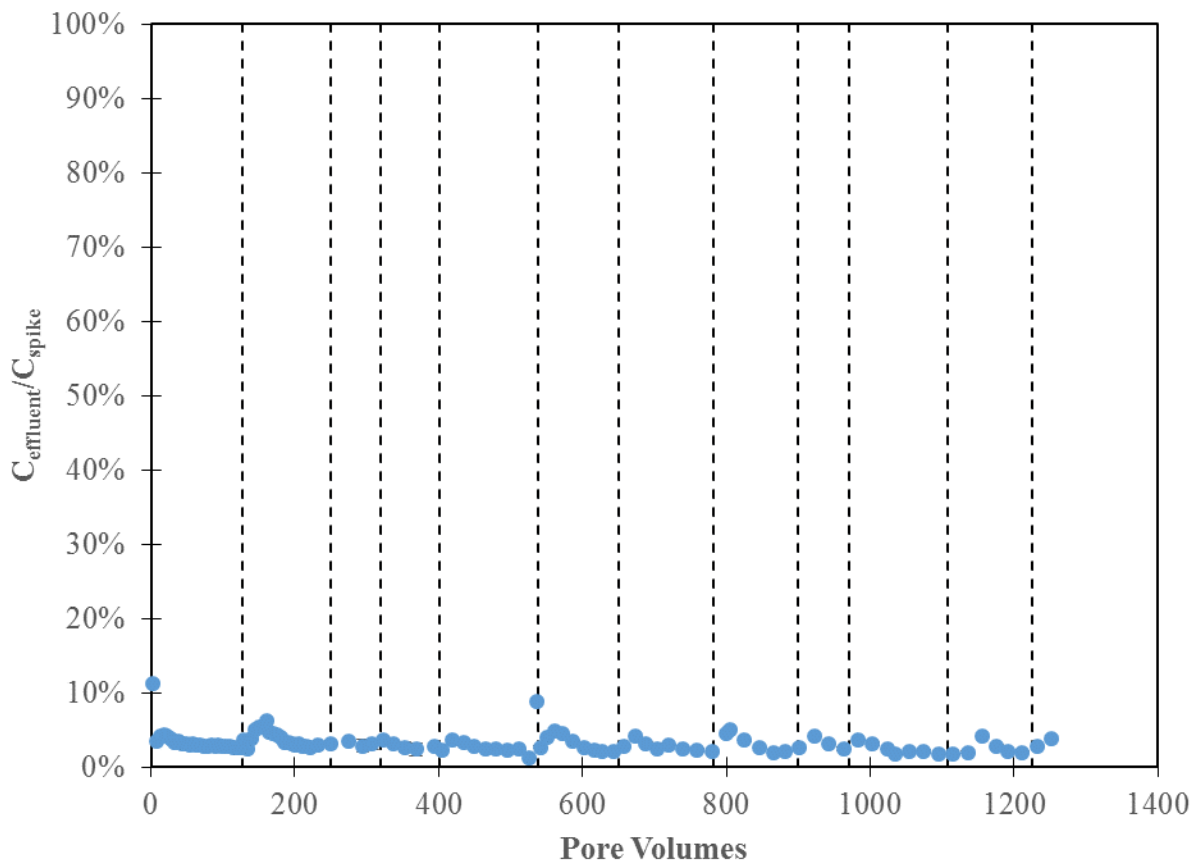


Figure 2-43. Continuous input of 20 ppb Nd + 0.007 M NaCl + 0.003 M NaHCO₃ into mini column packed with dolomite at 1.5 mL/hr flow rate, Note: dotted lines represent points where the injection syringe was refilled.

Mineral Characterization

The BET surface area was measured by the FIU Mechanical Engineering department and was reported as 1.6991 m²/g.

Milestones and Deliverables

The milestones and deliverables for Project 2 for FIU Year 6 are shown on the following table. A deliverable for Task 1, a progress report on the experimental results on autunite mineral biodissolution (subtask 1.2) was submitted to DOE and site contacts on 2/15/2016. A second deliverable for Task 1, Literature Review of Geophysical Resistivity Measurements and Microbial Communities (Subtask 1.3.3), was also submitted to DOE and site contacts on 3/18/2016. FIU has reforecasted the milestones and deliverables associated with the SRS surface water modeling of Tims Branch task as described in the narrative above under Task 3. The new reforecast dates are noted in the table below. As such, milestone 2015-P2-M3, complete input of MIKE SHE model configuration parameters for simulation of evapotranspiration (Subtask 3.1), which was due on February 29, 2016 was reforecast and completed on March 31, 2016. Milestone 2015-P2-M4, Complete input of MIKE SHE model configuration parameters for simulation of unsaturated flow (Subtask 3.1), which was originally due 3/31/2016 has been reforecast to 4/29/16. The circumstances and end path forward, including the new reforecast dates for this project task, have been closely coordinated with the stakeholders at SRS and DOE HQ. FIU discussed the issue via teleconference with the SRNL collaborators and confirmed the agreement on new milestone and deliverable dates with an email sent to SRS and DOE HQ contacts on February 26, 2016.

FIU Performance Year 6 Milestones and Deliverables for Project 2

Task	Milestone/Deliverable	Description	Due Date	Status	OSTI
Project	2015-P2-M1	Submit draft papers to Waste Management 2016 Symposium	11/6/2015	Complete	
Task 1: Hanford Site	Deliverable	Progress report on the experimental results on autunite mineral biodissolution (Subtask 1.2)	2/15/2016	Complete	OSTI
	Deliverable	Progress report on batch experiments for ammonia injection task (Subtask 1.3.1)	6/22/2016	On Target	OSTI
	Deliverable	Literature Review of Geophysical Resistivity Measurements and Microbial Communities (Subtask 1.3.3)	3/18/2016	Complete	
Task 2: SRS	Deliverable	Progress report on batch experiments on sodium silicate application in multi-contaminant systems (Subtask 2.1)	4/11/2016	On Target	OSTI
	Deliverable	Progress report on the synergy between colloidal Si and HA on the removal of U(VI) (Subtask 2.4)	4/21/2016	On Target	OSTI
	Deliverable	Progress report on column experiments to investigate uranium mobility in the presence of HA (Subtask 2.5)	5/20/2016	On Target	OSTI
Task 3: Tims Branch	2015-P2-M2	Complete refinement of MIKE SHE model configuration	12/30/2015	Complete	

		parameters for the simulation of overland flow using revised model domain (Subtask 3.1)			
	2015-P2-M3	Complete input of MIKE SHE model configuration parameters for simulation of evapotranspiration (Subtask 3.1)	2/29/2016 Reforecast to 3/31/16	Complete	
	2015-P2-M4	Complete input of MIKE SHE model configuration parameters for simulation of unsaturated flow (Subtask 3.1)	3/31/2016	Reforecast to 4/29/16	
	Deliverable	Progress Report for Subtask 3.1: Modeling of surface water and sediment transport in the Tims Branch ecosystem	4/29/2016	Reforecast to 5/31/16	OSTI
	Deliverable	Progress Report for Subtask 3.2: Application of GIS technologies for hydrological modeling support	4/29/2016	Reforecast to 5/31/16	OSTI
	2015-P2-M5	Complete input of MIKE SHE model configuration parameters for simulation of flow in the saturated zone (Subtask 3.1)	6/30/2016	Reforecast to 7/29/16	
Task 4: Sustainability Plan	Deliverable	Draft sustainable remediation report for the M1 air stripper	12/18/2015	Complete	OSTI

Work Plan for Next Quarter

Task 1: Remediation Research and Technical Support for the Hanford Site

Subtask 1.1 – Sequestering Uranium at the Hanford 200 Area Vadose Zone by in situ Subsurface pH Manipulation using NH₃ Gas

- Continue with isopiestic measurements.
- Initiate sequential extraction experiments with uranium-bearing solids with various composition,
- Prepare uranium samples in epoxy and ship them to PNNL to finalize sample preparations for the EMRA analysis.
- Conduct EMRA analysis at FIU.
- Digest sample precipitates followed by KPA and/or ICP-OES analysis.

Subtask 1.2. Investigation on Microbial-Meta-Autunite Interactions - Effect of Bicarbonate and Calcium Ions

- Replicate the exact conditions (U, Ca and P concentrations) along with three different bicarbonate concentrations in mineral-free experiments.

Subtask 1.3. Evaluation of Ammonia Fate and Biological Contributions During and After Ammonia Injection for Uranium Treatment

- Equilibrium batch sorption experiments will continue to be optimized to understand sorption of U and NH₃ under conditions relevant to the Hanford Site based on the lessons learned.
- Aqueous speciation modeling will be completed for comparison with the experimental results.
- Statistical analysis will be used to compare the samples that had pH adjusted by NaOH versus by NH₄OH (t-test).
- Sequential extraction results will be finalized and reported.

Task 2: Remediation Research and Technical Support for Savannah River Site

Subtask 2.1. FIU's Support for Groundwater Remediation at SRS F/H –Area

- Determine the surface area of different SRS soil fractions and express sorption results as mg of U(VI) per surface unit.
- Perform desorption experiments in different SRS soil fractions
- Perform batch experiments with different concentrations of Ca²⁺ and Mg²⁺, using Ca(NO₃)₂ and Mg(NO₃)₂ respectively.

Subtask 2.2 – Monitoring of U(VI) Bioreduction after ARCADIS Demonstration at F-Area

- Initiate a summary of the results.

Subtask 2.3. Sorption Properties of the Humate Injected into the Subsurface System

- Perform FTIR of SRS sediments + Huma-K but at concentrations higher than 50 ppm to investigate surface complexation.
- Perform kinetics of Huma-K sorption on SRS sediments at different times (less than 30 min) to complete the experiment.
- Study the effects of salts (NaNO₃) on desorption of Huma-K.
- Initiate experiments on uranium adsorption kinetics onto SRS sediments.

Subtask 2.4 – The synergetic effect of HA and Si on the removal of U(VI)

- Complete experiments with 30 ppm of HA and compare data with previously obtained data for 10 and 50 ppm of HA.
- Repeat any necessary experiments for missing data or questionable data.
- Initiate sediment samples analysis via SEM/EDS
- Complete draft progress report on synergy experiments.

Subtask 2.5 – Investigation of the migration and distribution of natural organic matter injected into subsurface systems

- Initiate column experiments with 0.5 PV huma-K sorption/desorption followed by uranium injection to study the effect of sorbed huma-K on uranium mobility.
- Complete TOC analysis on sediments from previous experiments.
- Complete draft progress report on column experiments details the results obtained thus far for this task.

Task 3: Surface Water Modeling of Tims Branch

Subtask 3.1. Modeling of Surface Water and Sediment Transport in the Tims Branch Ecosystem

- Complete input of MIKE SHE model configuration parameters for simulation of unsaturated flow.
- Complete input of MIKE SHE model configuration parameters for simulation of flow in the saturated zone.
- Complete progress report for subtask 3.1: modeling of surface water and sediment transport in the Tims Branch ecosystem.

Subtask 3.2. Application of GIS Technologies for Hydrological Modeling Support

- Geospatial distribution of ET over time including the creation of a raster data set for ET in SRS and Tims Branch.
- Preparation of timeseries datasets of Leaf Area Index and Root Depth to generate raster datasets.
- Preparation of a groundwater table GIS shapefile. This may require revisiting the available water table shapefiles and adding current data from various online sources.
- Continue with preliminary MIKE 11 model development which involves delineation of stream network, and generation of cross-sections and chainages for Tims Branch major and minor tributaries.
- Complete progress report for subtask 3.2: application of GIS technologies for hydrological modeling support.

Subtask 3.3. Biota, Biofilm, Water and Sediment Sampling in Tims Branch

- Dr. Mahmoudi is working on the identification and mapping of key points along the Tims Branch stream for data collection and will coordinate with Dr. Seaman from SREL with respect to the parameters required, the frequency of data collection and who will collect the data. FIU anticipates student support for this effort during the DOE Fellows 2016 summer internships stationed at SRS/SRNL.
- FIU undergraduate student and DOE Fellow Awmna Rana was granted an internship opportunity as part of the SREL REU in Radioecology during summer 2016 under the mentorship of Dr. John Seaman with whom FIU has been collaborating on this task. It is anticipated that while stationed at SRS, there will be an opportunity for this student to

provide support for some of the sampling and data collection required to support the Tims Branch model development.

Task 4: Sustainability Plan for the A/M Area Groundwater Remediation System

- This task was completed and a technical report submitted to DOE and SRNL on Dec. 15, 2015 entitled, “A Sustainability Analysis for the M1 Air Stripper and Pumps of the M Area Groundwater Remediation System at the Savannah River Site.” No additional effort is planned on this task.

Task 5: Remediation Research and Technical Support for WIPP

- Work in collaboration with LANL to continue parallel experiments including mini-columns and batch experiments with Nd(III) for 0.01 – 5 M NaCl.
- Begin model development for mini column experiments in PHREEQC.
- Investigate and apply kinetic models to fit batch sorption data.
- Develop a technical report based on work performed at CEMRC Carlsbad facilities between February 15 to April 8, 2016.

Project 3

Waste and D&D Engineering & Technology Development

Project Manager: Dr. Leonel E. Lagos

Project Description

This project focuses on delivering solutions under the decontamination and decommissioning (D&D) and waste areas in support of DOE HQ (EM-13). This work is also relevant to D&D activities being carried out at other DOE sites such as Oak Ridge, Savannah River, Hanford, Idaho and Portsmouth. The following tasks are included in FIU Year 6:

Task No	Task
Task 1: Waste Information Management System (WIMS)	
Subtask 1.1	Maintain WIMS – database management, application maintenance, and performance tuning
Subtask 1.2	Incorporate new data files with existing sites into WIMS
Task 2: D&D Support to DOE EM for Technology Innovation, Development, Evaluation and Deployment	
Subtask 2.1	D&D Technology Demonstration & Development and Technical Support to SRS's 235-F Facility Decommissioning
Subtask 2.2	Technology Demonstration and Evaluation
Subtask 2.3	Support to DOE EM-13 and the D&D Community
Task 3: D&D Knowledge Management Information Tool	
Subtask 3.1	Web and Mobile Application for D&D Decision Model
Subtask 3.2	Mobile Applications/Platforms for DOE Sites
Subtask 3.3	Development & Integration of International KM-IT Pilot for UK Collaboration
Subtask 3.4	Outreach and Training (D&D Community Support)
Subtask 3.5	Data Mining and Content Management
Subtask 3.6	D&D KM-IT Administration and Support

Task 1: Waste Information Management System (WIMS)

Task 1 Overview

This task provides direct support to DOE EM for the management, development, and maintenance of a Waste Information Management System (WIMS). WIMS was developed to receive and organize the DOE waste forecast data from across the DOE complex and to automatically generate waste forecast data tables, disposition maps, GIS maps, transportation details, and other custom reports. WIMS is successfully deployed and can be accessed from the web address <http://www.emwims.org>. The waste forecast information is updated at least

annually. WIMS has been designed to be extremely flexible for future additions and is being enhanced on a regular basis.

Task 1 Quarterly Progress

The Waste Information Management System (WIMS) was developed to receive and organize the DOE waste forecast data from across the DOE complex and to automatically generate waste forecast data tables, disposition maps, GIS maps, transportation details, and other custom reports. WIMS is successfully deployed and can be accessed from the web address <http://www.emwims.org>. During this reporting period, FIU performed database management, application maintenance, and performance tuning to the online WIMS in order to ensure a consistent high level of database and website performance.

The 2016 data set has been collected by DOE. The completed data set is expected to be sent to FIU in the April 2016 timeframe. The revised waste forecast data will be received as formatted data files and, to incorporate these new files, FIU will build a data interface to allow the files to be received by the WIMS application and import it into SQL Server. SQL server is the database server where the actual WIMS data is maintained. FIU will complete the data import and deploy onto the test server for DOE testing and review. Once FIU has incorporated feedback from the data review, the new data will be deployed on the public server. The 2016 waste data will replace the existing previous waste data and will become fully viewable and operational in WIMS.

A professional poster titled, “Waste Information Management System with 2015-16 Waste Streams,” was prepared and presented during the March 6-10 Waste Management 2016 conference in Phoenix, AZ (Figure 3-1).

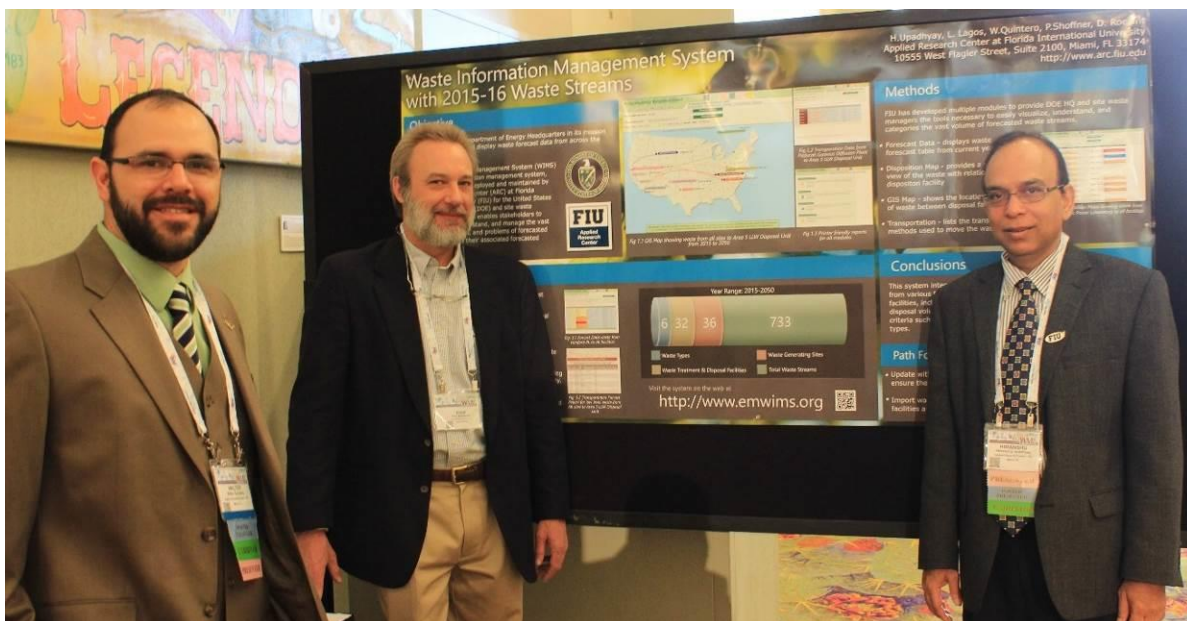


Figure 3-1. WIMS poster being presented at WM16.

Task 2: D&D Support to DOE EM for Technology Innovation, Development, Evaluation and Deployment

Task 2 Overview

This task provides direct support to DOE EM for D&D technology innovation, development, evaluation and deployment. For FIU Year 6, FIU will assist DOE EM-13 in meeting the D&D needs and technical challenges around the DOE complex. FIU will expand the research in technology demonstration and evaluation by developing a phased approach for the demonstration, evaluation, and deployment of D&D technologies. One area of focus will be working with the Savannah River Site to identify and demonstrate innovative technologies in support of the SRS 235-F project. FIU will further support the EM-1 International Program and the EM-13 D&D program by participating in D&D workshops, conferences, and serving as subject matter experts.

Task 2 Quarterly Progress

Task 2.1.1: Incombustible Fixatives

The objective of this research task is to improve the operational performance of fixatives by enhancing their fire resiliency. Most fixatives begin to see degradation between 200-400 degrees, at which time radioisotopes could potentially be released into the environment. The layering or combining of an intumescent coating with the fixative is being investigated as a way to mitigate the release of radioisotopes during fire and/or extreme heat conditions. Since 9/11/2001, there have been significant improvements in fire retardant/fire resistant technologies, with intumescent coatings being at the forefront of this development. Intumescent coatings develop a thick char to insulate the substrate and protect it from fire and extreme heat conditions. Applying that technology to fixatives through layering and combining should increase its fire resiliency and mitigate the risk of contamination under those extreme conditions.

The completion of the Phase I proof of principle series of tests provided sufficient data to support the hypothesis that fire resiliency of fixatives used in D&D activities can be enhanced by layering them with an intumescent coating. Phase II testing, including controlled tests on uncontaminated coupons using different substrates by incrementally increasing the temperatures in a muffle furnace, started in December 2015. For Phase II, ARC is applying each of the 5 fixatives to coupons in accordance with the manufacturer's directions (fixative-only coupons), and then applying the various fixatives plus a layer of intumescent coating to a second series of coupons (fixatives plus intumescent coating). Coupons include 4" x 4" red oak and sheet metal in order to facilitate placement in the muffle furnace. The same application and curing procedures as Phase I are being followed.

ARC is subjecting the cured fixative-only coupons as well as the fixative-plus-intumescent-coating coupons to incrementally increasing temperatures (e.g.; 100°F, 200°F, 300°F, and so forth) in a muffle furnace for a set time period at each temperature, allowing the coupons to cool, and then recording the effect of the heat on the fixative. Effects observed and recorded include the amount of weight lost, thickness degradation, and a visual inspection for evidence of failure, including peeling, cracking, blistering, abnormal discoloration, or loss of adhesion. The intent is to determine at what temperature each of the designated fixatives begin to breakdown and

display negative effects that could degrade its intended purpose, specifically fixing radioactive contaminants.

All fixatives began to exhibit minor mass loss starting at temperatures as low as 200°F, but most significant degradation appeared to occur around 500-600°F (Figure 3-2 through 3-6). The fixatives lost anywhere from 50% to upwards of 90% mass when exposed to incremental temperature increases (200-800°F).

The results of exposing Fixative A to increased temperatures are shown in Figure 3-2. After exposure to 400°F, the fixative exhibited discoloration, expansion, and minor mass loss. After exposure to 600°F, the fixative exhibited additional discoloration, bubbling, continued expansion, off gassing, desiccation and increased mass loss. After exposure to 800°F, significant mass loss, extreme discoloration, desiccation, cracking, and flaking were evident; even slight abrasion with the fixative resulted in total loss of adhesion.



Figure 3-2. Fixative A, from left: after exposure to 400°F, 600°F, and 800°F.

The results of exposing Fixative B to increased temperatures are shown in Figure 3-3. After exposure to 200°F, the fixative exhibited slight discoloration, expansion, and minor mass loss. After exposure to 400°F, the fixative exhibited additional discoloration, bubbling, continued expansion, off gassing, and increased mass loss. After exposure to 500°F, significant discoloration, continued expansion, off gassing, additional mass loss, desiccation, cracking, and brittle composition were evident. After exposure to 800°F, extreme discoloration, significant mass loss, desiccation, cracking and flaking were evident; even slight abrasion with the fixative resulted in total loss of adhesion.



Figure 3-3. Fixative B, from left: after exposure to 200°F, 400°F, 600°F, and 800°F.

The results of exposing Fixative C to increased temperatures are shown in Figure 3-4. After exposure to 200°F, the fixative exhibited slight discoloration, bubbling, expansion, off gassing and minor mass loss. After exposure to 500°F, the fixative exhibited significant discoloration, continued expansion, off gassing, increased mass loss, desiccation, cracking, and brittle composition. After exposure to 800°F, extreme discoloration, significant mass loss, desiccation, cracking and flaking were evident; even slight abrasion with the fixative resulted in total loss of adhesion.

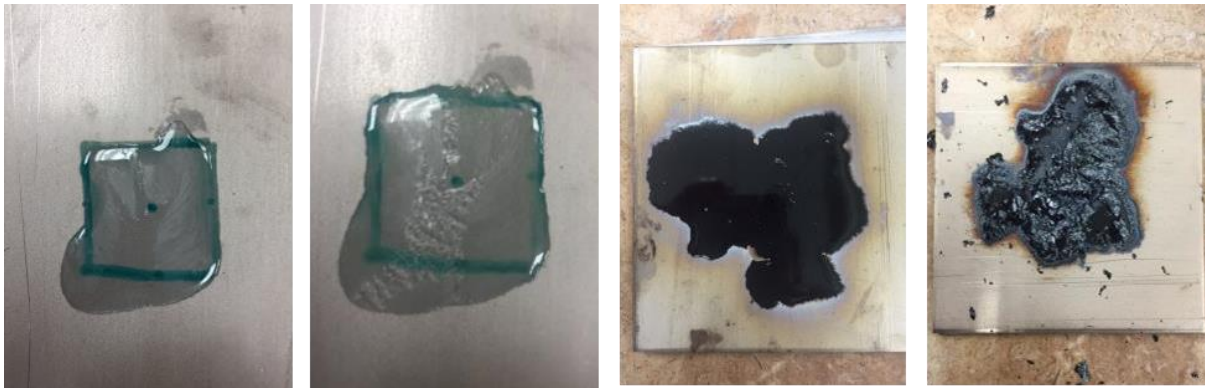


Figure 3-4. Fixative C, from left: before exposure and after exposure to 200°F, 500°F, and 800°F.

The results of exposing Fixative D to increased temperatures are shown in Figure 3-5. After exposure to 500°F, the fixative exhibited slight discoloration, bubbling, expansion, off gassing, and mass loss. After exposure to 700°F, the fixative exhibited significant discoloration, continued expansion, off gassing, increased mass loss, desiccation, cracking, and brittle composition. After exposure to 800°F, extreme discoloration, significant mass loss, desiccation, cracking and flaking were evident; even slight abrasion with the fixative resulted in total loss of adhesion.

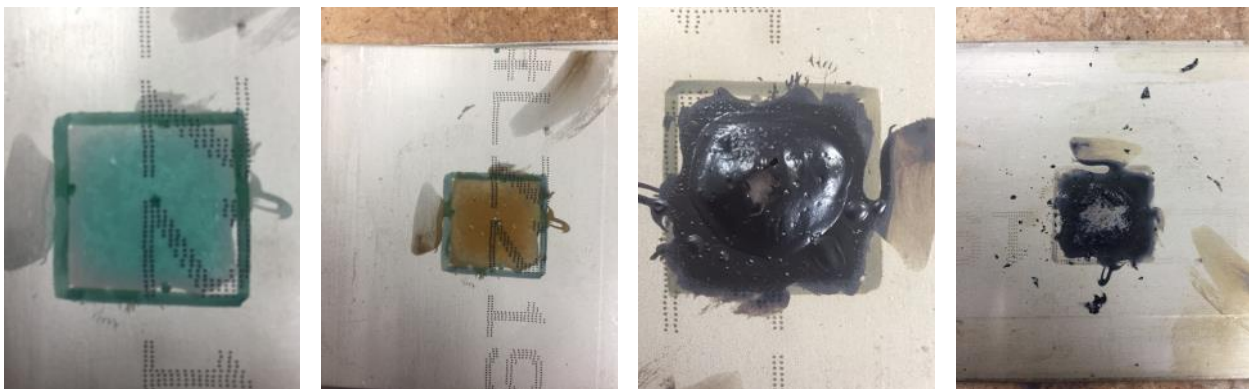


Figure 3-5. Fixative D, from left: before exposure and after exposure to 500°F, 700°F, and 800°F.

The results of exposing Fixative E to increased temperatures are shown in Figure 3-6. After exposure to 500°F, the fixative exhibited slight discoloration, off gassing, and mass loss. After exposure to 700°F, the fixative exhibited significant discoloration, continued expansion, off

gassing, increased mass loss, desiccation, cracking, and brittle composition. After exposure to 800°F, extreme discoloration, significant mass loss, desiccation, cracking and flaking were evident; even slight abrasion with the fixative resulted in total loss of adhesion.

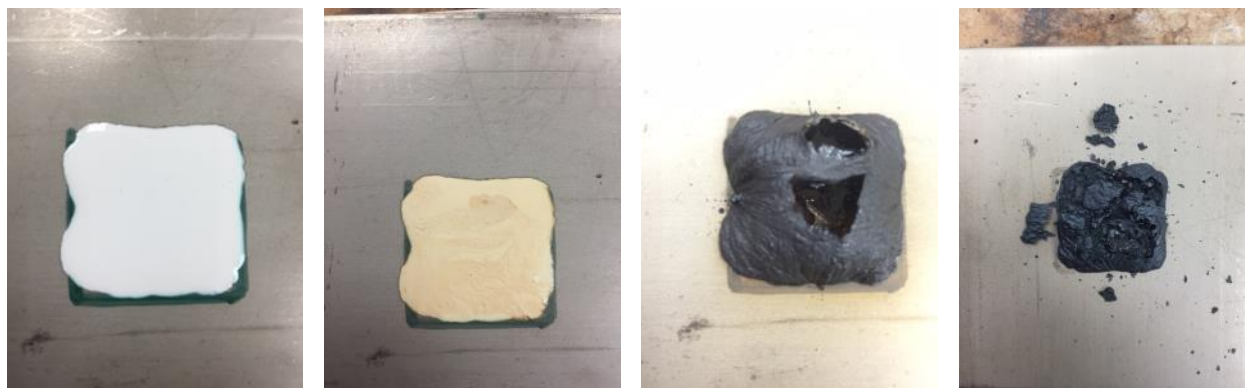


Figure 3-6. Fixative E, from left: before exposure and after exposure to 500°F, 700°F, and 800°F.

After discussion with the SRNL collaborators, FIU also performed additional proof-of-principle testing in January. The concept discussed and subsequently tested was the potential for an intumescent coating on the exterior of a surface to provide thermal protection for a fixative on the interior of a surface, given the increased probability of a fire starting outside the hot cell area.

FIU prepared and tested three (3) steel coupons (4" x 4" and ¼" thick), as follows:

- A steel coupon with a fixative applied to both sides was exposed to a direct flame 3 to 4" away on one side. The fixative on the side exposed to the flame proved flammable and actively burned. The fixative on the back side not exposed to the flame completely bubbled and burst due to the heat transfer and off-gassing.
- A steel coupon was prepared with a fixative and a layer of intumescent coating on both sides. The coupon was then exposed to a direct flame, ~3-4 inches away. Charring occurred on the side exposed to the direct flame and the underlying fixative remained intact. Furthermore, the back side did not exhibit any signs of off-gassing or damage. When using the intumescent coating layer, temperature differences between 150° and 300° F were observed between the front of the coupon exposed to the direct flame and the back of the coupon. By producing an immediate char when exposed to flame, the intumescent coating instantly creates a thermal barrier, providing a protective layer to the fixative and substrate beneath.
- A steel coupon was prepared with a 1-cm strip of fixative down the center and edged by an intumescent coating on two sides. Two propane torches were set at both outer edges (~1¾") from the center line. Immediate charring occurred at both outer edges of the steel coupon and appeared to prevent heat transfer to the exposed fixative for upwards of 5 minutes (Figure 3-7).

Similar testing was then performed using sheetrock substrates and yielded the same general observational results.



Figure 3-7. Charred intumescent coating provided thermal protection to bordering fixative.

FIU performed data analysis on the results of the Phase II testing performed to date, including controlled tests on uncontaminated coupons using different substrates, five commercially available fixatives, and a commercially available intumescent coating. ARC subjected the cured fixative-only coupons as well as the fixative-plus-intumescent-coating coupons to incrementally increasing temperatures (e.g.; 100°F, 200°F, 300°F, and so forth) in a muffle furnace for a set time period at each temperature, allowing the coupons to cool, and then recording the effect of the heat on the fixative. The intent was to determine at what temperature each of the designated fixatives begin to breakdown and display negative effects that could degrade its intended purpose, specifically fixing radioactive contaminants. All fixatives began to exhibit minor mass loss starting at temperatures as low as 200°F, but most significant degradation appeared to occur between 600°F and 800°F (Figure 3-8). The fixatives lost anywhere from 50% to upwards of 90% mass when exposed to incremental temperature increases (200-800°F).

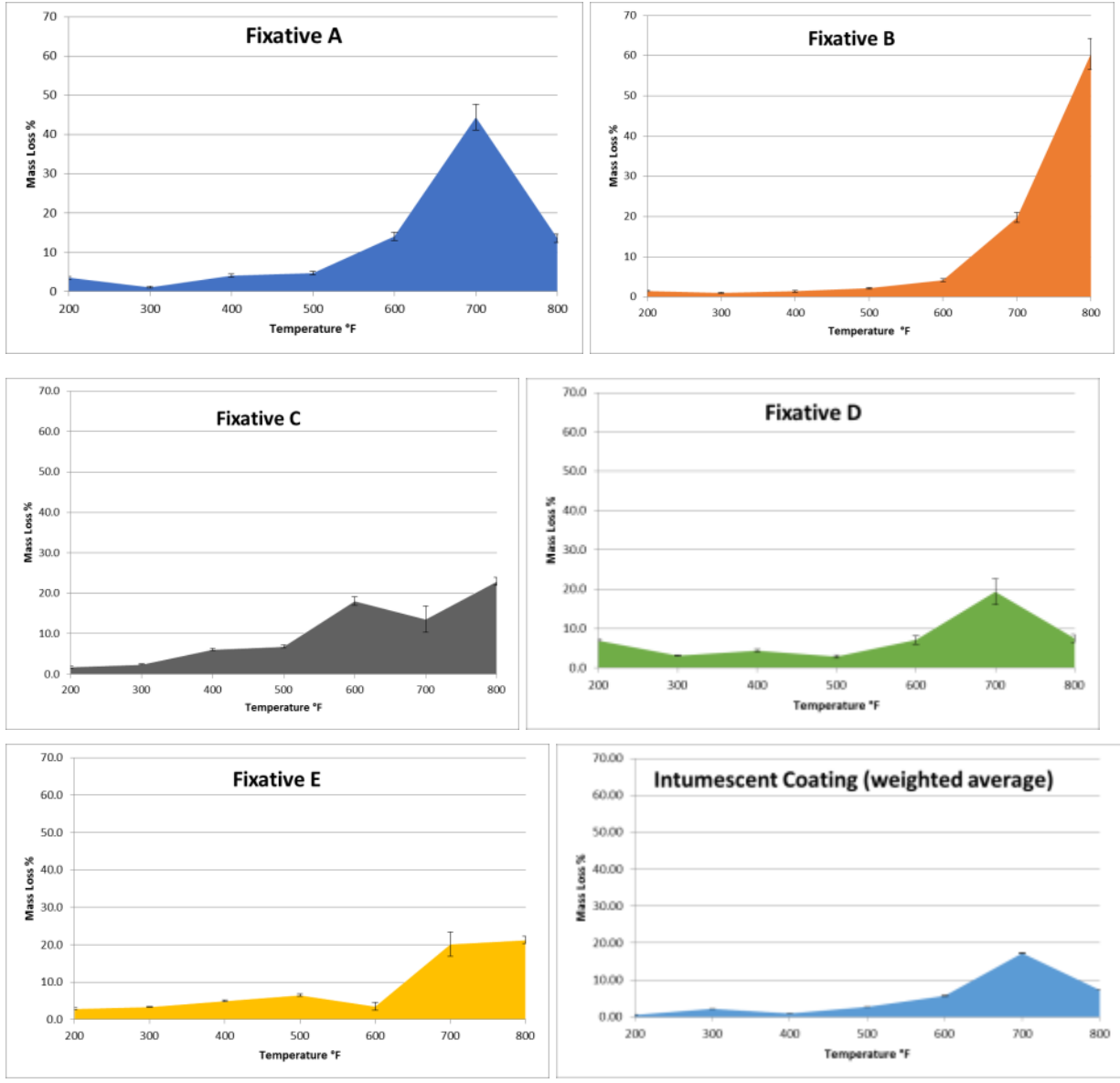


Figure 3-8. Mass loss of fixatives and intumescent coating versus temperature in muffle furnace.

As shown in Table 3-1, the intumescent coating mass loss is significantly lower than for the fixative products.

Table 3-1. Total Mass Loss

Fixative	Total Mass Loss (%)
A	85.2 ± 7.4
B	90.6 ± 8.2
C	71.6 ± 2.1
D	51.3 ± 7.8
E	62.6 ± 4.1
IC	40.5 ± 0.2

The next objective of the experiment was to test if layering the IC over a fixative would reduce the total mass loss of the sample. Sample coupons were prepared by layering the IC over Fixative A on a glass petri dish. The choice of the substrate was due to the transparency of the glass that allowed the investigators to visually inspect the fixative sample during cooling intervals. Once subjected to heat in the muffle furnace, the mass loss of the sample cannot be specifically attributed to either the fixative or the IC. However, if one assumes that the previous mass loss profiles measured individually remain consistent for the combined sample, then the combined mass loss profile can be predicted. By comparing the predicted combined mass loss with the actual combined mass loss, we can determine if the IC layer inhibited the mass loss of the fixative. Specifically, if the IC layer provided mass loss protection to the fixative layer, the actual total mass loss of the combined sample should be less than predicted.

Figures 3-9 and 3-10 show the mass loss profile of the IC + Fixative A samples compared to the predicted mass loss profiles.

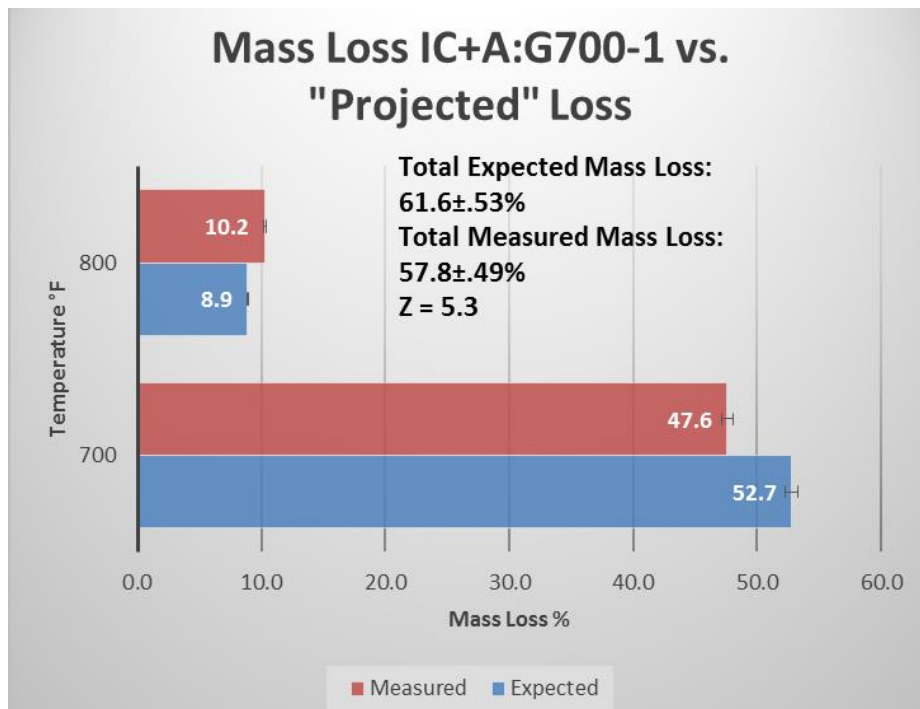


Figure 3-9. Mass loss profile of layered IC+Fixative A coupon #1 (predicted and actual).

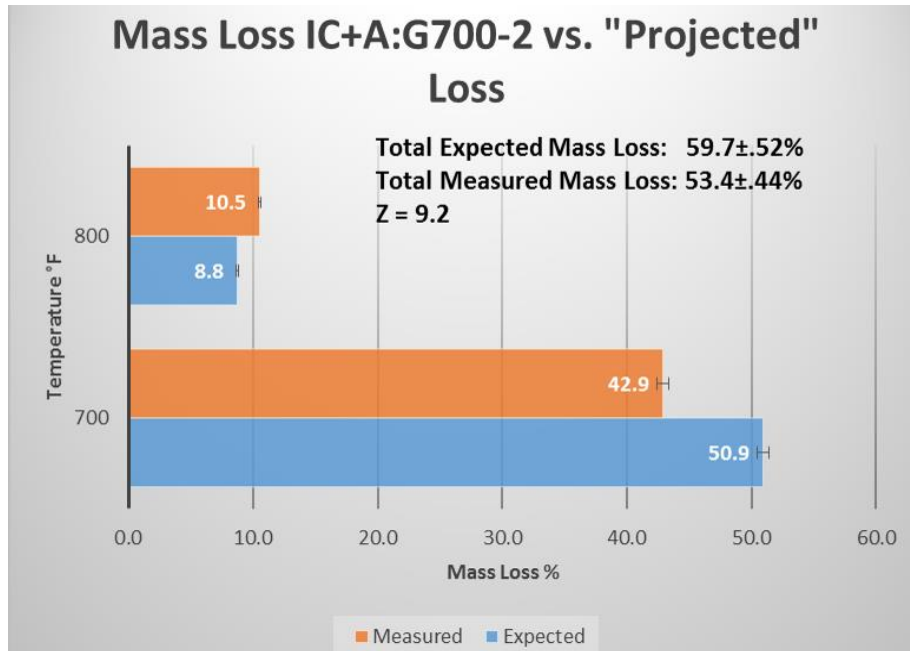


Figure 3-10. Mass loss profile of layered IC+Fixative A coupon #2 (predicted and actual).

As shown in these figures, the intumescent coating surpassed expectations in reducing the total mass loss when layered over the fixative. For coupon #1, the total measured mass loss was $47.8 \pm 0.49\%$ versus an expected mass loss of $61.6 \pm 0.53\%$. For coupon #2, these results were repeated, with slightly better protection being afforded by the intumescent coating; total measured mass loss was $53.4 \pm 0.44\%$ versus an expected total mass loss of 59.7% .

FIU and SRNL commenced detailed discussions with SRS 235-F site personnel to define the operational, safety, and regulatory requirements for deploying an intumescent coating as a fire resilient fixative in support of the SRS 235-F hot cells. A major component associated with the safety personnel revolves around fire resiliency of the material, which is a key advantage of intumescent coatings. All of the intumescent coatings FIU is currently baselining have all been certified by independent laboratories against the following ASTM, NFPA, UL, and UBC fire testing standards:

- UL 263 / UL 723 / ASTM E-119 / ASTM E-84 / ASTM E-2768/ UL 10B
- NFPA: 251 / NFPA: 255 / NFPA: 703 / NFPA: 252
- ULC S101 / ULC S102 / UBC 8.1 / UL 1715 / UBC 26-3 / UBC 7-1

Additional testing protocols are being discussed and developed in order to address several of the other safety, regulatory, and operational requirements highlighted by the site.

FIU has completed the purchase of three additional commercial-off-the-shelf intumescent coatings to baseline. These include Intumax, Interchar, and Fire Dam. FIU will baseline these intumescent coatings utilizing the same testing protocols developed by FIU and SRNL during the proof-of-principle phase in order to ensure integrity in the testing, evaluation, and direct comparison of the various intumescent materials. FIU has initiated discussions with SRNL to develop a new testing protocol designed to determine the actual protection afforded by a fixative in mitigating/preventing the release of radioisotopes during fire and extreme heat conditions.

Lastly, FIU received and is reviewing the schematics and approved equipment list received from SRS 235-F site personnel on the facility hot cells. FIU will begin planning for a full scale demonstration for applying the final down-selected intumescent coating under the same operational and safety constraints encountered in the SRS 235-F hot cell.

FIU prepared and presented a professional presentation titled, “A Novel Approach to Mitigating the Potential Release of Radioisotopes under Fire Conditions: Enhancing Fire Resiliency in Facilities and Fixatives during D&D and Storage Activities,” during the March 6-10 Waste Management 2016 conference in Phoenix, AZ (Figure 3-11). In addition, a poster titled, “Fixatives Decision Model on KM-IT Platform,” was prepared and presented by DOE Fellow Jorge Deshon at the student poster session at the Waste Management Symposia in Phoenix.



Figure 3-11. Joe Sinicrope presenting at WM16.

Task 2.1.2: Development of a Decision Model for Contamination Control Products

A poster titled, “Fixatives Decision Model on KM-IT Platform,” was prepared and presented at the Student Poster Competition session at the Waste Management Symposia in Phoenix.

During this reporting period, FIU continued to review and update the contamination control product list. FIU has developed a web-based decision model on the D&D KM-IT framework to aid in the selection of appropriate contamination control products (fixatives, strippable coatings, and decontamination gels) during D&D activities. The web-based application was sent to DOE for review on January 15, 2016. Subsequently, FIU incorporated some changes based on comments received from DOE. The decision model has been made available through the D&D Knowledge Management Information Tool portal for beta testing and input from field site users.

Task 2.1.3: Robotic Technologies for SRS 235-F

A poster titled, “Cooperative Robotic Scheduling and Path Planning for D&D Applications,” was prepared and presented by DOE Fellow Sebastian Zanolgo during the student poster session at the Waste Management Symposia in Phoenix.

The SRS 235-F facility has a need to identify a remote system that can make one-time entry to highly contaminated areas. The one-time-entry requirement indicates that the technology will not be retrieved at the end of the work but would remain inside the facility due to the high levels of contamination. FIU will perform research to identify robotic technology systems applicable to the challenges and needs of the SRS 235-F Facility. Research will include working with SRNL

to define the requirements for the robotic technology and utilizing the Robotic Database in D&D KM-IT to search and identify potential technologies that meet the defined requirements. A summary report will be developed to document the results.

Task 2.1.4: Fogging Research and Evaluation

A poster titled, “Innovative Process for Abatement of Mercury,” was prepared and presented by DOE Fellow Janesler Gonzalez during the student poster session at the Waste Management Symposia in Phoenix. The poster presents the research performed by the DOE Fellow during his summer 2015 internship at INL. This task has been completed.

Task 2.2: Technology Demonstration and Evaluation

A poster titled, “ASTM Testing Standards Development for D&D Technologies” was prepared and presented by DOE Fellow Jesse Viera at the student poster session at the Waste Management Symposia in Phoenix.

The primary objective of this task is to standardize and implement proven processes to refine and better synchronize DOE-EM technology needs, requirements, testing, evaluation, and acquisition by implementing a three-phased technology test and evaluation model. The development of uniformly accepted testing protocols and performance metrics is an essential component for testing and evaluating D&D technologies.

Mr. Joseph Sinicrope attended the ASTM International Conference in San Antonio, TX on January 24-27, 2016, where he presented an executive brief to support the initiative of developing and promulgating uniform testing protocols and performance metrics for D&D technologies across the stakeholder community and outlined the proposed way ahead for bringing this initiative to fruition (milestone 2015-P3-M2.2). Mr. Sinicrope was elected Chairman for the E10.03 Subcommittee on Radiological Protection for Decontamination and Decommissioning of Nuclear Facilities and Components. Subsequently, FIU began identifying and inviting potential members across the stakeholder community to join the subcommittee. This effort will assist in moving forward a specified task associated with ARC's DOE-EM Cooperative Agreement, specifically implementation of a Technology Test and Evaluation Model that incorporates uniform testing protocols and capability assessments for technologies used in deactivation and decommissioning activities.

FIU is leading the standards development process for D&D technologies through the ASTM International E10.03 Subcommittee. A draft agenda for the scheduled June Working Group on this initiative was developed and distributed to the working group members. New members from SRNL and INL were recruited into the Working Group, and clear objectives for the June meeting were outlined. These include:

1. Confirm/modify operational characteristics and requirements for fixatives used in support of D&D technologies. We will capture these and then begin a DRAFT standard for D&D coatings similar to ASTM E-2731 above.
2. Begin INITIAL standards development for testing protocols related to determining radiation resiliency of fixatives used for long-term D&D requirements.

3. Begin INITIAL standards development for testing protocols related to determining the decontamination factor (DF) of fixatives/decon gels on contaminated concrete for D&D (and possibly other substrates).
4. Begin INITIAL standards development for testing protocols related to fixative/decon gel/coating performance on contaminated steel for D&D.

A general approach was agreed upon as a starting point for the working group members. There are some existing testing protocols associated with various R&D efforts for D&D technologies that have gained informal acceptance. Identifying these, codifying them, then reformatting into the ASTM standard and staffing across community stakeholders for review will allow the formal process of standards development to occur. This will allow for the development of not only uniform testing protocols and performance metrics to justify test and evaluation methods, but also facilitate institutional objectives related to capturing, preserving, and sharing information.

FIU finalized the manuscript titled, “The Expanding Nuclear Niche and Growing Requirement for Standardized Testing Protocols and Performance Metrics for D&D Technologies,” for publication in the March/April 2016 ASTM International’s Standardization News magazine.

Task 3: D&D Knowledge Management Information Tool (KM-IT)

Task 3 Overview

The D&D Knowledge Management Information Tool (KM-IT) is a web-based system developed to maintain and preserve the D&D knowledge base. The system was developed by Florida International University’s Applied Research Center (FIU-ARC) with the support of the D&D community, including DOE-EM (EM-13 & EM-72), the former ALARA centers at Hanford and Savannah River, and with the active collaboration and support of the DOE’s Energy Facility Contractors Group (EFCOG). The D&D KM-IT is a D&D community driven system tailored to serve the technical issues faced by the D&D workforce across the DOE Complex. D&D KM-IT can be accessed from web address <http://www.dndkm.org>.

Task 3 Quarterly Progress

A professional poster titled, “Robotics Technologies on Knowledge Management Information Tool (KM-IT) Platform,” was prepared and presented during the March 6-10 Waste Management 2016 conference in Phoenix, AZ (Figure 3-12). In addition, a poster titled, “Fixatives Decision Model on KM-IT Platform,” was prepared and presented by DOE Fellow Jorge Deshon at the student poster session at the Waste Management Symposia in Phoenix.

FIU also hosted a booth in the exhibitor hall during the conference (Figure 3-13). FIU hosted workshops on D&D KM-IT during the conference by providing live demonstrations of the system and showing the available features and the newly added content, with emphasis on the robotic technologies. During the operation of the exhibitor booth and poster presentation of D&D KM-IT, FIU encouraged conference attendees to become active users of the system as well as to register as subject matter specialists. Significant interest was shown in the knowledge management of D&D as reflected by the increase in user registrations during the conference, increasing the total number of registered users from 846 to 903 (+57). In addition, the number of subject matter specialists increased from 93 to 104 (+11).



Figure 3-12. Robotics on D&D KM-IT poster being presented at WM16.



Figure 3-13. DOE Fellows and ARC staff at FIU booth during WM16 Exhibit Hall.

DOE Fellows and other FIU students are supporting D&D KM-IT by reviewing the information in the vendor and technology modules and updating contact information. As of April 13, the system included a total of 1263 technologies and 941 vendors.

The FIU team completed the development of a desktop decision support model for fixatives and deployed it on the test server for DOE review on January 15, 2015 (milestone 2015-P3-3.2). The FIU team incorporated revisions to the web-based decision support model for fixatives based on comments received from DOE, including the addition of a product disclaimer statement and the removal of product cost information. A screenshot of the Decision Model search page and one of the product data sheets are included as Figures 3-6 and 3-7. The D&D Decision Model can assist in the selection of commercially available fixatives, strippable coatings, and decontamination gels for application during D&D activities. The model includes a comprehensive database of commercially available fixatives and other contamination control products and is capable of filtering and sorting the available products according to the criteria entered by the user. The initial product list was from the former DOE Hanford ALARA Center. This list was thoroughly reviewed in order to eliminate products which were discontinued or not commercially available and an extensive search was conducted to add newer commercial products which fit the criteria. Manufacturers were also contacted to update the product list. The decision model has been made available for beta testing by field site users who can provide feedback on ways to improve the tool. FIU is also beginning the design and development of a mobile application for this tool.

Benefits of the D&D Decision Model include:

1. Cuts down research time to identify contamination control products to use depending on site-specific conditions.
2. Provides an instant overview of the commercially available products filtered and sorted for the criteria entered.
3. Provides access to concise information on over 40 commercially available contamination control products.
4. Can be easily expanded to include more criteria or newly available products.

Figure 3-14 is a screenshot of the decision model search options and Figure 3-15 shows an example fixative product data sheet.

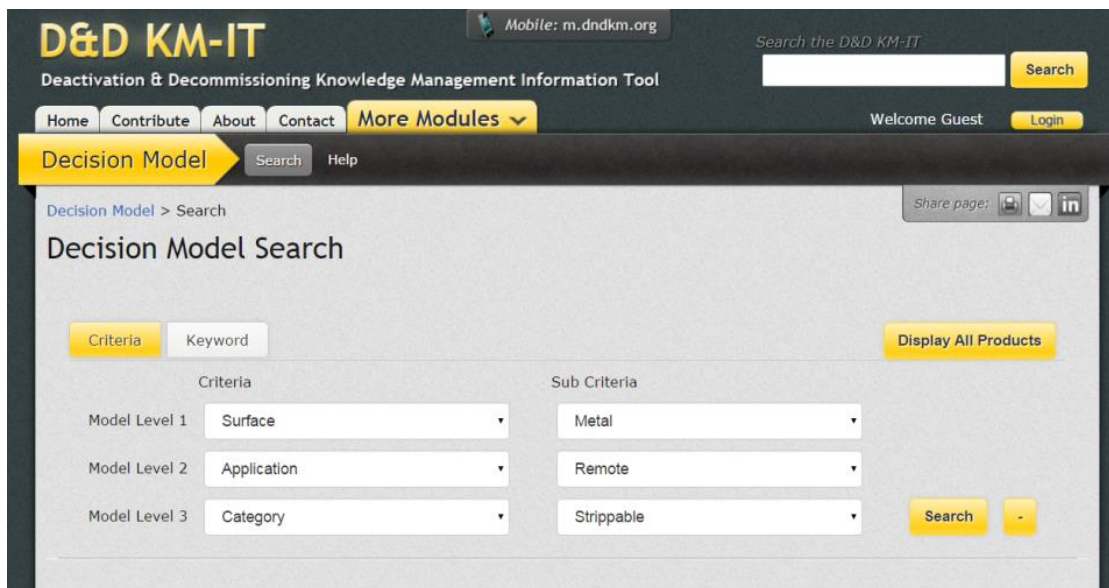


Figure 3-14. Fixative Decision Model search page.

D&D KM-IT
Deactivation & Decommissioning Knowledge Management Information Tool

Home Contribute About Contact **More Modules** v

Welcome Guest Login

Decision Model Search Help

Back to Decision Model > Product Factsheet

CC STRIP

Instructions
CC Strippable can be brushed, rolled, misted or spray applied. Spray application can best be accomplished with a hand pump, metal canister spray unit with fan tip. This is the final step in a two step approach, previously using the CC Wet.

Product Use
To decontaminate any contaminated surface

Previous Use
Used in an experimental radiological dispersal exercise by Homeland Security. (See project profile)

Advantages
Strippable coating. Removes radiological beryllium and other hazardous contamination.

Product URL
<http://instacote.com/cc-strip.htm>

Vendor
Pegasus International Inc.
Schenley, Pennsylvania , United States
(724) 845-2838
www.pegasus-international.com
More...

Comments

Product Data

Combustion:	NA
Cost:	\$490.00 per 5 gallon pail
Coverage:	320 ft ² /gal
PH:	7-9
Ingredients:	Butyl acrylate polymer (25067 - 01-0) <51%
SG:	1.0 - 1.2
Viscosity:	NA
Solubility In Water:	100%
Volatile Percentage:	NA
Incompatibility:	None Known
Conditions To Avoid:	Do not allow freezing
Hazardous Decomposition:	NA
HMIS Rating:	Health - Flammability - Reactivity - Hazard -
Thickness:	Thick enough that it could be removed
Density:	NA
ShelfLife:	1 Year
FlashPoint:	Will not flash ignite

Figure 3-15. Example product data sheet from the Fixative Decision Model.

FIU developed a draft newsletter to announce the participation of STEM students from FIU and other U.S. colleges and universities at the upcoming Waste Management Symposia from March 6-10, 2016 in Phoenix, AZ. The activities include the student poster competition, a student/industry reception, a student panel session, and a student resume job portal hosted by the conference. The draft newsletter was sent to DOE for review and subsequently revised before being distributed to the WM16 attendee list (Figure 3-16).

D&D KM-IT

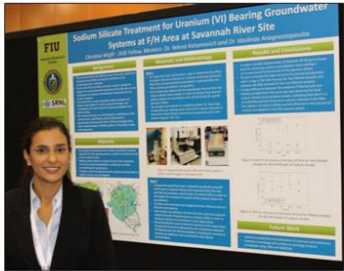

Knowledge Management Information Tool

STEM Student Participation at WM2016

*** | FACEBOOK:LIKE | ***

Dear *|FNAME|*, will you be attending Waste Management 2016? Be sure to take advantage of the opportunities to meet the next generation of scientists and engineers that will continue moving our industry forward into the future. You will be able to meet and see these students in action throughout the WMI conference: participating in the WMS Student Exhibition/Competition, working as student assistants in the various sessions and panels, participating in the Student/Industry Reception on Monday evening, representing and speaking on behalf of their generation in panel session 42, and enjoying WM16 in general.

Student Poster Exhibition/Competition - Students from colleges and universities from across the United States will be presenting their research topics during the Student Poster Exhibition/Competition on Monday afternoon (Session 031) of the conference in the Exhibit Hall. All posters will remain on display through Wednesday of the conference.


WM15 Student Poster Winner - Christine Wipfli (DOE Fellow)

Student/Industry Reception - Student/Industry Reception - WMS will be hosting a special student reception on Monday evening (6 pm - 8 pm) to promote interaction between the student attendees and industry representatives. Everyone is encouraged to attend and talk to some of the brightest and most accomplished science, technology, engineering, and mathematics (STEM) students as they approach the completion of their education and look forward to starting their professional careers.

Student Panel Session 42: In panel session "Graduating Scientists and Engineers..."

opportunity to connect and interact with students participating in WM16.


The Waste Management Symposia provides an excellent forum for government and industry to meet and greet the next generation of scientists and engineers that will continue moving our industry forward into the 21st Century. WMS provides an excellent opportunity for the "next generation" to learn first-hand the industry's challenges. So take the time to meet some of these great students and share your experiences, knowledge, and lessons learned. You will be amazed at the readiness and eagerness of these students to learn and find solutions to our industry's most difficult challenges. [Florida International University's Applied Research Center](#) is proud to join WMS in welcoming the next generation of scientist and engineers to the [2016 Waste Management Symposia](#).



FIU DOE Fellows at FIU booth during WM15 Exhibit Hall

Meet the "next generation"

Visit the Florida International University's booth (#409) to learn more about STEM student research fueling DOE-EM projects like the [D&D KM-IT](#).



March 6-10, 2016
Phoenix, Arizona
#WMS2016

WM2016 CONFERENCE
MARCH 6 - 10, 2016
PHOENIX CONVENTION CENTER

Figure 3-16. Screenshots of the newsletter announcing STEM student participation at WM2016.

FIU revised the D&D KM-IT overview presentation to incorporate additional comments received from DOE, including adding information regarding interactions with the IAEA as well as corporate knowledge management efforts. The revised presentation was sent to DOE on February 10, 2016. This presentation is planned for use to DOE management.

FIU developed a quarterly update document for the *D&D KM-IT Strategic Approach for the Long-Term Sustainability of Knowledge* document and sent it to DOE on February 10, 2016. The strategic plan for D&D KM-IT is a living document. The projected schedule and status evolve over time as the recommended strategic approaches are implemented. The update document, developed on a quarterly basis, provides an update to the table of recommended actions contained in the original document.

Also during this reporting period, FIU finalized the update of the DOE Technical Fact Sheet for D&D KM-IT, primarily including an update of the system statistics, and sent the document to DOE on February 10, 2016.

FIU completed the development of a metrics progress for outreach and training activities for D&D KM-IT and submitted to DOE on February 29, 2016. This document provides a

performance year 6 mid-year report of the progress being made towards accomplishing the outreach and training goals and objectives set forth in the document titled, “Metric Definition for D&D KM-IT Outreach and Training,” which was developed during performance year 5 and expanded on the outreach and training activities for D&D KM-IT as described in the annual PTP by defining specific metrics and capturing the tools and techniques that will be applied to track and report the results. Outreach and training is a critical element towards the long-term sustainability of knowledge and essential for the long-term strategic vision of D&D KM-IT: it will continue to grow and mature into a self-sustaining system through the active participation of the D&D community it was designed to serve.

FIU completed the development of a Google Web Analytic report for D&D KM-IT for the fourth quarter of 2015 (October to December) and submitted it to DOE on February 11, 2016. This report included information from Google Analytics and Google Web Master tools and a narrative to explain the results. Figure 3-17 shows an infographic of the web analytics for the fourth quarter of 2015. The web analytics were similar to prior fourth quarter reports; there was a drop of some of the key metrics, including Pageviews, Pages per Session and Average Session Duration. However, during the fourth quarter, the site also welcomed 13.42% more visitors and had an increase of 7.69% in the number of sessions. Other interesting results include the Picture Library module becoming one of the top 3 most visited modules and Japan joining the top 5 countries that visit D&D KM-IT.

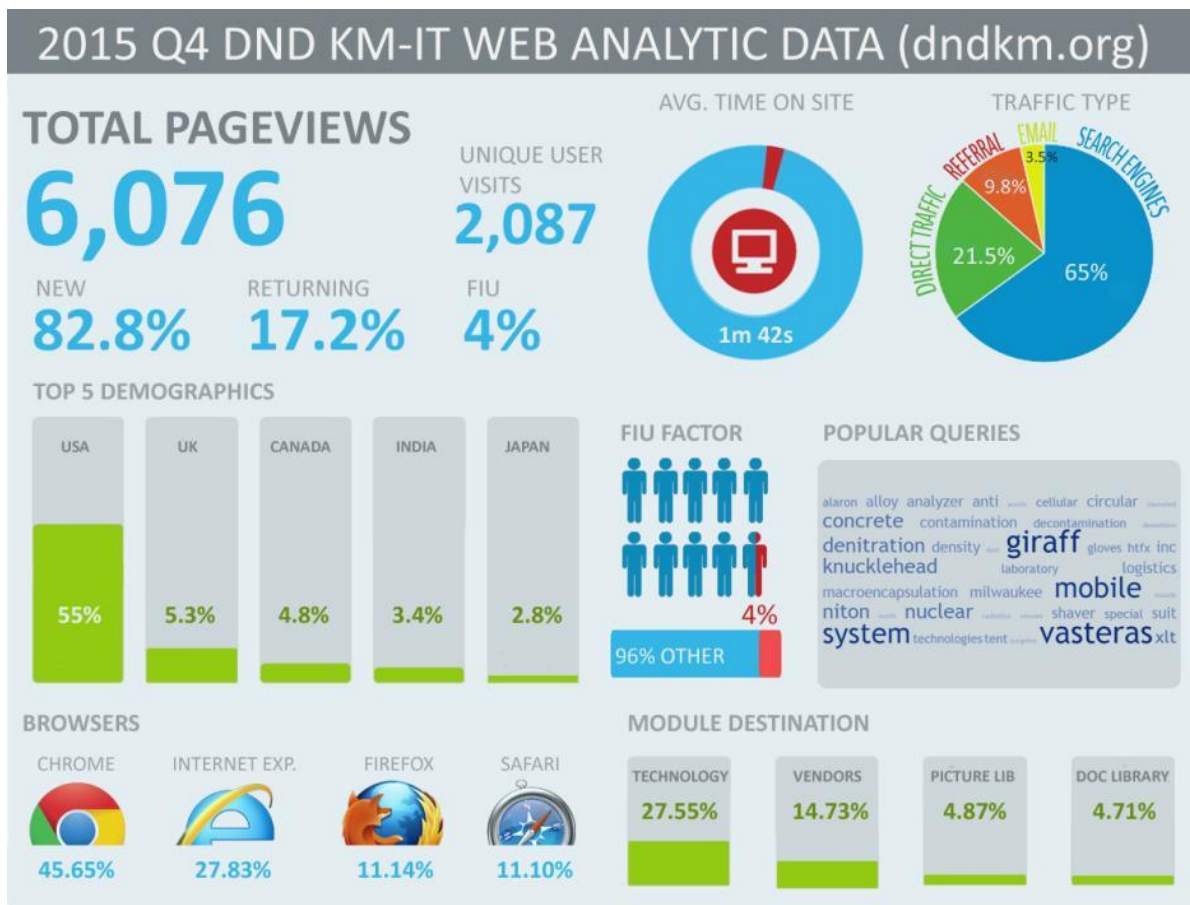


Figure 3-17. Web analytic infographic for 4th quarter of 2015.

FIU supported the completion of a draft case study on D&D KM-IT at the request of DOE for an International Atomic Energy Agency (IAEA) report titled, “Challenges and Approaches to Knowledge Management for Decommissioning and Environmental Remediation.” The IAEA report provides guidance to decision makers in government and private industry, including regulators, facility operators and contractors. It covers the planning, implementation and sustenance of critical nuclear and institutional knowledge necessary for the safe and efficient management of decommissioning and environmental remediation projects. The draft case study on D&D KM-IT was sent to IAEA by DOE on March 22, 2016.

FIU completed development and integration of the Global Knowledge Sharing Platform (for collaboration with the United Kingdom), FIU milestone 2015-P3-M3.3, and sent the link to DOE for their review on March 4, 2016 (Figure 3-18).

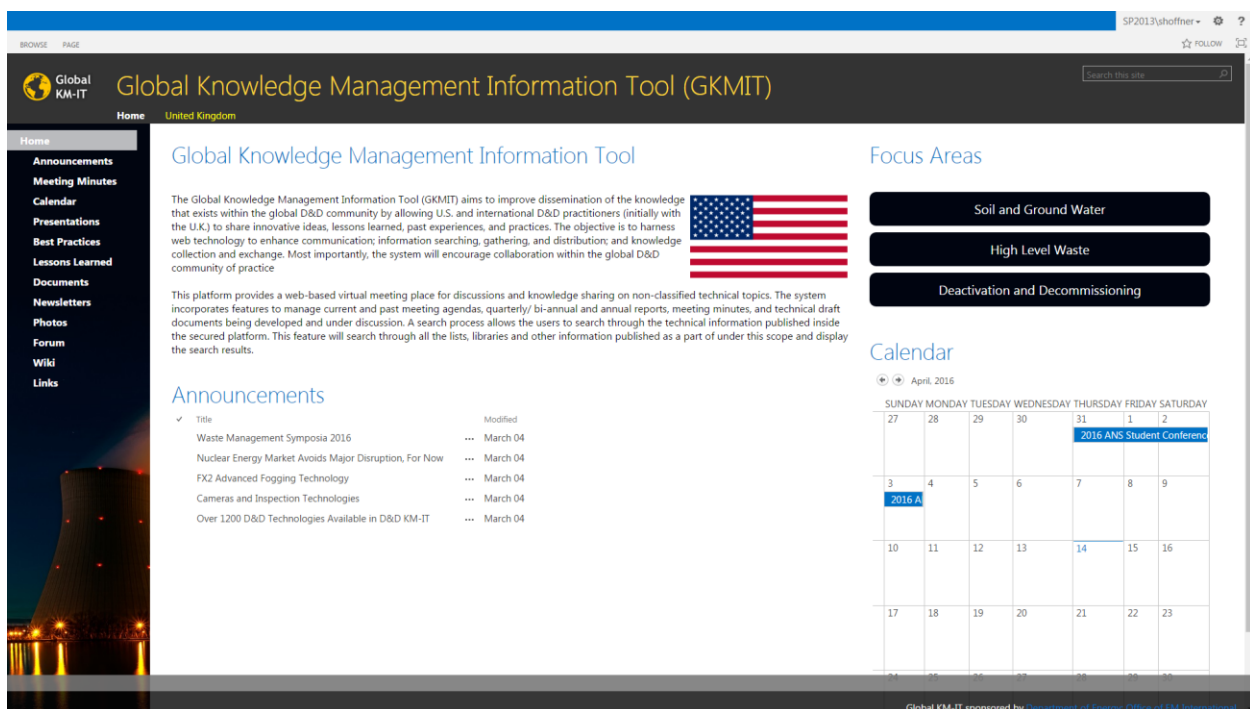


Figure 3-18. Screenshot of the Global Knowledge Management pilot.

The platform was developed based on the protocols and standards for knowledge sharing of non-classified information with a focus on the U.K. and includes features like Newsletters, Meeting Minutes, Technology, Lessons Learned, Best Practices, Documents, Announcements, Calendars, Link, FAQ, Wikis, etc. The Global Knowledge Sharing Platform aims to improve dissemination of the knowledge that exists within the global D&D community by allowing U.S. and international D&D practitioners (initially with the U.K.) to share innovative ideas, lessons learned, past experiences, and practices. The objective is to harness web technology to enhance communication; information searching, gathering, and distribution; and knowledge collection and exchange. Most importantly, the system will encourage collaboration within the global D&D community of practice. A search process allows the users to search through the technical information published inside the secured platform. This feature will search through all the lists,

libraries and other information published as a part of under this scope and display the search results.

FIU is also developing a set of infographics for use in sharing knowledge and information about the DOE EM Cooperative Agreement and the research being performed at FIU for DOE EM. The first one to be developed was for the DOE-FIU Science and Technology Workforce Development Program. The most recent infographic provided an overview of the DOE EM Cooperative Agreement. After several reviews at FIU and DOE and subsequent revision iterations, this infographic was revealed during the FIU Research Review presentations in early April. This completes a deliverable for a draft infographic due to DOE by July 25, 2016.

Milestones and Deliverables

The milestones and deliverables for Project 3 for FIU Year 6 are shown on the following table. Milestone 2015-P3-M2.2 was met with the participation in the ASTM International conference and embedded ASTM E10 committee meeting on January 24-27, 2016. In addition, milestone 2015-P3-M3.2 was met with the deployment of the pilot web-based D&D Decision Model application to DOE for review on January 15, 2016. A deliverable on the Preliminary Metrics Progress Report on Outreach and Training Activities for the D&D KM-IT task was complete and sent to DOE by the due date of February 29, 2016. FIU completed development and integration of the Global Knowledge Sharing Platform (for collaboration with the United Kingdom), FIU milestone 2015-P3-M3.3, and sent the link to DOE for their review on March 4, 2016. A deliverable, to host a D&D workshop with the D&D community, was completed during the Waste Management conference. A second deliverable was completed by developing a draft infographic on the DOE EM Cooperative Agreement, which was revealed during the FIU Research Review presentations in early April. Milestone 2015-P3-M3.4, the addition/editing of four Wikipedia articles, originally due by March 31, has been reforecast to April 15 due to the coordination needed for the planned FIU Research Review presentations to DOE in early April. The circumstances and path forward, including the new reforecasted date for this project task, have been closely coordinated with the stakeholders at DOE HQ, and was discussed and agreed upon with the DOE Project Lead during regular project teleconferences on March 17 and March 31, 2016.

FIU Performance Year 6 Milestones and Deliverables for Project 3

Task	Milestone/ Deliverable	Description	Due Date	Status	OSTI
Task 1: WIMS	2015-P3-M1.1	Import 2016 data set for waste forecast and transportation data	Within 60 days of data receipt	On Target	
	2015-P3-M1.2	WM 2016 Paper for WIMS	11/6/2015	Complete	
Task 2: D&D	2015-P3-M2.1	Completion of Phase 1 testing of incombustible fixatives	12/31/2015	Complete	
	2015-P3-M2.2	Participate in ASTM E10 Committee Meeting to introduce a requirement for standardized D&D testing protocols & performance metrics	01/31/2016	Complete	
	Deliverable	Summary Report on Robotic Technologies for SRS 235-F Facility	05/29/2016	On Target	OSTI

	Deliverable	Draft Test Plan for Phase II incombustible fixatives testing and evaluation	06/30/2016	On Target	OSTI
	2015-P3-M2.3	Participate in ASTM International's Executive Steering Committee Meeting to solicit final approval for development of standardized testing protocols and performance metrics for D&D technologies.	06/30/2016	On Target	
	Deliverable	Decision brief to DOE-EM 13 on recommended technologies to test for FY'17 using FIU's 3-Phased Technology Test and Evaluation Model.	07/29/2016	On Target	
	Deliverable	Draft technical reports for demonstrated technologies	30-days after demo	On Target	OSTI
	Deliverable	Draft Tech Fact Sheet for technology evaluations/ demonstrations	30-days after demo	On Target	
Task 3: D&D KM-IT	2015-P3-M3.1	Waste Management Symposium Paper for D&D KM-IT	11/06/2015	Complete	
	Deliverable	First D&D KM-IT Workshop to DOE EM staff at HQ	11/30/2015 TBD**	Reforecast	
	2015-P3-M3.2	Deployment of pilot web-based D&D Decision Model application	01/16/2016	Complete	
	2015-P3-M3.3	Completion of development & integration of International KM-IT pilot for UK collaboration	03/04/2016	Complete	
	Deliverable	Preliminary Metrics Progress Report on Outreach and Training Activities	02/29/2016	Complete	
	Deliverable	First D&D KM-IT Workshop to D&D community	03/31/2016	Complete	
	2015-P3-M3.4	Four Wikipedia integration edits/articles	03/31/2016 Reforecasted to 04/15/16	Reforecast	
	2015-P3-M3.5	Deployment of pilot mobile application for D&D Decision Model	05/20/2016	On Target	
	Deliverable	Second D&D KM-IT Workshop to DOE EM staff at HQ	05/31/2016**	On Target	
	Deliverable	First infographic to DOE for review	07/25/2016	Complete	
	Deliverable	Second infographic to DOE for review	08/08/2016	On Target	
	Deliverable	Metrics Progress Report on Outreach and Training Activities	08/15/2016	On Target	
	Deliverable	Second D&D KM-IT Workshop to D&D community	08/25/2016	On Target	
	Deliverable	Draft Security Audit Report	30-days after audit	On Target	
	Deliverable	D&D KM-IT Web Analysis Report	Quarterly	On Target	
Deliverable	Draft Tech Fact Sheet for new modules or capabilities of D&D KM-IT	30-days after deployment of new module	On Target		

****Completion of this deliverable depends on scheduling and availability of DOE EM staff**

Work Plan for Next Quarter

- Task 1: Perform database management, application maintenance, and performance tuning to WIMS.
- Task 1: Receive 2016 data set for waste forecast and transportation data from DOE and complete integration into WIMS.
- Task 2: Complete execution of the phase II testing for evaluating a set of contamination control products and intumescent coatings, selected by FIU and SRS. Begin development of a test plan for the next phase of testing.
- Task 2: Participate in ASTM International's E10 Committee on Nuclear Technologies and Applications and E10.03 - Radiological Protection for Decontamination and Decommissioning of Nuclear Facilities and Components at the June 2016 conference in Chicago. Lead the working group to support the initiative of developing and promulgating uniform testing protocols and performance metrics for D&D technologies across the stakeholder community.
- Task 2: Collaborate with SRNL to define the requirements for robotic technologies to support D&D activities at the SRS 235-F facility as well as across the DOE complex.
- Task 3: Design and development a pilot mobile application for the D&D Decision Model for the selection of fixatives.
- Task 3: Develop quarterly website analytics report and submit to DOE for review.
- Task 3: Complete the D&D KM-IT Workshop to DOE EM staff at HQ, based on scheduling and availability of DOE EM staff.
- Task 3: Complete four new Wikipedia integration edits/articles in support of D&D topics.
- Task 3: Perform outreach and training, community support, data mining and content management, and administration and support for the D&D KM-IT system, database, and network.

Project 4

DOE-FIU Science & Technology Workforce Development Initiative

Project Manager: Dr. Leonel E. Lagos

Project Description

The DOE-FIU Science and Technology Workforce Development Initiative has been designed to build upon the existing DOE/FIU relationship by creating a “pipeline” of minority engineers specifically trained and mentored to enter the Department of Energy workforce in technical areas of need. This innovative program was designed to help address DOE’s future workforce needs by partnering with academic, government and DOE contractor organizations to mentor future minority scientists and engineers in the research, development, and deployment of new technologies, addressing DOE’s environmental cleanup challenges.

Project Overview

The main objective of the program is to provide interested students with a unique opportunity to integrate course work, Department of Energy (DOE) field work, and applied research work at ARC into a well-structured academic program. Students completing this research program would complete the M.S. or Ph.D. degree and immediately be available for transitioning into the DOE EM’s workforce via federal programs such as the Pathways Program or by getting directly hired by DOE contractors, other federal agencies, and/or STEM private industry.

Project Quarterly Progress

Fellows continue their support to the DOE-FIU Cooperative Agreement by actively engaging in EM applied research and supporting ARC staff in the development and completion of the various tasks. The program director continues to work with DOE sites and HQ to fully engage DOE Fellows with research outside ARC where Fellows provide direct support to mentors at DOE sites, DOE-HQ, and DOE contractors. All Fellows also participated in a weekly meeting conducted by the program director, a conference line has been established to enable DOE Fellows conducting internship to join to weekly meeting and update program director on their internship. During each of these meetings, one DOE Fellow presents the work they performed during their summer internship and/or EM research work they are performing at ARC.



DOE Fellow Christine Wipfli was selected for a one year internship position with the International Atomic Energy Agency (IAEA), stationed at the agency headquarters in Vienna, Austria. Ms. Wipfli, currently pursuing an undergraduate degree in environmental engineering, will be working with the Division of Nuclear Fuel Cycle and Waste Technology to assist in managing global environmental remediation projects. The IAEA is an international organization which reports to both the United Nations General Assembly and Security Council, and works for the safe, secure and

peaceful uses of nuclear science and technology. Last summer, Ms. Wipfli also participated in an internship at the Department of Energy’s Office of Environmental Management headquarters in Washington, D.C., where she gained valuable knowledge and insight into the field of Radioactive Waste Management (RWM). Ms. Wipfli joined the DOE Fellows Program in fall of 2014 and has received three awards for poster competitions at FIU and at national conferences. Her expected graduation date is December of 2017.



DOE Fellow Silvana Di Pietro was awarded the Roy Post Foundation Scholarship. This is a Waste Management Symposia sponsored scholarship and she'll receive the award at the upcoming Waste Management Conference in Phoenix, AZ.

The American Nuclear Society (ANS) student section at Florida International University (FIU) was officially launched on January 28, 2016 with a visit to FIU from ANS president Eugene “Gene” Grecheck for a special ceremony to present the Student Section Charter. Chapter officers include Ryan Sheffield (President), Maximiliano Edrei (Vice President), Awmna Rana (Secretary), Janesler Gonzalez (Committee Head), and Jesse Viera (Treasurer). Dr. Leonel Lagos from FIU’s Applied Research Center is serving as the FIU Chapter Faculty Advisor. Figures 4-1 and 4-2 show photographs from the event.



Figure 4-1. ANS President Gene Grecheck (back row, middle), new FIU ANS Student Section officers (front row), and FIU faculty and staff.



Figure 4-2. ANS President Gene Grecheck (back row, middle) with new FIU ANS Student Section officers.

FIU developed an electronic newsletter to send out to all Waste Management 2016 attendees to highlight the opportunities at the conference to interact with the next generation of scientists and engineers, including students from FIU and other U.S. colleges and universities. Activities included in the newsletter:

Student Poster Presentation – Students from Florida International University (FIU) and other colleges and universities from across the United States will be presenting their research topics during the Student Poster Presentation on Monday afternoon (Session 031) of the conference in the Exhibit Hall. All posters will remain on display through Wednesday of the conference.

Student/Industry Reception – WMS will be hosting a special student reception on Monday evening (6 pm – 8 pm) to promote interaction between the student attendees and industry representatives. Everyone is encouraged to attend and talk to some of the brightest and most accomplished STEM students as they approach the completion of their education and look forward to starting their professional career.

DOE-FIU Workforce Development Program – DOE Fellows will be manning FIU’s booth #733 in the exhibitor hall. Please plan to come by the booth to talk to them and learn about the Applied Research Center at FIU. FIU-ARC provides support to the U.S. Department of Energy (DOE) Office of Environmental Management (EM) in their mission of accelerated risk reduction and cleanup of the environmental legacy from the nation’s Manhattan Project nuclear weapons program. FIU-ARC is currently executing applied research in radioactive waste processing, facility deactivation and decommissioning (D&D), soil and groundwater remediation, and information technology (IT) applications for environmental management. FIU-ARC also provides hands-on research to FIU

science, technology, engineering, and mathematics (STEM) students via its student workforce development and training program (DOE Fellows Program).

Dr. Brady Lee from PNNL presented “Hanford: An Introduction to Waste Issues and Associated Biogeochemical Tasks Supporting Site Remediation” to the DOE Fellows and ARC staff as part of the DOE Fellows Lecture Series on February 3, 2016. Figure 4-3 shows pictures from this event.



Figure 4-3. Dr. Brady Lee presenting at the DOE Fellows Lecture Series.

On February 8-9, 2016, FIU hosted a visit from representatives from the National Nuclear Laboratory (NNL) in the United Kingdom, including Steve Thompson (Business Manager, NNL), Anthony Banford (Chief Technology Officer, NNL), and Keith Miller (Head of Marketing, NNL) (Figure 4-4). Other distinguished guests included Benjamin Rivera (DOE EM International Program) and Dr. Kevin Cooper (Dean of Applied Research & Entrepreneurial Activities, Indian River State College Regional Center for Nuclear Education and Training). FIU was represented by Henry Artigues (Director of Research Development, FIU’s Office of Research & Economic Development), Dr. Inés Triay (ARC Executive Director) and Dr. Leonel E. Lagos (Principal Investigator for DOE-FIU Cooperative Agreement and ARC Director of Research), as well as ARC staff and DOE Fellows from the FIU-DOE Workforce Development Program.



Figure 4-4. National Nuclear Laboratory (NNL) representatives Steve Thompson, Anthony Banford, and Keith Miller with Dr. Leonel Lagos, ARC staff and DOE Fellows.

During the visit, ARC presented the research being performed for the DOE EM and NNL provided a presentation on their research activities. NNL representatives also had the opportunity to meet with faculty from the FIU nuclear program as well as tour the ARC facilities. During these tours, ARC staff and DOE Fellows had the opportunity to showcase their DOE EM research (Figure 4-5):

- **Robotics and Sensors Laboratory**
 - Development of Inspection Tools for DST Primary Tanks
 - Pipeline Corrosion and Erosion Evaluation
- **Non-Metallic Materials Testing Laboratory**
 - Evaluation of Nonmetallic Components in the Waste Transfer System
- **IT and Cyber Research Laboratory**
 - D&D Knowledge Management Information Tool (D&D KM-IT)
 - Waste Information Management System (WIMS)
- **Engineering Technology Laboratory**
 - Evaluation of FIU's SLIM for Estimating the Onset of Deep Sludge Gas Release Events
- **Radiological Laboratory**
 - Remediation Research and Technical Support for the Hanford Site
- **Test and Evaluation Facility**
 - Incombustible Fixatives - Fire Resiliency Testing
- **Modeling, Simulation & GIS Laboratory**
 - Modeling of Surface Water and Sediment Transport
 - Application of GIS Technologies for Hydrological Modeling Support
- **Soil and Groundwater Laboratory**

- Remediation Research and Technical Support for Savannah River Site



Figure 4-5. ARC lab tours to UK NNL visitors.

During their visit to FIU, NNL also presented as part of the DOE Fellows Lecture Series. Dr. Steve Thomson spoke on the “UK Experience Relevant to US Nuclear Clean-up Missions.” In addition, Mr. Keith Miller gave another talk on “An overview of NNL” and Dr. Anthony Banford spoke on “Research, Development and Demonstration in Waste Management and Decommissioning.”

DOE Fellows participated in the Engineering Expo held by FIU on Friday, February 26, 2016 and showcased their hands-on research related to DOE EM in the ARC Robotics Laboratory. The **FIU Engineering Expo** is the college’s premier community outreach event organized annually and welcoming more than 1,400 K-12 students from Miami Dade and Broward County Schools (elementary, middle and high schools) to the FIU Engineering Center to engage FIU students, researchers and staff, and to discover the endless possibilities of STEM. All of the college’s research and learning labs were opened for tours, there are contests, presentations and hands-on projects. The event provides exposure to science and engineering for local public school students to encourage them to consider a career in the engineering and science professions, where minorities are under-represented.

DOE Fellows Alejandro Garica, Alexis Smoot, Christopher Strand, Gene Yllanes, Sarah Bird, Sebastian Zanlongo and Yoel Rotterman attended and successfully completed hands-on radiation safety training and obtained certifications to work with radioactive materials.

The DOE Fellows program director continued communications to coordinate with DOE-HQ, DOE sites, DOE national laboratories, and DOE contractors for placement of DOE Fellows for summer 2016 internships. Planned internships for spring/summer 2016 include:

Table 4-1. Spring/Summer 2016 Internships

Project	DOE Fellow	Location	Internship Mentor	Comments
1	Erim Gokce	WRPS	Ruben Mendoza/ Dennis Washenfelder	High Level Waste
	Gene Yllanes	SRS	Mike Serrato	Mechanical Systems & Custom Equipment Development and Imaging & Radiation Systems
	Max Edrei	NETL	Chris Gunter	High Level Waste CFD
	Sebastian Zanlongo	LANL	David Mascarena	LANL Robotics Group
2	Alejandro Garcia	PNNL	Brady Lee	Masters
	Alejandro Hernandez	SRNL	Miles Denham	Soil & Groundwater
	Alexis Smooth	DOE HQ	Skip Chamberlain	Soil & Groundwater EM-12
	Awmna Rana	REU/SREL	John Seaman (SREL)	MSIPP Internship or SRNL
	Christopher Strand	LANL	Bill Foley	Soil & Groundwater
	Hansel Gonzalez	SRNL	Miles Denham	PhD
	Sarah Bird	DOE HQ	Skip Chamberlain	Soil & Groundwater (EM-12)
	Silvina Di Pietro	PNNL	Jim Szecosdy/Nik Qafoku	PhD

DOE Fellow Alejandro Garcia completed a 10-week spring 2016 internship at PNNL. His efforts during this reporting period included preparations for the column experiments related to the spectral induced polarization (SIP) signatures of microbial activity designed to remediate uranium-contaminated vadose zone sediment.

DOE Fellow Christine Wipfli began a one year internship at the International Atomic Energy Agency (IAEA) in March 2016. Christine is interning in the Waste Technology Section, Division of Nuclear Fuel Cycle & Waste Technology at IAEA's Headquarters in Vienna, Austria (Figure 4-6). DOE EM included a write up on Christine's achievement, titled "IAEA Awards DOE Fellow Internship," in the Volume 8, Issue 5, of the EM Update newsletter dated March 16, 2016 (https://content.govdelivery.com/accounts/USDOEOEM/bulletins/13c48e1#link_1457990261444).



Figure 4-6. DOE Fellow Christine Wipfli as she started her internship at IAEA in March 2016.

The DOE Fellows who participated in a summer 2015 internship are preparing and presenting an oral presentation at the weekly DOE Fellows meetings. The schedule for these presentations is provided below.

Table 4-2. Presentations on Summer 2015 Internships

DOE Fellow	Internship Location	Summer Mentor(s)	Date
John Conley	WRPS, Richland, WA	Terry Sams/ Dave Shuford	Sept 11, 2015
Andrew De La Rosa	Oak Ridge National Lab – Cyber & Information Security Research	Joseph Trien	Sept 18, 2015
Kiara Pazan & Aref Shehadeh	SRNL, Savannah River, SC	Miles Denham/ Margaret Millings	Oct 09, 2015
Christine Wipfli	DOE-HQ EM-12, Cloverleaf, Germantown, Maryland	Skip Chamberlain/ Kurt Gerdes	Nov 20, 2015
Maximiliano Edrei	National Energy Technology Lab, Morgantown, WV	Chris Guenther	Nov 20, 2015
Natalia Duque	SRNL, Savannah River, SC	Ralph Nichols/ Carol Eddy-Dilek/ Brian Looney	Dec 10, 2015
Yoel Rotterman	DOE-HQ EM-13, Forrestal, Washington D.C.	Albes Ganoa/ John De Gregory	Feb 22, 2016
Ryan Sheffield	DOE-HQ EM-20, Cloverleaf, Germantown, Maryland	James Poppiti	Feb 29, 2016
Jorge Deshon	SRNL, Savannah River, SC	John Bobbitt/ Steven Tibrea	Feb 29, 2016
Jesse Viera	Idaho National Lab	Rick Demmer/ Steve Reese	Apr 11, 2016

Anthony Fernandez / Meylyn Planas	Washington River Protection Solutions (WRPS), Richland, WA	Ruben Mendoza/ Gregory Gauck	Apr 25, 2016
---	---	---------------------------------	--------------

DOE Fellows completed preparation and participated in the Waste Management 2016 Symposia (WM16) in Phoenix, AZ, from March 6-10, 2016. The DOE Fellows completed technical posters, presentation materials, written biographies, resumes, and brief videos for the WM conference to introduce themselves and their research. Among the many distinguished industry leaders that the FIU students met during the conference, they had the chance to take photos with Dr. Monica Regalbuto, Associate Principal Deputy Assistant Secretary for Environmental Management (Figure 4-7).



Back Row (left to right): Yoel Rotterman, Jorge Deshon, Erim Gokce, Anthony Fernandez, Jesse Viera, Natalia Duque, Christopher Strand, Janesler Gonzalez

Next row down (left to right): Christine Wipfli, Ryan Sheffield

Next row down (left to right): Silvina Di Pietro, Maximiliano Edrei, Sebastian Zanlongo, Robert Larriere, John Conley

Next row down (left to right): Awmna Rana, Hansel Gonzalez, Alejandro Fernandez

Front row (left to right): Leonel Lagos, Ines Triay, Monica Regalbuto, Meylyn Planas, Gene Yllanes

Figure 4-7. DOE Fellows at WM16 with Program Director Leonel Lagos and DOE EM's Monica Regalbuto

A total of twenty (20) DOE Fellows attended WM16 and presented technical posters during Session 31 (Student Posters: The Next Generation – Industry Leaders of Tomorrow) on Monday, March 7, 2016. The posters presented the DOE-EM research that they have performed at FIU's ARC and during their summer internships at DOE sites, HQ, and national research laboratories, in the research areas of high level waste/waste processing, soil and groundwater modeling and remediation, and deactivation and decommissioning. The titles of the DOE Fellow posters presented during the Student Poster Competition at WM16:

1. Kinetic and Mechanism Studies of U(VI) Bearing Groundwater Treated with Sodium Silicate at the Savannah River Site - Alejandro Hernandez (DOE Fellow)
2. Nonmetallic Materials Testing for Hanford's HLW Transfer System - Anthony Fernandez (DOE Fellow)

3. Application of Geospatial Tools to Support Development of a Hydrological Model of the Tims Branch Watershed, Aiken, SC - Awnna Rana (DOE Fellow)
4. Cooperative Robotic Scheduling and Path Planning for D&D Applications - Sebastian Zanlongo (DOE Fellow)
5. A Study of Sodium Silicate Treatment for the U(VI)-impacted Acidic Groundwater at Savannah River Site's F/H Area - Christine M. Wipfli (DOE Fellow)
6. Topographic Analysis of Timeseries Data to Support the Hydrology Model of the Tims Branch Watershed, Aiken, SC - Christopher Strand (DOE Fellow)
7. Modifications and Enhancements to the Robotic Pipe Inspection Tool to be utilized for the DOE High Level Waste Project at the Hanford Site - Erim Gokce (DOE Fellow)
8. Rapid Imaging of Solids in High Level Waste Tanks at Hanford - Gene Yllanes (DOE Fellow)
9. Study of an Unrefined Humate Solution as a Possible Remediation Method for Groundwater Contamination at SRS - Hansell Gonzalez Raymat (DOE Fellow)
10. Innovative Process for Abatement of Mercury - Janesler Gonzalez (DOE Fellow)
11. ASTM Testing Standards Development for D&D Technologies - Jesse Viera (DOE Fellow)
12. Stainless Steel Corrosion: Feed Properties Affecting Material Selection for LAWPS Piping at Hanford Site - John Conley (DOE Fellow)
13. Fixatives Decision Model on KM-IT Platform - Jorge Deshon (DOE Fellow)
14. Radial Jet Impingement Correlation Investigation - Maximiliano Edrei (DOE Fellow)
15. Heat Transfer Calculations for the Use of an Infrared Temperature Sensor - Meilyn Planas (DOE Fellow)
16. A Model to Simulate Flow in Tims Branch, Savannah River Site, SC - Natalia Duque (DOE Fellow)
17. The Characterization of Uranium Phases Produced by the NH₃ Injection Remediation Method under Hanford 200 Area Conditions - Robert Lapierre (DOE Fellow)
18. Development of a Miniature Motorized Inspection tool for the Hanford DOE Site Tank Bottoms - Ryan Sheffield (DOE Fellow)
19. Ammonia Gas Injection for Remediation of Uranium Contamination - Silvina Di Pietro (DOE Fellow)
20. Green & Sustainable Remediation Analysis of a Packed Tower Air Stripper Used to Remediate Groundwater Contaminated with CVOCs - Yoel Rotterman (DOE-Fellow)

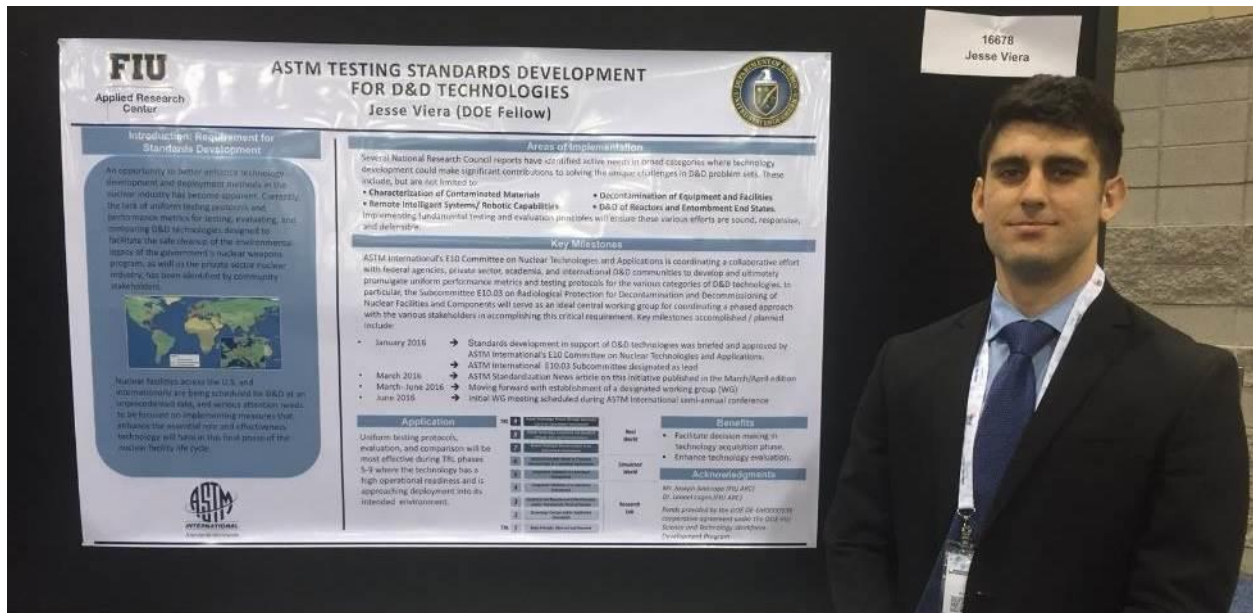


Figure 4-8. Jesse Viera presenting at the WM16 student poster session.

DOE Fellow Robert Lapierre presented during professional session 81, on “Characterization of U(VI)-Bearing Precipitates Produced by Ammonia Gas Injection Technology for Unsaturated Sediments” and DOE Fellow Ryan Sheffield presented during professional session 95 on “Development of Inspection Tools for the AY-102 Double-shell Tank at the Hanford DOE Site.” (Figure 4-9). DOE Fellow Yoel Rotterman presented a professional poster during session 71 on “DOE Climate Change Vulnerability and Adaptation Planning.”



Figure 4-9. DOE Fellow Ryan Sheffield presenting at WM16.

DOE Fellows Program Director, Dr. Lagos, and DOE Fellow Christine Wipfli participated in a conference panel during session 42 on Tuesday, March 8, titled “Graduating Scientists and Engineers: Wants and Needs – Does it Differ Between Countries” (Figure 4-10). During this panel session, students had an opportunity to interact with government and industry representatives to discuss their wants and needs as they get ready to transition into the workforce.

Other panel members included DOE EM-70, Ms. Melody Bell (Associate Deputy Assistant Secretary for Human Capital), and Pacific Northwest National Lab, Ms. Hope Lee (Manager for PNNL Environmental Management Group)



Figure 4-10. Panel members for Session 42 at WM16.

In addition, DOE Fellows Program Director, Dr. Lagos, also led session 43 “Young Professional in Nuclear Science and Engineering, an International Perspective” (Figure 4-11). Panel members included young nuclear professionals from the Young Generation Nuclear from the US and the UK. The panel also include a young nuclear professional representing Savannah River Site.



Figure 4-11. Panel members for Session 43 at WM16.

The 2016 Roy G. Post Foundation Scholarship at the Graduate Student Level was awarded to DOE Fellow Silvina Di Pietro during the WM2016 Conference Honors and Awards Luncheon on Tuesday, March 8, 2016 (Figure 4-12).



Figure 4-12. DOE Fellow Silvina Di Pietro awarded Roy G. Post Foundation Scholarship at WM16.

The DOE Fellows joined staff from the Applied Research Center at Florida International University to host a booth (#409) in the exhibitor hall during the conference, interacting with conference attendees on how FIU-ARC provides support to the DOE EM in their mission of accelerated risk reduction and environmental legacy cleanup. DOE Fellows also participated as Student Assistants during the conference, assisting conference organizers and presenters during the technical sessions.

Finally, the conference hosted a Networking Reception for Students and Young Professionals on the evening of Monday, March 7, to promote interaction between the student attendees and industry representatives.

FIU also developed and sent an electronic newsletter to send out to all Waste Management 2016 attendees to highlight the opportunities at the conference to interact with the next generation of scientists and engineers, including students from FIU and other U.S. colleges and universities. Activities included in the newsletter:

Student Poster Exhibition/Competition – Students from colleges and universities from across the United States will be presenting their research topics during the Student Poster Exhibition/Competition on Monday afternoon (Session 031) of the conference in the Exhibit Hall. All posters will remain on display through Wednesday of the conference.

Student/Industry Reception – Student/Industry Reception – WMS will be hosting a special student reception on Monday evening (6 pm – 8 pm) to promote interaction between the student attendees and industry representatives. Everyone

is encouraged to attend and talk to some of the brightest and most accomplished science, technology, engineering, and mathematics (STEM) students as they approach the completion of their education and look forward to starting their professional careers.

Student Panel Session 42 – In panel session “Graduating Scientists and Engineers: Wants and Needs,” students have an opportunity to interact with government and industry representatives to discuss their wants and needs as they get ready to transition onto the workforce. This session is scheduled for Tuesday morning at 8:30 am. This year, the next generation will be represented by Ms. Christine Wipfli (FIU DOE Fellow).

Student Resume Job Portal – The [WMS Student Resume Portal](#) is designed to help connect potential employers with student candidates. In this portal, you can access student resumes and information.

FIU continues to aggressively identify federal entry-level career opportunities within DOE with a particular emphasis on federal positions within DOE EM, the national labs, or DOE tier-1 contractors. The following DOE Fellows have recently accepted offers of employment: 1) Kiara Pazan with AECOM, 2) Aref Shehadeh with Nova Consulting Group, Inc., 3) Meilyn Planas with Florida Power & Light (FPL), and 4) Andrew De La Rosa with Lockheed Martin, 5) Brian Castillo with Stryker, 6) Janesler Gonzalez with Velossa Tech, and 7) Jorge Deshon with Lockheed Martin.



DOE Fellow, Kiara Pazan Joins AECOM

Kiara Pazan graduated with a Bachelor of Science degree in environmental engineering at Florida International University in the fall of 2015. When inducted into the DOE/FIU Science & Technology Workforce Development Program in the fall of 2014, she started working under the mentorship of Dr. Ravi Gudavalli in the development and optimization of soil and groundwater remediation and treatment technology. She was involved in developing an integrated model for the migration and distribution of natural organic matter injected into subsurface systems for the Savannah River Site. Her objectives were to investigate sorption and desorption parameters of humic acid (HA) injection through column experiments and determine transport parameters to model migration and distribution of HA injected in the subsurface for *in situ* treatment. In the summer of 2015, Kiara interned at Savannah River National Laboratory (SRNL). Her main project involved processing diffusion samplers that were deployed in the F-Area to further test the effects on sorption of uranium by humate-loaded sediments, under the mentorship of Dr. Miles Denham. Diffusion samplers, which were filled with sediment and different humate concentrations, were deployed into a well to equilibrate with the groundwater. This method provides a major advantage as it can be performed in existing monitoring wells, rather than needing to perform additional drilling. She analyzed the groundwater, pore water, and sediment of

the samplers for uranium, tritium, iodine (I-129), and total organic carbon (TOC). **Upon graduation, Kiara joined AECOM as an Environmental Engineer.**



DOE Fellow, Andrew De La Rosa Joins Lockheed Martin

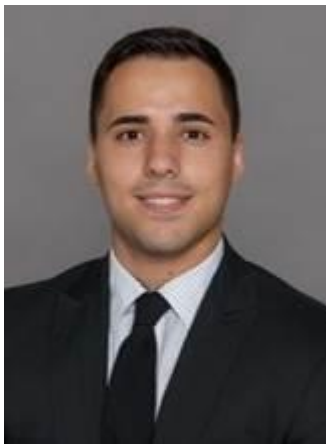
Andrew De La Rosa is a graduate student at Florida International University studying computer engineering with specialization in networks and cybersecurity. He graduated in the fall of 2014, earning his bachelor's degree in computer engineering. When inducted into the DOE/FIU Science & Technology Workforce Development Program in the fall of 2014, he started working with Dr. Himanshu Upadhyay on "Malware Forensics on Mobile Devices for DOE-EM Applications," analyzing the malware signatures from a mobile device and comparing them to the signatures from a desktop. In the summer of 2015, Andrew interned for the Computational Sciences and Engineering Division at Oak Ridge National Laboratory (ORNL). Under the mentorship of Dr. Joseph Trien, Andrew's main role was to learn and test the Hyperion toolset. The Hyperion Project's goal is to provide a software behavior computational algorithm designed to catch programs that are malicious. It is a tool comprised of programmable semantics and structuring based off the original code, by analyzing binaries and using mathematical precision to uncover the program's intended and unintended behaviors. The next generation of Hyperion is currently under development, where more powerful computational processing is performed as well as up-scaling for larger sized programs, while also implementing customization based on the user's preferences. **Recently, Andrew accepted a position as a Cyber Intel Analyst at Lockheed Martin.**

DOE Fellow, Aref Shehadeh Joins Nova Consultant Ltd.



Aref Shehadeh graduated with a Bachelor of Science degree in environmental engineering at Florida International University in the fall of 2015. When inducted into the DOE/FIU Science & Technology Workforce Development Program in the fall of 2014, he started working under the mentorship of Dr. Yelena Katsenovich on the project task titled "Monitoring of U(VI) bioreduction after ARCADIS demonstration at SRS F-Area." ARCADIS implemented the *in situ* injections of a carbohydrate substrate to establish anaerobic reactive zones for metal and radionuclide remediation via the enhanced anaerobic reductive precipitation (EARP) process at the Savannah River Site (SRS) F-Area. In the summer of 2015, Aref interned with the Department of Environmental Management (DOE EM) at Savannah River National Laboratory (SRNL), working on the remediation of iodine-129 (I-129) in the SRS F-Area, which was caused by a large radionuclide plume stemming from an old seepage basin. Dr. Miles Denham, Aref's mentor, proposed the use of silver chloride (AgCl) to react with the I-129 in the

sediments to create a binding effect and prevent further spreading of the plume. Based off Dr. Denham's proposal, Aref was in charge of researching the particle size and structure of AgCl, created in a laboratory setting, and helped determine the optimal size to use for future *in situ* remediation. Recently, **Aref joined Nova Consultants Ltd. as an Assistant Engineer.**



DOE Fellow, Brian Castillo Joins Stryker

Brian Castillo is an undergraduate student at Florida International University pursuing a Bachelor of Science degree in biomedical engineering. He is expected to graduate spring of 2016. When inducted into the DOE/FIU Science & Technology Workforce Development Program in the fall of 2014, he started working under the mentorship of Dr. Dwayne McDaniel on data analysis of high-level waste pipelines to determine wear rates due to erosion and corrosion. **Recently, Brian accepted an employment offer from Stryker.**



DOE Fellow, Janesler Gonzalez Joins Velossa Tech

Janesler Gonzalez is an undergraduate student at Florida International University pursuing a Bachelor of Science degree in mechanical engineering. When inducted into the DOE/FIU Science & Technology Workforce Development Program in the fall of 2014, he was under the mentorship of Mr. Joseph Sinicrope working on the development of advanced fogging technologies for use in contaminated buildings at the Savannah River Site. Working in conjunction with Savannah River National Laboratories (SRNL) and Idaho National Laboratories (INL), Janesler researched ways to test the efficiency of fogging technologies that will disseminate fixative agents for eliminating airborne contamination and shielding from existing radiation within the walls. In the summer of 2015, Janesler interned at INL under the mentorship of Mr. Stephen Reese and Mr. Rick Demmer. His objectives included decontamination and decommissioning efforts such as mercury abatement through the use of an advanced strippable fogging technology. He was also a part of projects that included supporting the development of a scrubber designed for hazardous gas emissions from spent fuel and pyro-processing for the extraction of useful materials in nuclear waste. **Janesler has accepted a position as a student intern at Velossa Tech.**

DOE Fellow, Jorge Deshon Joins Lockheed Martin



Jorge Deshon is an undergraduate student pursuing a Bachelor of Science in computer engineering with a specialization in data system software, computer architecture and microprocessor design, and network engineering. He is expected to graduate spring of 2016. Jorge is working under the mentorship of Himanshu Upadhyay. As a DOE Fellow in the DOE-FIU Science & Technology Workforce Development Program, Jorge is supporting on the mobile development of the Deactivation and Decommissioning Knowledge Management Information Tool (D&D KM-IT). **Jorge Deshon has accepted an offer of employment as a Software Engineer Associate**

with Lockheed Martin.

DOE Fellow, Meilyn Planas Joins Florida Power and Light



Meilyn Planas is an undergraduate student pursuing a bachelor’s degree in electrical engineering with an expected graduation date of April 2016. As a DOE Fellow, Meilyn is supporting the deactivation and decommissioning research into using intumescent coatings to improve the fire resiliency of fixative coatings. She also assisted in the development of a computer based model to will guide end users in the selection of appropriate contamination control products for the needed site application. **Meilyn has accepted an offer of employment with Florida Power and Light.**

DOE Fellows spring recruitment efforts were initiated on March 21 and will run through April 15. Recruitment campaigns were conducted by placing recruitment tables at the College of Engineering and at the main FIU campus in the Physics & Chemistry building and Computer Science building. Large group of students showed interest in the program and a signup sheet was used to collect student information. Emails were sent to interested students with information on requirements and components of the program along with application procedure and application checklist. Deadline for FIU students to submit applications for DOE Fellowship will be April 15, 2016. Applications will be reviewed by ARC researches and staff and interviews will be conducted during the month of April.

During this reporting period, the Fellows continued their research in the four DOE EM applied research projects under the cooperative agreement and research topics identified as part of their summer internships at DOE sites, national labs, and/or DOE HQ. Each DOE Fellow is assigned to DOE EM research projects as well as ARC mentors. A list of the current Fellows, their classification, areas of study, ARC mentor, and assigned project task is provided below.

Table 4-3. Project Support by DOE Fellows

Name	Classification	Major	ARC Mentor	Project Support
Alejandro Garcia	Graduate - B.S.	Geoscience	Dr. Yelena Katsenovich	FIU’s Support for Groundwater Remediation at PNNL

Alejandro Hernandez	Undergrad - B.S.	Chemistry	Dr. Vasileios Anagnostopoulos	Groundwater Remediation at SRS F/H -Area
Alexis Smoot	Undergrad - B.S.	Envr. Eng.	Dr. Ravi Gudavalli	Synergistic Effects of Silica and Humic Acid on U(VI) Removal
Anthony Fernandez	Undergrad - B.S.	Mechanical Eng.	Mr. Amer Awwad	Evaluation of Nonmetallic Components in the Waste Transfer System
Awmna Kalsoom	Undergrad - B.S.	Chemistry	Ms. Angelique Lawrence	Surface Water Modeling of Tims Branch
Christine Wipfli	Undergrad - B.S.	Envr. Eng.	Dr. Vasileios Anagnostopoulos	Groundwater Remediation at SRS F/H Area
Christopher Strand	Undergrad - B.S.	Civil & Env. Eng.	Dr. Noosha Mahmoudi	Surface Water Modeling of Tims Branch
Claudia Cardona	Graduate - Ph.D.	Envr. Eng.	Dr. Yelena Katsenovich	Sequestering Uranium at the Hanford 200 Area Vadose Zone
Erim Gokce	Undergrad - B.S.	Mechanical Eng.	Mr. Anthony Abrahao	Development of Inspection Tools for DST Primary Tanks
Gene Yllanes	Undergrad - B.S.	Electrical Eng.	Dr. David Roelant	Evaluation of FIU's SLIM for Estimating the Onset of Deep Sludge Gas Release Events
Hansell Gonzalez	Graduate - Ph.D.	Chemistry	Dr. Yelena Katsenovich	Sorption Properties of Humate Injected into the Subsurface System
Iti Mehta	Undergrad - B.S.	Mechanical Eng.	Dr. Aparna Aravalli	Investigation Using an Infrared Temperature Sensor to Determine the Inside Wall Temperature of DSTs
Janesler Gonzalez	Undergrad - B.S.	Mechanical Eng.	Mr. Joseph Sinicrope	Incombustible Fixatives
Jesse Viera	Undergrad - B.S.	Mechanical Eng.	Mr. Joseph Sinicrope	Incombustible Fixatives
John Conley	Undergrad - B.S.	Mechanical Eng.	Mr. Amer Awwad	Evaluation of Nonmetallic Components in the Waste Transfer System
Jorge Deshon	Undergrad - B.S.	Computer Eng.	Dr. Himanshu Upadhyay	Information Technology for Environmental Management
Maximiliano Edrei	Graduate - M.S.	Mechanical Eng.	Dr. Dwayne McDaniel	Computational Fluid Dynamics Modeling of HLW Processes in Waste Tanks
Meilyn Planas	Undergrad - B.S.	Electrical Eng.	Mr. Joseph Sinicrope	Incombustible Fixatives
Natalia Duque	Graduate - M.S.	Envr. Eng.	Dr. Noosha Mahmoudi	Surface Water Modeling of Tims Branch
Orlando Gomez	Graduate - Ph.D.	Physics	Mr. Joseph Sinicrope	Incombustible Fixatives
Robert Lapierre	Graduate - M.S.	Chemistry	Dr. Yelena Katsenovich	Sequestering Uranium at the Hanford 200 Area Vadose Zone

Ryan Sheffield	Undergrad - B.S.	Mechanical Eng.	Mr. Hadi Fekrmandi	Development of Inspection Tools for DST Primary Tanks
Sarah Bird	Undergrad - B.S.	Envr. Eng.	Dr. Ravi Gudavalli	Modeling of the Migration and Distribution of Natural Organic Matter injected into Subsurface Systems
Sebastian Zanolongo	Graduate – Ph.D.	Computer Science	Dr. Dwayne McDaniel	TBD
Silvina Di Pierto	Graduate - Ph.D.	Chemistry	Dr. Hilary Emerson	Evaluation of Ammonia for Uranium Treatment
Yoel Rotterman	Undergrad - B.S.	Mechanical Eng.	Mr. Joseph Sinicrope	Incombustible Fixatives

Highlights of DOE EM Research Being Conducted by DOE Fellows

DOE Fellow Robert Lapierre has studied the ammonia gas injection method proposed for the sequestration of uranium contamination for the remediation of the unsaturated region of the Hanford Site subsurface. The technology uses the reactive gas amendment to reduce the potential for the downward migration of uranium contaminants into groundwater. The research has included the laboratory scale application of the technology using a synthetic porewater solution designed to be relevant to the Hanford 200 Area vadose zone. With a focus on characterizing the uranium products, a host of complimentary techniques, including SEM/EDS and X-ray diffraction analysis, have been used to reveal the structure of phases formed and to investigate the effect of varying constituent concentrations.

DOE Fellow Ryan Sheffield has been developing an inspection tool for the refractory cooling channels of tank AY-102 at the Hanford Site with the guidance of Washington River Protection Solutions. This inspection tool will provide critical live video feedback to the engineers on site, and will serve as a basis to locate the leak that is present in the tank. This inspection tool will pioneer the inspection of tanks and be capable of inspecting other tanks as well with minor modifications.

DOE Fellow Meilyn Planas helped develop and implement a computer-based decision model that will guide end users looking for products to deactivate and decommission (D&D) facilities located at DOE sites such as the Savannah River National Lab. Her current task revolves around increasing the fire resiliency of various fixatives by layering with an intumescent coating. If proven successful, this task will bring about many new standards to which other fixatives may be tested against.

DOE Fellow Maximiliano Edrei has been pursuing efforts in computational fluid dynamics (CFD) based evaluation and validation of correlations proposed in the analytical work of the radial wall jets produced in the pulse jet mixing (PJM) process of low level waste. These proposed correlations that describe the radial wall jet thickness and maximum velocity along the radial direction were obtained from an experiment which does not completely resemble the geometric conditions

of the PJM vessels. These correlations are important in ascertaining whether criticality will be reached within the vessels during the PJM process.

DOE Fellow John Conley, working alongside FIU’s Applied Research Center, has been tasked with conducting a post service examination of hose-in-hose transfer line (HIHTL) nonmetallic components to improve the existing technical basis for component service life. John is conducting multi-stressor testing on the typical nonmetallic materials used at the Hanford tank farms. Baseline tests have been performed on the nonmetallic materials, and material aging is currently ongoing. Once the materials have been aged, testing will be repeated to determine the long term effect of multiple stressors on the nonmetallic materials.

DOE Fellow Yoel Rotterman performed an analysis of the mechanical components of the A/M groundwater remediation system at the Savanna River Site (SRS) to recommend site modifications that would offer the potential for less electrical power consumption and lower groundwater pumping rates of the system. The three main recommendations made were: A solar photovoltaic system for powering the A/M Area groundwater remediation system, the determination and use of an optimal speed for the blower motor that is sufficient to run the countercurrent stripper and removes the volatile organic contaminants to below the required level, and a groundwater modeling analysis be completed to optimize the pumping rate for each recovery well and for the entire system that provides hydrologic containment and maximizes the concentration of contaminants pumped to the stripper.

Milestones and Deliverables

The milestones and deliverables for Project 4 for FIU Year 6 are shown on the following table. Milestone 2015-P4-M4 was completed with the submission of twenty (20) student poster abstracts to WM16.

FIU Performance Year 6 Milestones and Deliverables for Project 4

Milestone/ Deliverable	Description	Due Date	Status	OSTI
2015-P4-M1	Draft Summer Internships Reports	10/16/15	Complete	
Deliverable	Deliver Summer 2015 interns reports to DOE	10/30/15 Reforecast	Complete 11/30/15	OSTI
Deliverable	List of identified/recruited DOE Fellow (Class of 2015)	10/30/15	Complete	
2015-P4-M2	Selection of new DOE Fellows – Fall 2015	10/30/15	Complete	
2015-P4-M3	Conduct Induction Ceremony – Class of 2015	11/05/15	Complete	
2015-P4-M4	Submit student poster abstracts to Waste Management Symposium 2016	01/16/16	Complete	
Deliverable	Update Technical Fact Sheet	30 days after end of project	On Target	

Work Plan for Next Quarter

- Continue research by DOE Fellows in the DOE-EM applied research projects under the cooperative agreement and research topics identified as part of their summer internships.
- Complete spring 2016 campaign to recruit DOE Fellows into the program.
- Complete coordination of internship placements for summer 2016 at DOE sites, national laboratories, DOE-HQ, and DOE contractors and make arrangements for travel and housing. DOE Fellows will begin summer internships in June 2016.